EU-SOPAC Project Report 50
Reducing Vulnerability of Pacific ACP States

TUVALU TECHNICAL REPORT

High-Resolution Bathymetric Survey

Fieldwork undertaken from 19 September to 24 October 2004

October 2008

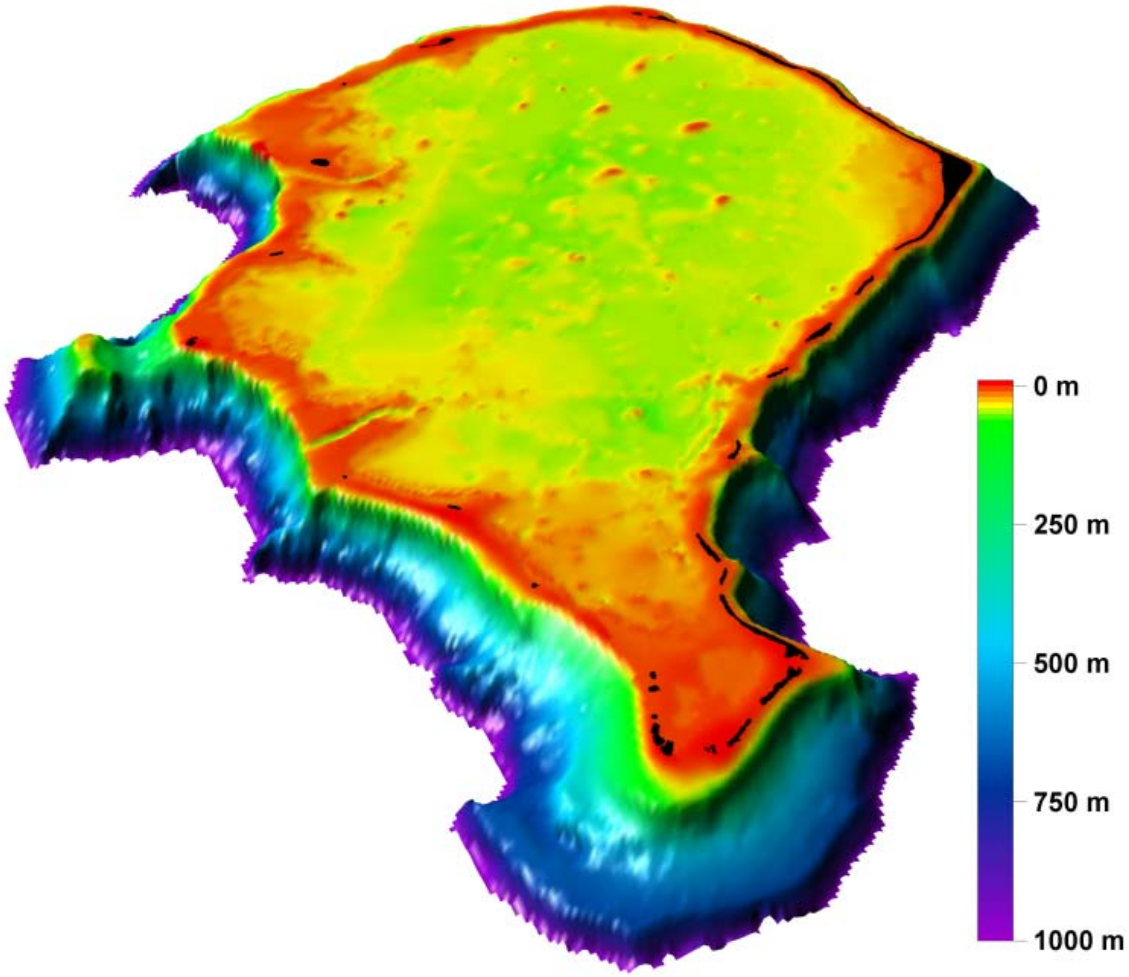

Three-dimensional perspective image of the Funafuti atoll bathymetry.

Prepared by:
Jens Krüger
SOPAC Secretariat
July 2008

PACIFIC ISLANDS APPLIED GEOSCIENCE COMMISSION
c/o SOPAC Secretariat
Private Mail Bag
GPO, Suva
FIJI ISLANDS
http://www.sopac.org
Phone: +679 338 1377
Fax: +679 337 0040
www.sopac.org
director@sopac.org

Important Notice

This report has been produced with the financial assistance of the European Community; however, the views expressed herein must never be taken to reflect the official opinion of the European Community.

TABLE OF CONTENTS

LIST OF FIGURES

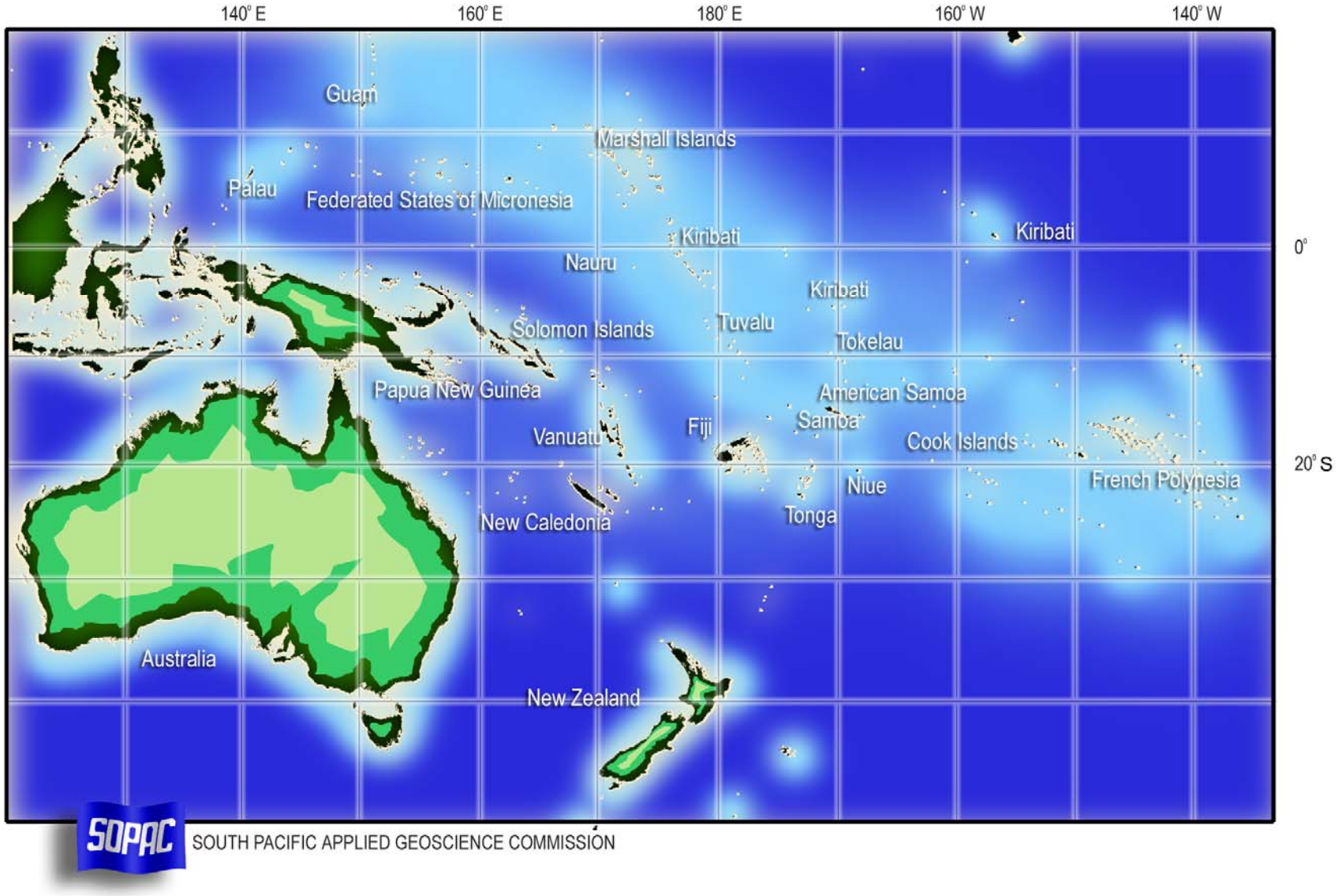

Figure 1. *Location map of Pacific Island countries and territories constituting SOPAC*

Acronyms and their meaning	
ACP	African, Caribbean, and Pacific
ADV	Acoustic Doppler velocimeter
ARGO	Array for real-time geostrophic oceanography
ASCII	American standard code for information interchange
CD	Chart datum
CTD	Conductivity – temperature – depth
DTM	Digital terrain model
EEZ	Exclusive economic zone
EU	European Union
GDEM	Generalised digital environmental model
GEBCO	General bathymetry chart of the oceans
GPS	Global positioning system
LAT	Lowest astronomical tide
MBES	Multibeam echosounder
MRU	Motion reference unit
MSL	Mean sea level
NOAA	National Oceanic and Atmospheric Administration
PI-GOOS	Pacific Islands Global Ocean Observing System
RTK	Real-time kinematic
S2004	Global bathymetry grid merging GEBCO and predicted depths from satellite altimeter measurements
SOPAC	Pacific Islands Applied Geoscience Commission
TAO	Tropical atmosphere ocean array
UTC	Universal time co-ordinated (Greenwich meridian time, GMT)
UTM	Universal transverse Mercator
WGS	World geodetic system

EXECUTIVE SUMMARY

Krüger, J. 2008: High-Resolution Bathymetric Survey of Tuvalu. *EU EDF 8 – SOPAC Project Report 50*. Pacific Islands Applied Geoscience Commission: Suva, Fiji, vi + 58 p. + 9 charts.

The Pacific Islands Applied Geoscience Commission (SOPAC) carried out a marine survey for Tuvalu in the waters around all nine atolls and low reef islands, namely, Nanumea, Niutao, Nanumanga, Nui, Vaitupu, Nukufetau, Funafuti, Nukulaelae, Niulakita. The objective was to investigate the seabed and provide information about water depths around the islands using a multibeam echosounder (MBES). This work was initiated by the SOPAC/EU Reducing Vulnerability of Pacific ACP States Project.

This report describes the high-resolution bathymetric mapping survey carried out over a period of five weeks in September and October 2004. The survey achieved good coverage of the seafloor from approximately 10 m depth in the nearshore reef slope area, to an average offshore depth of some 2000 m, at an average slope angle of 27°.

The resultant data was used to produce nine bathymetry charts for Tuvalu at scales ranging from 1 : 20 000 to 1 : 50 000. Where available, high-resolution satellite imagery of the land surface and shallow reef was included. These new maps provide a descriptive picture of the island features and terrain, vividly revealing the size, shape and distribution of underwater features. They serve as the basic tool for scientific, engineering, marine geophysical and environmental studies, as well as for marine and coastal resource management.

A preliminary analysis of the high-resolution bathymetric data shows prominent terraces and associated seaward steep slopes (>60°) that dominate the islands flanks at water depths of approximately 100 m and 600 m. The shallow terraces at –100 m are interpreted to be drowned growth features that formed when sea level was at a lower level, thereby providing favourable conditions for marine life. These are likely to be features that are vertically stable through many sea level cycles.

The steep slopes at –600 m are associated with downslope channels and gullies presumed to transport sediment into deeper waters. These deeper features are therefore interpreted as erosional scarps, and many of them form relatively large-scale lateral submarine landslides. Some large lateral collapses were found to have headscarps extending into shallower water, with the capacity to deeply modify an island's geomorphology. Particularly on Funafuti it was found that convex seaward notches on the annular ring reef appear to be subaerial expressions of submarine landslide scars. However, the majority of the scarps were mapped in water depths averaging 600 m, which is believed to represent a region of structural discontinuity and therefore weakness on the edifices. The submarine landslides may be associated with areas where the toe of the limestone overlies weak transitional formations, such as subaerial volcanics or sedimentary rocks.

By gaining an understanding of how submarine landslides look and where they occur, we can begin to infer what triggered these failures, and how they control the present-day geomorphology of atolls. The discovery of the –100 m submerged terraces, presumed equilibrium features related to reef-building during earlier sea level stillstands, have the potential to be modern marine habitats of commercial importance (such as for black coral). It is recommended that these seabed features are investigated by remote sampling and underwater video.

1. INTRODUCTION

1.1 Background

A marine survey for Tuvalu was carried out around all nine atolls and low reef islands, namely, Nanumea, Niutao, Nanumanga, Nui, Vaitupu, Nukufetau, Funafuti, Nukulaelae, and Niulakita (Figure 2 and Figure 3). The objective was to investigate the seabed and provide information about water depths around the islands using a multibeam echosounder (MBES). The wave and current regime within Funafuti lagoon was also investigated through the deployment of acoustic Doppler current profilers at four locations, namely Pa'ava, Te Ava Fuagea, Payne Rock, and Te Atau Loa. The oceanographic data was collected in order to calibrate a water circulation model of Funafuti lagoon using MIKE21 hydrodynamic modelling software. The present report presents the results of the MBES survey (the oceanographic data and modelling results for Funafuti lagoon are covered elsewhere). This work was initiated by the SOPAC/EU Reducing Vulnerability of Pacific ACP States Project, under the European Development Fund (EDF9).

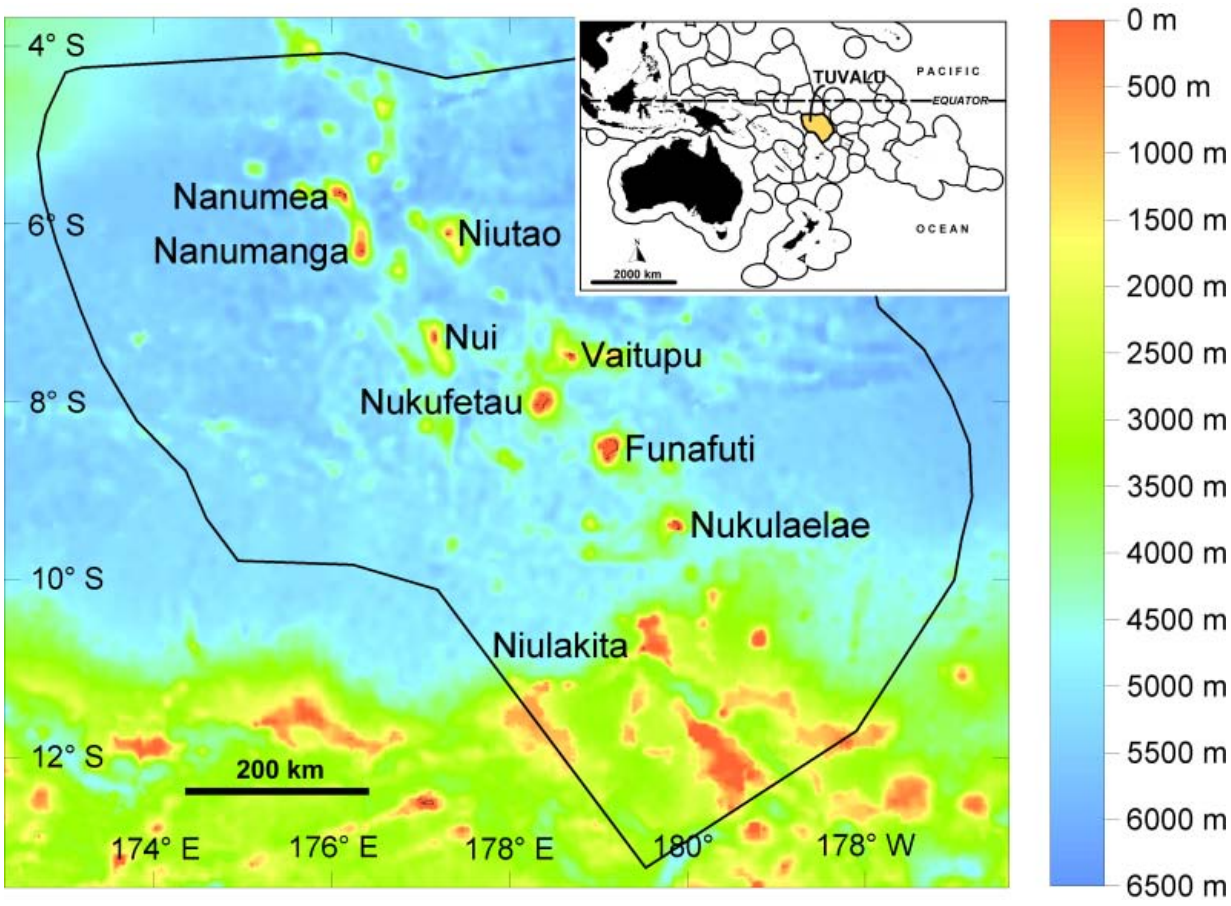

Figure 2. *Map of Tuvalu showing the location of atolls and islands, and approximate position of the exclusive economic zone. Bathymetric data shown are predicted water depths in metres (Smith and Sandwell 1997).*

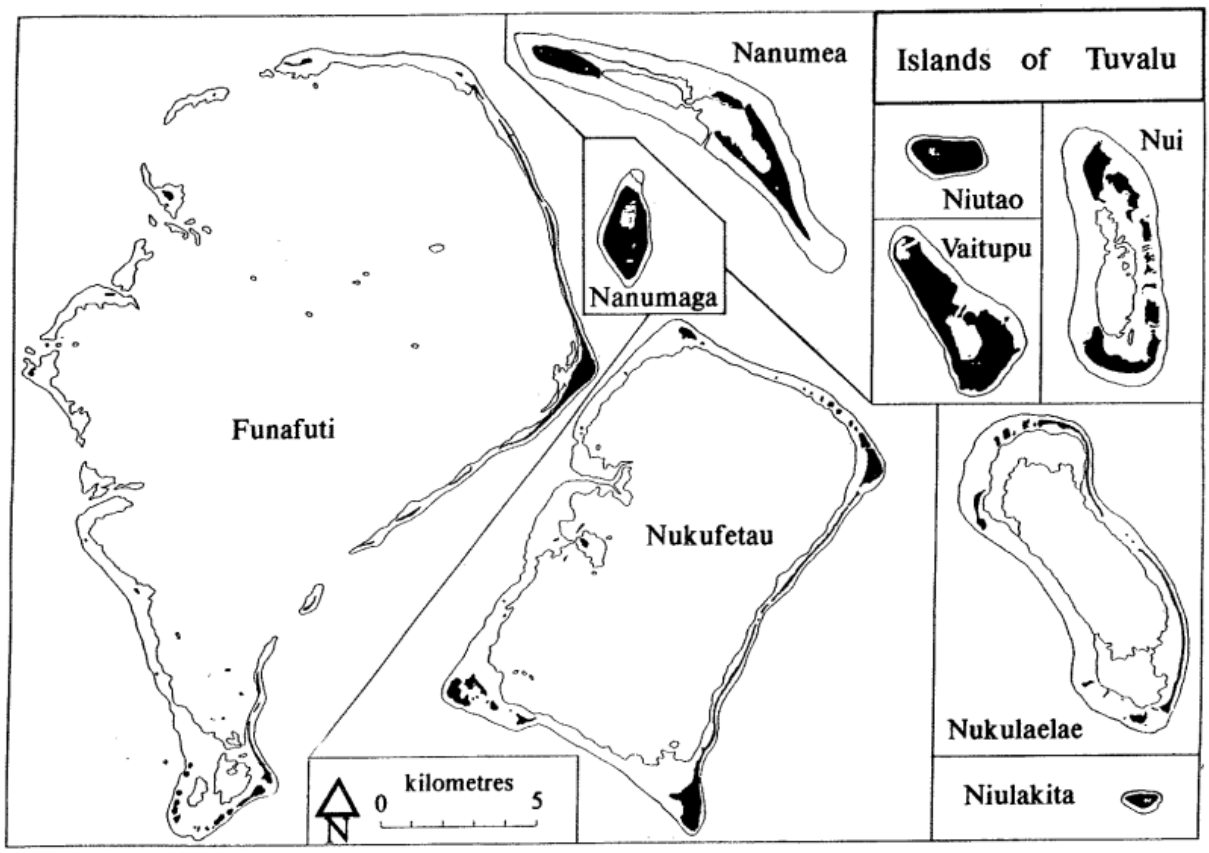

***Figure 3**. Relative size of the reefs and islands of Tuvalu. From McLean and Hoskins (1991).*

1.2 Geographic Situation and Geological Setting

Tuvalu consists of nine atolls and low-reef islands situated between 4° and 13.2°S latitude, and 172.7° and 176.8°E longitude, with an exclusive economic zone of approximately 900 000 km^2 (Figure 1 and Figure 2), land area of about 25 km^2, and a population estimated at 9600 (SOPAC 2000). The islands form a 680-km long linear cluster with a NNW to SSE orientation, suggesting that the group developed as part of a hotspot chain (Pelletier and Auzende 1996). Volcanic rocks dredged from the flanks of Niulakita are Cretaceous, or some 80 Ma (Duncan 1985).

Early geological investigations of the Tuvalu Group (formerly Elice Islands) were driven by the debate over concepts relating to the long-term development of mid-ocean coral atolls and Darwin's subsidence theory (Darwin 1842). Drilling explorations at Funafuti from 1896 to 1898 resulted in 340 m long cores comprising shallow-water carbonates without encountering basement volcanics (David and Sweet 1904). Subsequent analysis of the drill cores suggests a subsidence rate for Funafuti of approximately 30 m/Ma (Ohde et al. 2002). Additional studies on the deep structure of Funafuti comprised a magnetic survey (Creak 1904), and a single seismic refraction line inside the lagoon (Gaskell and Swallow 1953). These two data sets are interpreted to show a minimum of 500 m of limestone below the lagoon floor, with presumed underlying volcanics (Locke 1991). Gaskell and Swallow (1953) also report on a refraction line in Nukufetau lagoon, concluding that volcanics are capped by approximately 760 m of limestones. More recent investigations in the group relate to the search for phosphates and aggregates (Radke 1986; Smith et al. 1990, 1991; Cronan and Hodkinson 1990; Rogers 1992; Smith 1995), and mapping in the context of coastal geomorphology and management (McLean and Hoskins 1991, 1992; Kaly and Jones 1994; Xue and Malologa 1995; Xue 1996a, 1996b, 1996c; Ramsay and Kaly 2004; Webb 2005), as well as climate change and sea level rise (Lewis 1989; Dickinson 1999; Connell 2003; Church et. al. 2006; Patel 2006; Yamano et. al. 2007).

1.3 Previous Seabed Mapping Surveys

Publicly available marine charts do not currently cover the entire islands group, with inshore surveys dating from 1892 to 1954, but primarily limited to the 19th century (cf. Figure 9, top). Most bathymetric data within the EEZ and in nearshore areas originate from sparse single-beam soundings from oceanographic cruises. Pearce (2008) recently listed available bathymetry datasets as part of a geospatial inventory of Tuvalu.

Funafuti lagoon was surveyed by GIBB in 1983 (GIBB 1995) as shown in Figure 4; by the HMNZ Monowai, Royal New Zealand Navy, in 1983 (see Figure 5); and parts of the lagoon fronting Fongafale where surveyed by SOPAC in 1992 and 1993 (Smith 1995). Nukufetau lagoon was surveyed by Radke (1986) and Smith et al. (1990), and a bathymetric map was subsequently published as at a scale of 1 : 25 000 with contours at 5 m intervals (Smith 1992b) as shown in Figure 6. Nukulaelae Lagoon was previously surveyed by Smith et al. (1990), and compiled into a bathymetric map at a scale of 1 : 12 500 with contours at 2 m intervals (Smith 1992a), which is shown in Figure 7. A multibeam mapping cruise of the South Tuvalu banks was conducted as part of the SOPACMAPS project (IFREMER 1994) and is shown in Figure 8. Apart from MBES bathymetry, the SOPACMAPS project also consisted of sidescan sonar imagery, high-resolution sub-bottom profiler, six-channel seismic reflection, gravity and magnetic data and resultant interpretations. Maps of these products are held in hard copy format at the SOPAC library.

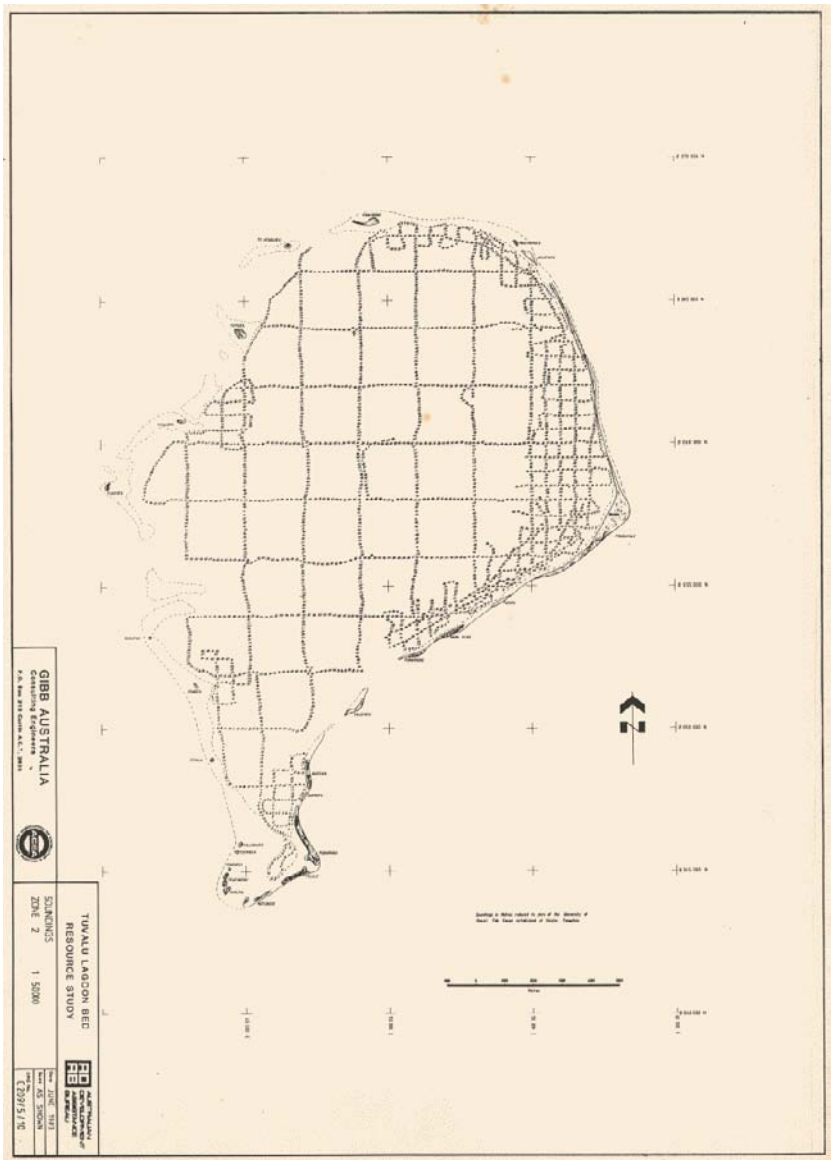

Figure 4. *Depth soundings in Funafuti lagoon by GIBB (1985). This data was collected by single-beam echosounder as part of a lagoon bed resource survey.*

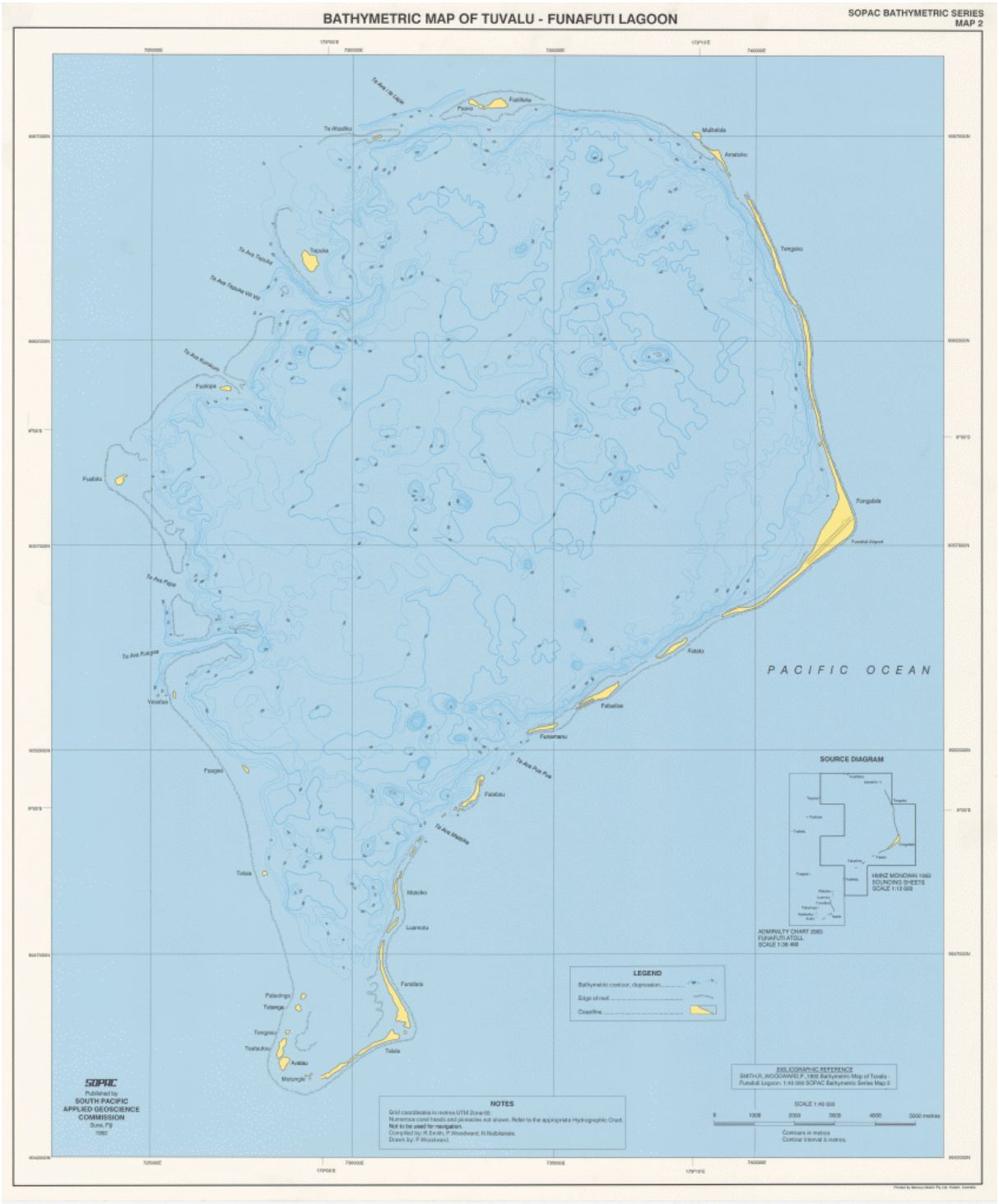

Figure 5. *Bathymetry map of Funafuti lagoon at a scale of 1 : 40 000 in the original, with contours at 5 m intervals based on HMNZ Monowai 1983 sounding sheets and Admiralty Chart 2983 (Smith and Woodward 1992). This map is available online at the SOPAC virtual library site (see www.sopac.org) as the Bathymetric Map Series No. 2.*

Figure 6. *Bathymetry map of Nukufetau lagoon at a scale of 1 : 25 000 in the original, with contours at 5 m intervals (Smith 1992a). This map is available online at the SOPAC virtual library site (see www.sopac.org) as the Bathymetric Map Series No. 4.*

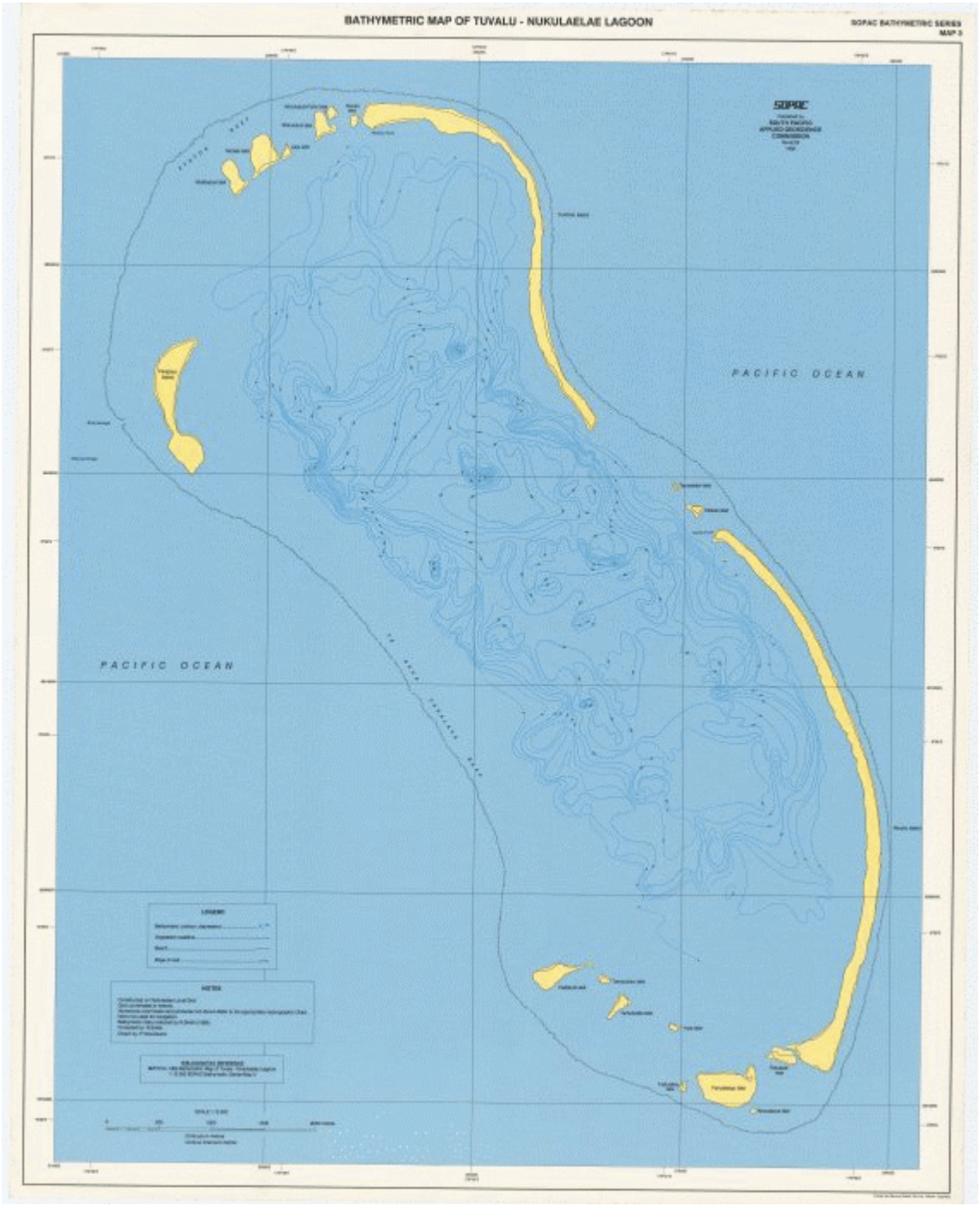

Figure 7. *Bathymetry map of Nukulaelae lagoon at a scale of 1 : 12 500 in the original, with contours at 2 m intervals (Smith 1992a). This map is available online at the SOPAC virtual library site (see www.sopac.org) as the Bathymetric Map Series No. 3.*

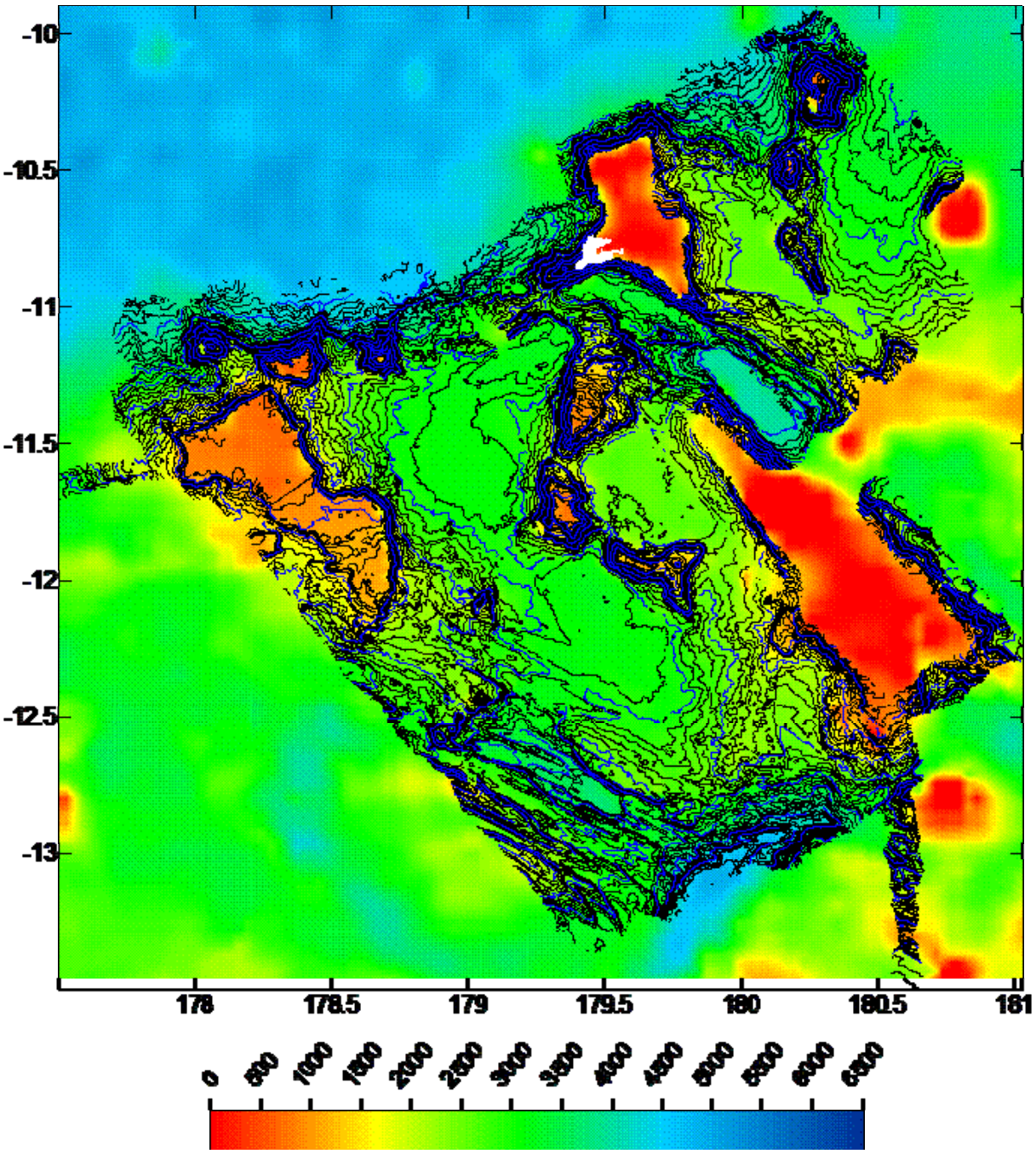

Figure 8. *Area of the South Tuvalu Banks Area covered by the SOPACMAPS project shown with blue and black contours (IFREMER 1994). Niulakita is located at 179°28'E 10°47'S, with the SOPAC/EU coverage (this report) shown in white. The coloured backdrop is predicted bathymetry in metres (Smith and Sandwell 1997).*

2. RESULTS

2.1 Bathymetry

The nearshore areas and submarine flanks of all nine atolls and low reef islands of Tuvalu were mapped by MBES in 2004 and compiled into bathymetric charts with scales ranging from 1 : 20 000 to 1 : 50 000 (see example in Figure 9 and the table below). The charts are available with this report as appendices. Charts ER0050.1 to ER0050.9 also include smaller-scale insets of 3D images, slope angle and shaded relief maps. The underlying bathymetric grid files and metadata used to produce the charts are available through the SOPAC GeoNetwork site. This report and charts are available through the SOPAC virtual library website.

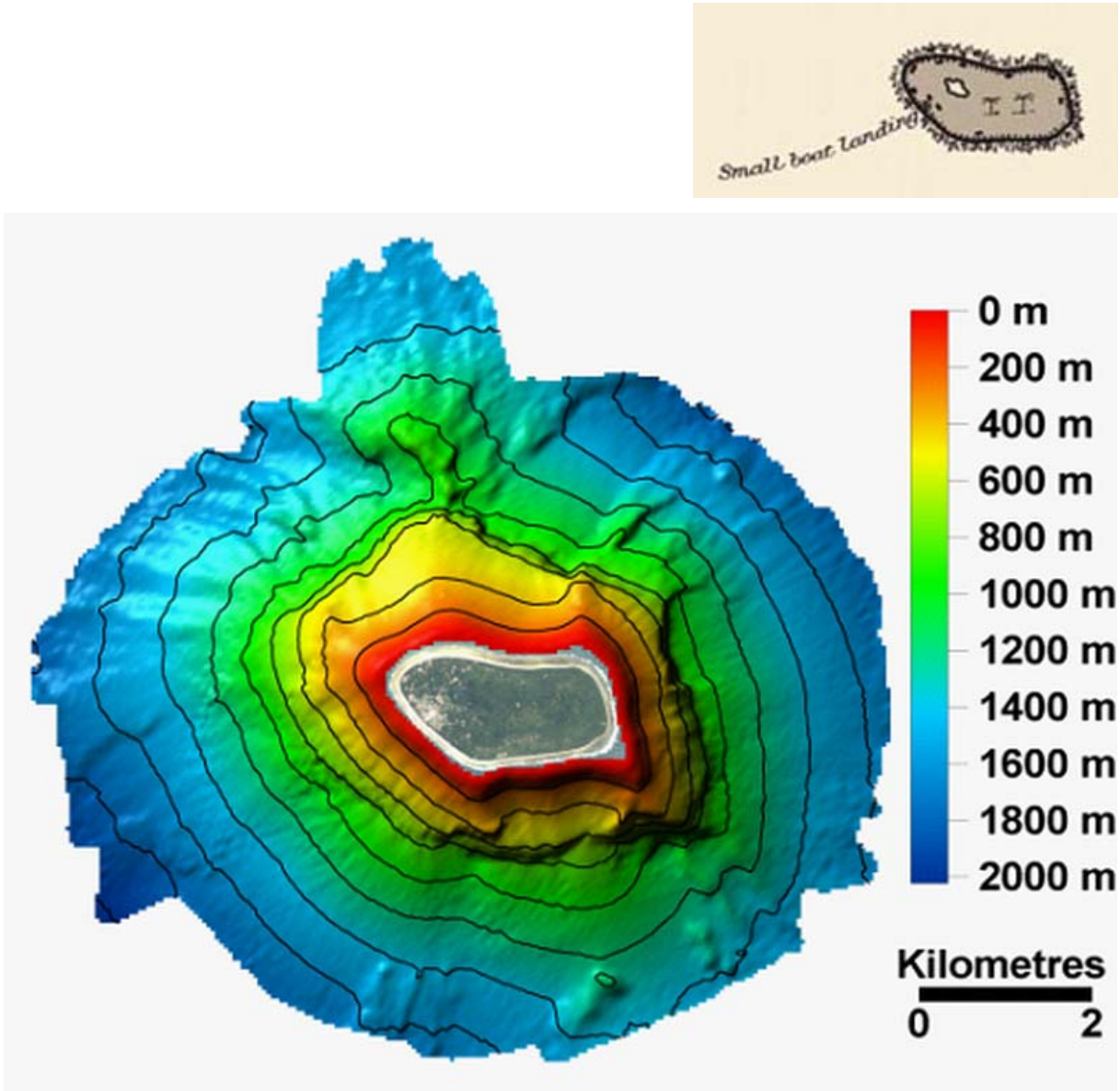

Figure 9. *Upper image: The low reef island of Niutao, as depicted on the marine chart AUS766, published in 1952. Main image: High-resolution satellite and bathymetry data as acquired for Niutao under SOPAC/EU in 2004. Contours are at 200 m intervals and north is up.*

The survey locations along with vital seabed statistics derived from the MBES data are tabulated below. The average slope angle using a 20 m gridded bathymetry was calculated to be 27° from the horizontal.

Islands of the Tuvalu Group		Location		Slope (º horizontal)			Depth (m)	
Name	Type	Lat	Long	Min	Max	Mean	Min	Max
Nanumea	Atoll island	176°06'E	5°39'S	0	72	25	12.1	2,511.7
Niutao	Low reef island	177°20'E	6°06'S	0	78	24	8.6	2,021.3
Nanumanga	Low reef island	176°19'E	6°17'S	0	77	26	9.2	2,054.2
Nui	Atoll island	177°09'E	7°13'S	0	79	23	2.5	2,466.5
Vaitupu	Atoll / low reef island	178°40'E	7°28'S	0	78	30	9.5	1,343.5
Nukufetau	Atoll island	178°22'E	7°59'S	0	77	39	7.4	1,922.3
Funafuti	Atoll island	179°07'E	8°30'S	0	79	26	0.3	2,224.2
Nukulaelae	Atoll island	179°50'E	9°23'S	0	77	27	9.0	1,878.0
Niulakita	Low reef island	179°28'E	10°47'S	0	73	23	7.2	2,148.7

2.1.1 Funafuti Composite Bathymetry Grid

As outlined in the introduction above, one of the objectives of the survey was to provide baseline data necessary to run and calibrate a numerical water circulation model of Funafuti. One fundamental component is a digital terrain model (DTM). The MBES data of Funafuti was therefore merged with all the other digital depth data available for Funafuti at the time of this study, as shown in Figure 10. This provided sufficient coverage over the shallow lagoon and deeper ocean atoll flank. The final DTM was created at a 100 m grid interval using Surfer 8.01 software, and the resultant surface is shown in Figure 13 and Figure 14, as well as on a small-scale inset as part of chart ER050.7.

Figure 11 shows that Funafuti lagoon is characterised by a wide (18 km) and deep (maximum depth recorded is 54.7 m) basin in its northern part, and a very narrow shallow basin in its southern part. A N-S cross-section through the 24.5-km long lagoon is shown in Figure 12.

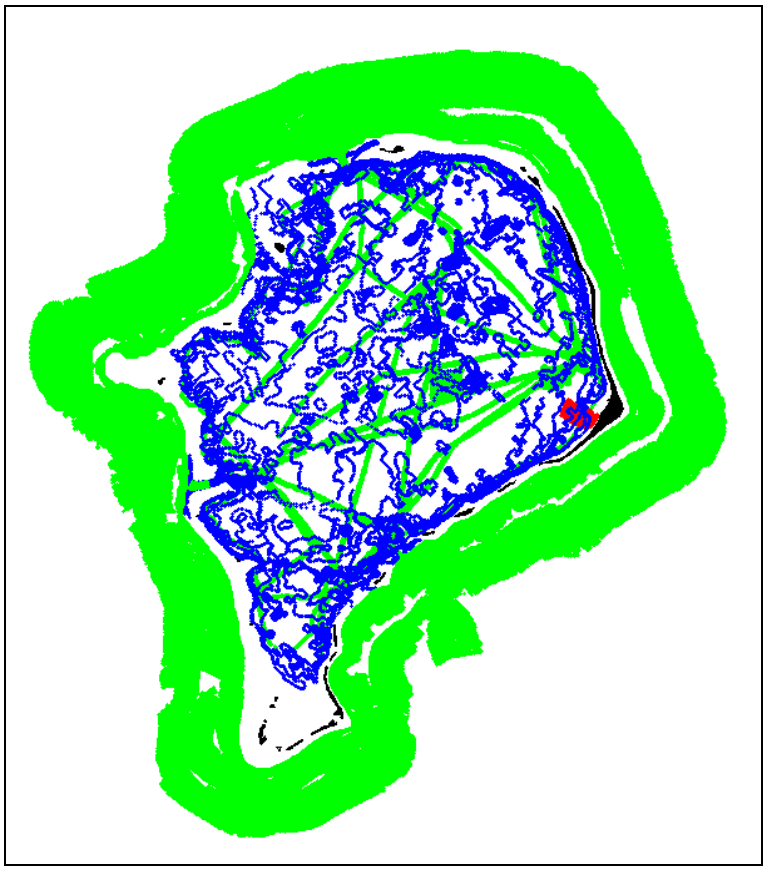

Figure 10. *Map showing the collation of depth data for Funafuti available in digital format, comprising (i) digitised contours from sounding sheets produced from the HMNZ Monowai, 1983 survey, shown in blue; (ii) MBES sounding points collected by SOPAC/EU 2004, in green; (iii) single-beam echosounder sounding collected by SOPAC (Smith 1995), in red.*

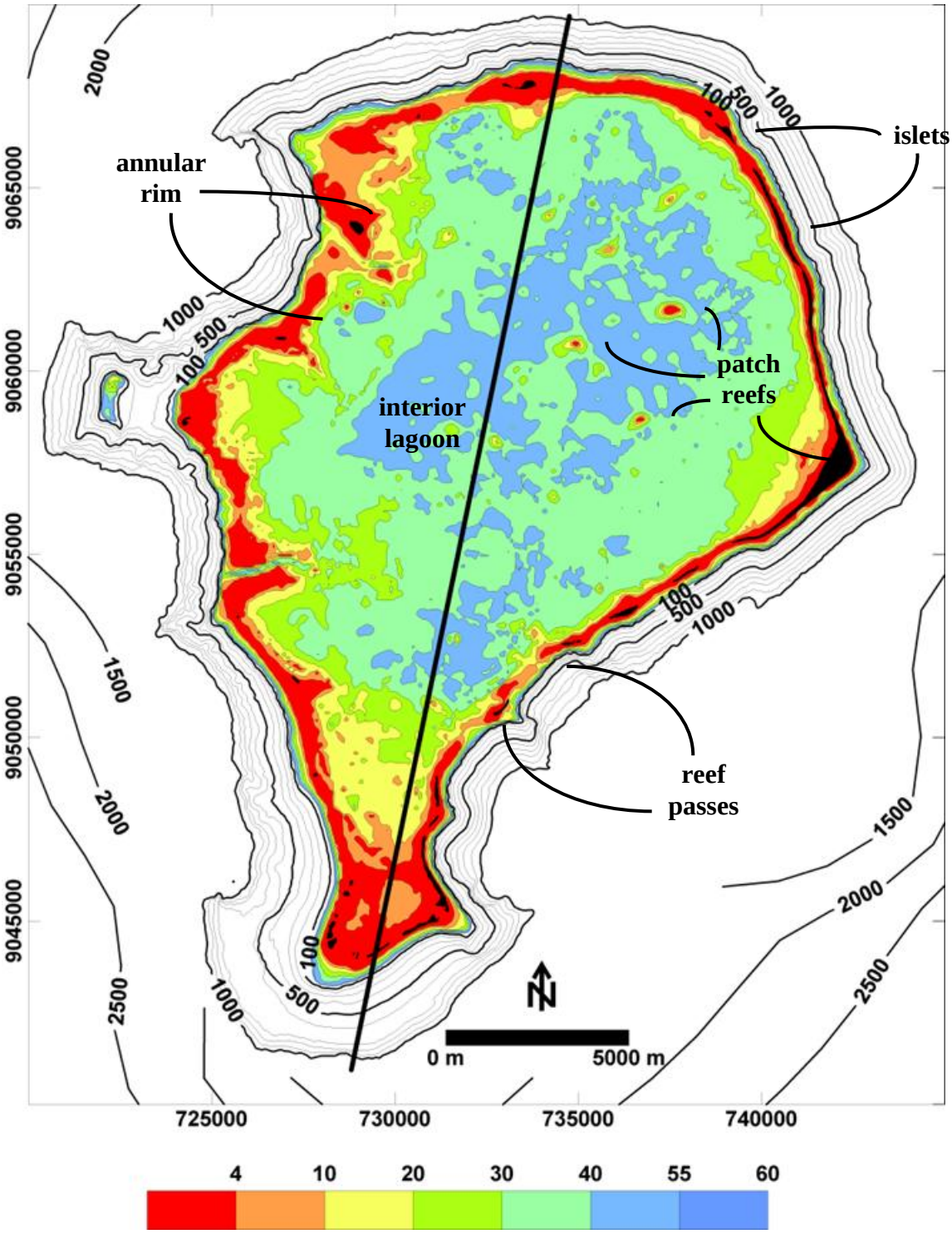

Figure 11. *Bathymetry and geography of Funafuti atoll. The bathymetry is compiled from: (i) HMNZ Monowai 1983 fair sheets (see Smith and Woodward 1992, and Figure 5), (ii) 2004 MBES data (this report), (iii) predicted bathymetry (Smith and Sandwell 1997). The reef rim (red) is shown as water depths of approximately 6 m below mean sea level (MSL), or 4 m below chart datum (CD). The descriptive geography is after Dickinson (2004). The bold N-S line is the cross section shown in Figure 12.*

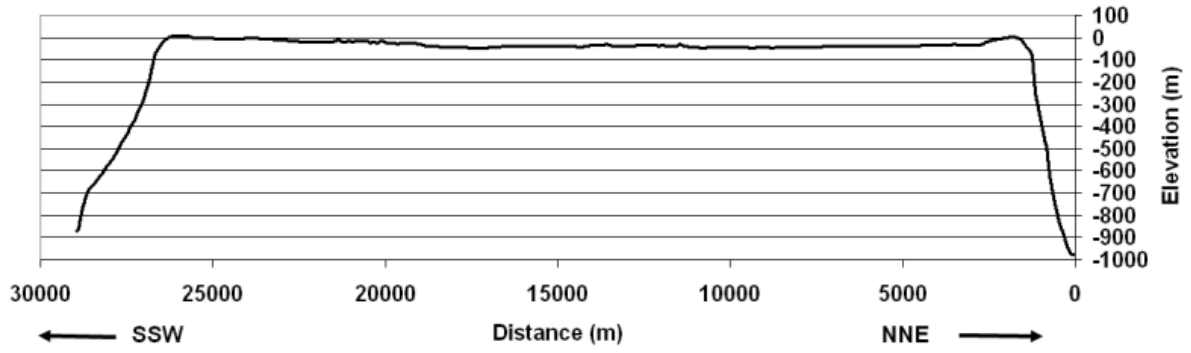

Figure 12. *N-S cross section through Funafuti lagoon shown in Figure 11. Note relatively distinct and wide terrace at the southern end at depth of 500–700 m.*

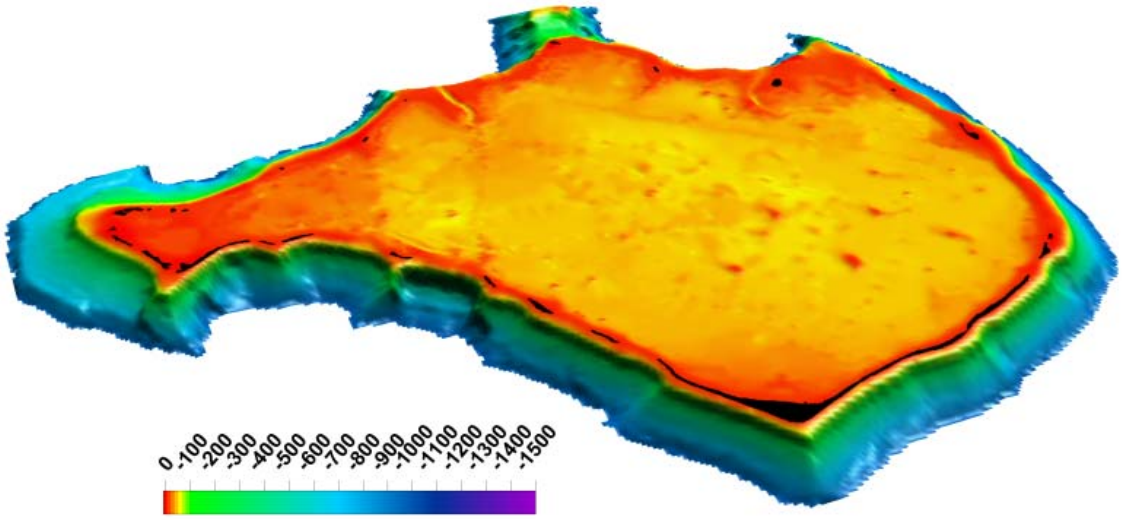

Figure 13. *Perspective image of Funafuti atoll looking west. Land is shown in black and depths are in metres. For detail see text.*

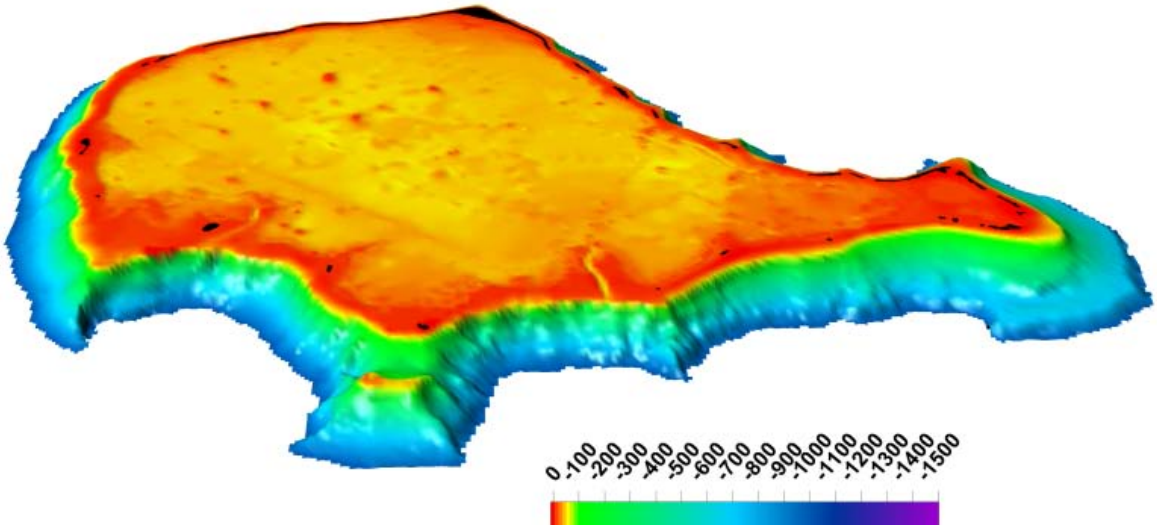

Figure 14. *Perspective image of Funafuti atoll looking east. Land is shown in black and depths are in metres. For detail see text.*

2.2 Seabed Morphology

What follows is a general description of the seabed geomorphology for each of the nine islands and atolls based on the 2004 MBES data. The interpretation is based on visual inspection of the charts, including the insets of contoured bathymetry, slope angle, shaded relief, and 3D views; and using the seabed features terms defined in detail in Section 4.11. The dominant seabed features evident from the bathymetry are the high-gradient slopes (~60º), and relatively large-scale lateral submarine landslides and channels that have deeply modified the islands' seabed geomorphology, as well as subaerial coastline.

2.2.1 Nanumea

Nanumea is an elongated atoll 13 km long along the NW-SE axis, and 2.4 km wide along the SW-NE axis, centred on 176°6'E and 5°39'S. The surveyed area extends to a maximum of approximately 5.3 km offshore from the coastline at the northwest tip of the atoll (see coverage map in Appendix 3). The bathymetry is shown on Chart 1 contoured at intervals of 20 m. The chart also includes smaller-scale insets of 3D images, slope angle and shaded relief maps.

The water depth within the survey area around Nanumea ranges from 12.1 to 2511.7 m. The minimum water depth occurs in the nearshore area on the outer reef slope, while the seabed deepens to the maximum at an average gradient of 25° near the seaward limits of the survey area. Locally, the seabed is expected to be quite irregular with gradients expected to be highly variable, ranging from 0 to 72°. The predicted bathymetry from Smith and Sandwell (1997) in Figure 2 shows that Nanumea stands some 5000 m above the surrounding ocean floor.

The island is encircled by a near-continuous scarp (slope angles >60°), located approximately 150 to 250 m seaward of the reef crest, 80 to 100 m below sea level, with scarp heights of approximately 100 m. The southwest flank of the edifice is characterised by a 750 m wide terrace that has a steep seaward slope (40 to 50°), which terminates in a 16.5-km long lateral scarp in water depths of 660 to 800 m, with scarp heights ranging from 100 to 160 m. The seabed regains mean slope values below this scarp. The effect of this steep lateral terrace is that the seafloor to the southwest of the edifice is generally deeper than for comparable areas of seabed to the northeast of the island. The southeasterly apex of the atoll exhibits a broad region of low overall slope, incised by several channels dipping to the ENE, with upslope scarps. To the northwest, the seafloor shows a stack of arcuate scarps that are sub-parallel to the atoll's NW-SE axis.

2.2.2 Niutao

Niutao Island, located at 6°06'S and 177°20'E, is a low reef island comprising a single island approximately 2.7 km long (E-W), 1.3 km wide (N-S). It is surrounded by a fringing reef and has a small central brackish-water pond. The surveyed area extends to an average of approximately 3.5 km from the coastline (see coverage map in Appendix 3). The bathymetry is plotted on Chart 2 with contours at intervals of 20 m. The chart also includes smaller-scale insets of 3D images, slope angle and shaded relief maps.

The water depth within the survey area around Niutao ranges from 8.6 to 2021.3 m. The minimum water depths occur in the nearshore area on the outer reef slope, while the seabed deepens to the maximum measured depth at an average gradient of 24° near the seaward limits of the survey area. Locally, the seabed is expected to be quite irregular with gradients expected to be highly variable, ranging from 0 to 78°. The predicted bathymetry from Smith and Sandwell (1997) in Figure 2 shows that Niutao rises some 5000 m from the surrounding ocean floor.

The seabed around Niutao shows numerous scarps, which can be generalised into two sets.

First, a continuous scarp encircles the island in close proximity (350 m) to the outer reef slope, with the headscarp situated in 60–80 m water depth, and a headscarp height of 120 m. The second set of deeper scarps are discontinuous and sub-parallel to Niutao's shoreline with headscarps 420–620 m below sea level, and headscarp heights of 220–380 m. Numerous channels are radially orientated downslope from the second set of scarps. The largest channel is 1.1 km wide, located in the northeast with sidewalls approaching angles of 45°.

2.2.3 Nanumanga

Nanumanga Island, located at 6°17'S and 176°19'E, is a low reef island comprising a single island approximately 3.7 km along the N-S axis, and 1.6 km wide in an E-W direction. The island is surrounded by a fringing reef, with small central brackish-water lagoons. The surveyed area extends to an average of approximately 4.0 km from the coast, with maximum coverage seaward of 7.3 km from the coastline to the north (see coverage map in Appendix 3). The bathymetry is shown on Chart 3 contoured at intervals of 20 m. The chart also includes smaller-scale insets of 3D images, slope angle and shaded relief maps.

The water depth within the survey area around Nanumanga ranges from 9.2 to 2054.2 m. The minimum water depths occur in the nearshore area on the outer reef slope of the fringing reef surrounding the island, and a shoal with dimensions approximately 1.0 km (N-S) by 0.3 km (E-W), located 4 km north of the island (minimum depth of 10.0 m). A ridge extends to the south of Nanumanga, in alignment with the island's N-S axis, shoaling to a depth of 300 m. Everywhere else, the seabed deepens to the maximum at an average gradient of 26° near the seaward limits of the survey area. Locally, the seabed is expected to be quite irregular with gradients expected to be highly variable, ranging from 0 to 77°. The predicted bathymetry from Smith and Sandwell (1997) in Figure 2 shows that Nanumanga stands some 5000 m above the surrounding ocean floor. From this morphological interpretation of Figure 18 it is evident that the island is situated at the centre of a 13-km long N-S orientated ridge, in contrast to the classic cone shape of a mid-ocean edifice which comprises circular bathymetric contours. The ridge makes up the external framework of the present day island, and is presumed to have been the result of a fissure eruption controlled by a structural discontinuity in the oceanic crust that governed the extrusion of lava.

The mapped scarps in the survey area around Nanumanga can be separated into those with headscarps occurring in water depths of approximately 80 to 100 m, and those that predominate at, or are deeper than, 500 m below sea level. Numerous channels were mapped with downslope directions perpendicular to the N-S trending ridge. The shallow scarps are circular and surround the island of Nanumanga itself, as well as the shoal 4 km to the north. These headscarps are in the order of 80 to 100 m high. The deeper scarps are generally N-S trending, following the isobaths of the ridge and saddle described above. The seabed is quite irregular along the saddle to the northeast of the survey area. The eastern flank of the saddle exhibits three stacked sub-parallel scarps flank, with a combined height extending through water depths ranging from 400 to 1000 m.

2.2.4 Nui

Nui is a N-S elongated atoll island approximately 8.1 km long and 2.5 km wide, centred on 7°13'S and 177°9'E. It has some eight major islands and a number of smaller islets, surrounding a central ponding lagoon system. There are no islands on the western leeward side of the lagoon. The surveyed area extends to an average of approximately 5.0 km offshore, however, there is a 500 m wide swath with no coverage, at a distance of approximately 2.5 km from the shoreline (see coverage map in Appendix 3). The bathymetry is shown on Chart 4 contoured at intervals of 20 m. The chart also includes smaller-scale insets of 3D images, slope angle and shaded relief maps.

The water depth within the survey area around Nui ranges from 2.5 to 2466.5 m. The minimum water depths occur in the nearshore area on the outer reef slope of the fringing reef surrounding the island, while the seabed deepens to the maximum at an average gradient of 23° near the seaward limits of the survey area. Locally, the seabed is expected to be quite irregular with gradients expected to be highly variable, ranging from 0 to 79°. The predicted bathymetry from Smith and Sandwell (1997) in Figure 2 shows that Nui stands some 5000 m above the surrounding ocean floor.

The atoll of Nui is surrounded by a scarp with a depth to the headscarp of approximately 100 m, and a headscarp height of 80 m. Beyond this, the general morphology of the seabed can be separated into a region with relatively steep slopes of 40° extending to approximately 1.5 km offshore to water depths of 700 m, and an offshore region where average gradients of 23° prevail. The seabed is relatively uniform compared to the other islands and atolls in the Tuvalu group, however some low-relief channels radiate from the atoll in a downslope direction.

2.2.5 Vaitupu

Vaitupu Island is located at 178°40'E and 7°28'S, and displays composite characteristics of atoll and low reef island forms, and was classified as a part-raised atoll with an enclosed lagoon by Scott and Rotondo (1983). The island is pear-shaped and approximately 5.2 km along the NW-SE axis, and 2.0 km along the SW-NW axis. A small ponding lagoon is located in the centre of the island, which is connected to the ocean by a shallow passage on the eastern side at high tide. The survey area extended approximately 1.8 km offshore from the coastline (see coverage map in Appendix 3). The bathymetry is shown on Chart 5 contoured at intervals of 20 m. The chart also includes smaller-scale insets of 3D images, slope angle and shaded relief maps.

The water depth within the survey area around Vaitupu ranges from 9.5 to 1343.5 m. The minimum water depths occur in the nearshore area on the outer reef slope, while the seabed deepens to the maximum at an average gradient of 30° near the seaward limits of the survey area. Locally, the seabed is expected to be quite irregular with gradients expected to be highly variable, ranging from 0 to 77°. The predicted bathymetry from Smith and Sandwell (1997) in Figure 2 shows that Vaitupu stands some 5000 m above the surrounding ocean floor.

The island is encircled by a steep scarp that exceeds slope angles of 60°, located approximately 300 m seaward of the reef crest with a water depth to the top of the headscarp and headscarp height of approximately 80 m and 120 m, respectively. Further offshore, the general morphology of the surveyed area can be separated into a region of regular seabed with sub-parallel isobaths in the east and south, and a scarp-enclosed seaward concave region to the west. The northwest apex of the island is dominated by a 1.2-km long arcuate headscarp in water depths of 260 m and a scarp height of 540 m. Several channels appear to be associated with this feature. The southwest has a set of two converging scarps 400 to 1120 m below sea level. These scarps to the northwest and south of the island are aligned in a cross-slope direction, and act as sidewalls to the lateral western slide.

2.2.6 Nukufetau

Nukufetau is a rectangular atoll with an enclosed lagoon some 14 km long (NE-SW axis) by 8.35 km wide (NW-SE axis), centred on 178°22'E and 7°59'S. The lagoon is surrounded by an outer reef platform with a natural reef channel in the southwest. Nukufetau lagoon was previously surveyed by Radke (1986) and Smith et al. (1990). The data from these surveys were published as a bathymetric map shown in Figure 6 (Smith 1992b). The area surveyed for this project varied from approximately 1.5 to 4.5 km offshore from the coastline (see coverage map in Appendix 3). The natural reef pass Te Ava Lasi allows a deep-water

passage for boat access to the lagoon, and part of the lagoon was mapped in a zigzag pattern. The bathymetry is shown on Chart 6 contoured at intervals of 50 m and 5 m for the ocean-side and lagoon, respectively. The chart also includes smaller-scale insets of 3D images, slope angle and shaded relief maps.

The water depth within the survey area ranges from 7.4 to 1922.3 m. The minimum water depths occur in the nearshore area on the outer reef slope, and along the western lagoon margin. The seabed deepens to the maximum at an average gradient of 27° near the seaward limits of the survey area, 4.5 km northwest of the channel. Locally, the seabed is expected to be relatively irregular with gradients expected to be highly variable, ranging from 0 to 77°. The predicted bathymetry from Smith and Sandwell (1997) in Figure 2 shows that Nukufetau stands some 5000 m above the surrounding ocean floor.

Nearshore areas with coverage of water depths less than 150 m show a steep cliff that exceeds slope angles of 60°, located approximately 250 m seaward of the reef crest, except at the southwest and southeast corners, where the scarp follows structural highs leading away from the atoll. The depth of the headscarp and scarp height are approximately 100 m and 150 m, respectively. The structural highs in the southwest and southeast corners are believed to be volcanic ridges that radiate out from the present-day atoll.

Further offshore, the general morphology of the seabed around Nukufetau can be separated into a region of relatively regular seabed, with contours sub-parallel to the reef rim in the north and northeast, and an area with numerous scarps to the south and west. The most dominant features to the west are two scarps with a NW-SE across-slope strike direction. Both scarps have their upper limits in water depths of approximately 400 m, leading into deeper waters with scarp heights of up to 400 m. These scarps are believed to be fault-controlled, extending into the lagoon where they are expressed as breaks in the reef rim (see satellite image on Chart 6), giving rise to the natural reef passes Te Ava Lasi to the south and Te Ava Amua to the north.

2.2.7 Funafuti

Funafuti is the largest atoll of the nine low reef islands and atolls that form the Tuvalu island chain. It comprises numerous islets around a central lagoon that is approximately 25.1 km (N-S) by 18.4 km (W-E), centred on 179°7'E and 8°30'S. An annular reef rim surrounds the lagoon, with several natural reef channels in the northwest, west, and southeast (Figure 11). The geomorphology and sedimentation of Funafuti has previously been described by Dickinson (1999), and Collen and Garton (2004). Past bathymetric and geophysical surveys carried out in Funafuti are listed in Section 1.3 and Section 2.1.1.

The area surveyed for this project varied from approximately 1.5 to 4.5 km offshore from the coastline (see coverage map in Appendix 3). Parts of the lagoon were mapped while underway for the purpose of deploying and retrieving oceanographic and GPS equipment. The acquired and processed MBES bathymetry is shown on Chart 7, contoured at intervals of 50 m and 5 m for the ocean-side and lagoon, respectively. The chart also includes smaller-scale insets of 3D images, slope angle, shaded relief, lagoon bathymetry, and interpreted seabed morphology. The interpreted seabed morphology is reproduced in Figure 15 to aid discussion.

Depths vary from 1 m in the lagoon, to 2224 m on the deeper margins of the atoll edifice flank. The atoll flank has an average seaward slope of 26°, which is highly variable with a maximum of 79°. The nearshore bathymetry of Funafuti is more complex than the other atolls and islands. However, a near continuous shoreline parallel terrace and break in slope in water depth of 100–150 m is observed approximately 100–450 m seaward of the modern reef, termed reef front slope in Figure 15. A 2-km wide submarine terrace is evident at the southern apex of the atoll flank. The landward upslope margin is at 250 m, while the seaward break in slope occurs in water depths of 700 m.

The northwest, southwest, and southeast flanks exhibit numerous stacked high gradient slopes (>60°), interpreted as mass movement features termed landslide scars in Figure 15. There is little evidence of these erosional features on the north or northeast flank. The dominant seabed feature is an amphitheatre-shaped submarine landslide on the northwest flank in water depths of about 150 m. The 10 km long shoreline-parallel scarp is flanked by a series of stacked cross-slope sidewall failures that have maximum slope angles approaching 80°. The largest of these is on the northern sidewall of the amphitheatre, about 3.5 km northeast of Tepuka island. The landward break in slope of the scarp occurs in water depth of 350 m, with a scarp height of 650 m, creating a near vertical drop off that terminates in 1000 m water depth. This submarine landslide complex has significantly altered the shape of the atoll, deeply incising the annular reef rim. Similar alterations are thought to have occurred particularly in the southwest and southeast of the atoll flank. This has the effect of creating seaward convex notches on the annular ring reef, and thereby controlling the subaerial shape and position of modern atoll islets and channel positions.

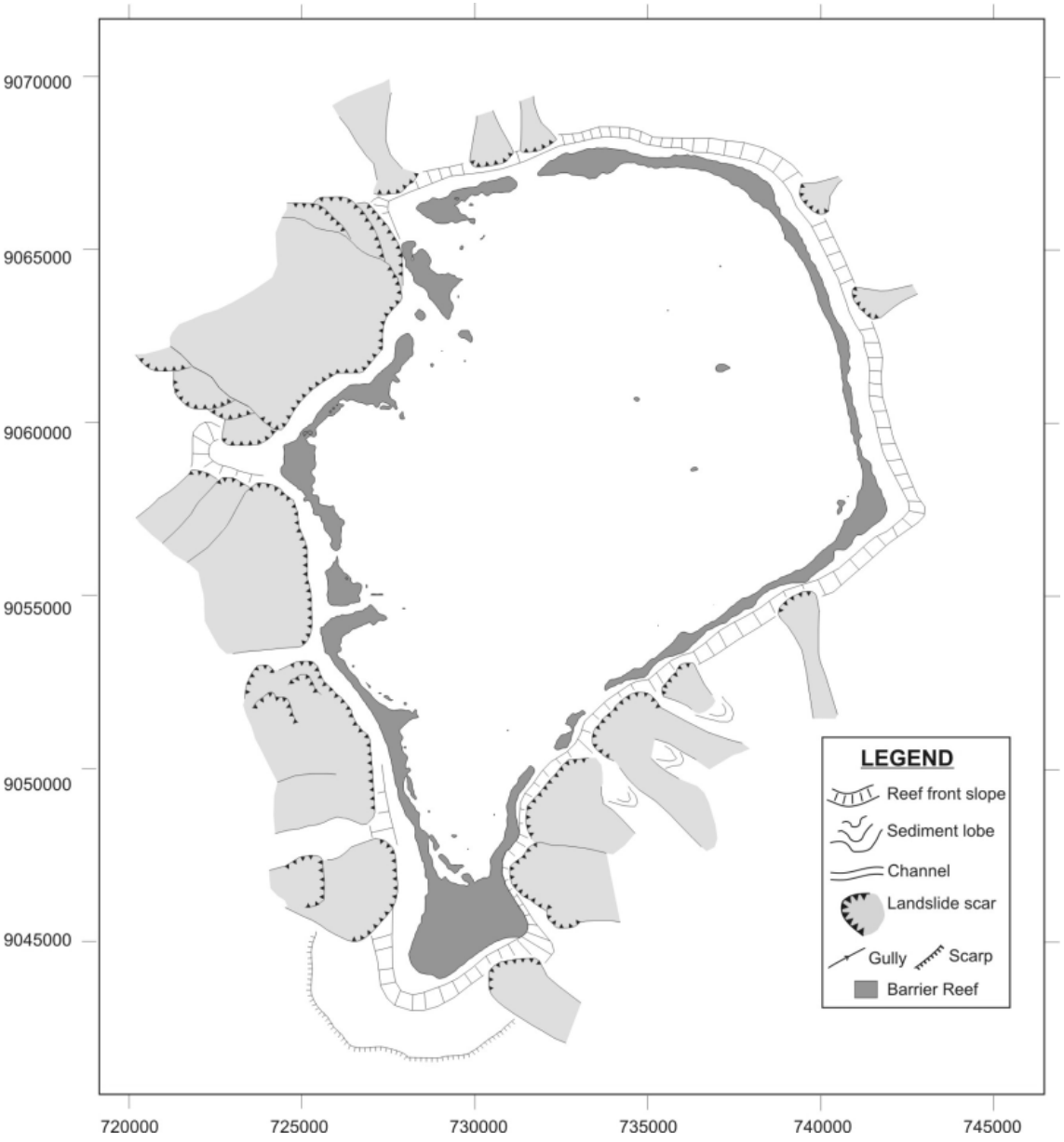

Figure 15. *Interpreted Funafuti seabed morphology. Note the numerous arcuate scarps that have altered the subaerial reef rim geometry, and broad terrace at the southern apex.*

2.2.8 Nukulaelae

Nukulaelae atoll is located at 179°50'E and 9°23'S, with dimensions of 10.8 km along the NW-SE axis and 4.7 km along the narrow SW-NE axis. The atoll is characterised by a central lagoon with some 20 vegetated islands predominantly on the eastern side of the atoll. Nukulaelae lagoon was previously surveyed by Smith et al. (1990). The data from this survey was compiled into a bathymetric map that is shown in Figure 7. The ocean-side surveyed for this report extends approximately 2.5 km offshore from the coastline (see coverage map in Appendix 1). The bathymetry is shown on Chart 8 contoured at intervals of 20 m. The chart also includes smaller-scale insets of 3D images, slope angle and shaded relief maps.

The water depth within the survey area around Nukulaelae ranges from 9.0 to 1878.0 m. The minimum water depths occur in the nearshore area on the outer reef slope, while the seabed deepens to the maximum at an average gradient of 27° near the seaward limits of the survey area. Locally, the seabed is expected to be quite irregular with gradients expected to be highly variable, ranging from 0 to 76°. The predicted bathymetry from Smith and Sandwell (1997) in Figure 2 shows that Nukulaelae stands some 6000 m above the surrounding ocean floor.

The island is encircled by a steep cliff that exceeds slope angles of 60°, located approximately 200–600 m seaward of the reef crest with a water depth to the top of the scarp and scarp height of 100 m and 100–240 m, respectively. Further offshore, the seabed is predominantly featureless, sloping in a seaward direction at the average angle 27°. Exceptions to this are the areas to the southeast and northwest. The southeast flank is dominated by a 5-km long lateral submarine failure originating in water depths ranging from 580 m in the north to 700 m at the southern extent. The scarp terminates at 1000 m below sea level, and scarp height therefore ranges from 420 to 300 m, north to south. This submarine landslide is shown in 3D perspective view in Figure 27, which also shows a bathymetric high thought to comprise the mass flow deposit out at a runout distance of approximately 1.5 km. Alternatively, it represents a remnant block of volcanic origin that has resisted erosion.

The north and northwest flank shows several scarps associated with downslope mass movement. The steepest of these is at the northwest margin of the surveyed area, with a scarp height of 420 m, with upslope and downslope break in slope margins in water depths of 300 and 720 m, respectively.

2.2.9 Niulakita

Niulakita is Tuvalu's southern-most as well as the smallest and most isolated island, located in the southern part of the EEZ of Tuvalu (Figure 2). The low reef island is located at 10°47'S and 179°28'E, with its long axis running E-W, measuring 1.2 km, and a N-S axis of 520 m. The surveyed area extends to a maximum of approximately 10.5 km offshore from the coastline at the southwest margin (see coverage map in Appendix 3). The bathymetry is shown on Chart 9 contoured at intervals of 20 m. The chart also includes smaller-scale insets of 3D images, slope angle and shaded relief maps.

The water depth within the survey area around Nanumea ranges from 7.2 m on the shallow banks surrounding the island, to 2149 m in the northwest offshore margin of the surveyed area. Maximum and minimum observed slopes were 73 and 23°, respectively. Figure 2 and Figure 16 show that Niulakita lies on the southwestern edge of the Kosciusko and Martha Bank (IFREMER 1994, and Kroenke 1995), which has been suggested as a possible reef reserve (Dahl 1980). These banks are not very well delineated on official marine charts, with Kosciusko and Martha Banks marked as obstructions with minimum water depths of 18 m. However the banks are clearly shown on the derived bathymetry shown in Figure 16. The submerged banks belong to the Melanesian Border Plateau, lying on the Pacific crust, north of the Vitias Trench paleo-lineament, which is part of the North Fiji Basin. The Vitias trench

lineament is considered to delineate the former subduction of the Pacific Plate below the Australia Plate (Augustin et al. 1996).

The South Tuvalu Banks area was surveyed in detail at a scale of 1 : 250 000, using multibeam bathymetry, sidescan sonar imagery, high-resolution sub-bottom profiler, six-channel seismic reflection, gravity and magnetic data (IFREMER 1994). The coverage of this survey near Niulakita is shown in Figure 8, and a synthesis of the SOPACMAPS project is provided by Kroenke (1995). The margins of the submerged reef platform (Martha Bank) were partly mapped to a distance of approximately 5 km east of Niulakita. The depth of the margin is presumed to be on average 20–30 m below sea level. More detailed mapping of these banks were limited due to time (reduced coverage of MBES in shallow water), and the shallow nature, and thus hazard to navigation of this feature. An arcuate scarp feature immediately south (1600 m from shoreline) of Niulakita is situated in 100 m of water, with a scarp height of 100 m. The survey data also shows a ridge extending to the southwest of Niulakita shoaling to 500 m, and with numerous erosional scarps on its southern flank.

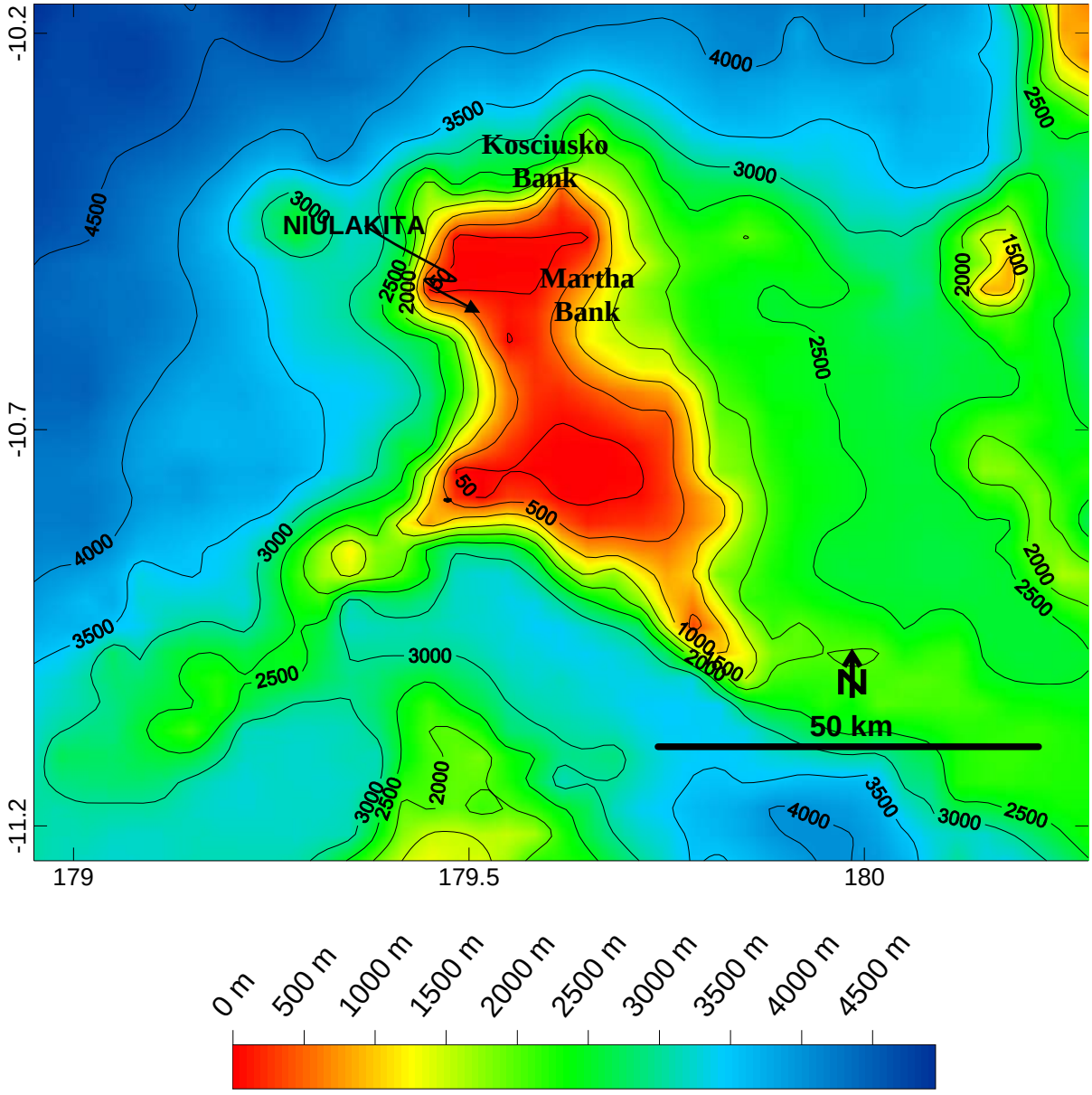

Figure 16. *Niulakita overview map. Bathymetric data are predicted water depths in metres (Smith and Sandwell 1997).*

3. INTERPRETATION

3.1 Shallow (–100 m) Terraces and Submerged Reefs

The nearshore bathymetry of all the atolls and islands in the Tuvalu group exhibit a narrow, near-continuous and shoreline sub-parallel terrace extending about 200–700 m from the base of the modern reef slope (1500 m for Niulakita). The break of slope at the seaward edge of this terrace occurs near the 100 m isobath (ranging from approximately 80 to 100 m). Seaward and downslope of the break in slope are escarpments with high slope gradients (exceeding 60°), with cliff heights ranging from 80 to 200 m.

Terraces or breaks in slope on the flanks of oceanic islands are not necessarily indicators of former sea level stands or purely erosional features. This was investigated through modelling by Paulay and McEdward (1990), who did not find marine erosion to be an important factor in generating forereef terraces. They concluded that reef terraces can readily form at depths and may be vertically stable through many sea level cycles. This is possible because sunlight provides adequate energy for photosynthesis to depths of 40 m (Sheppard 1982), and modern Halimeda has been reported at depths of 120 m (Webster et al. 2006). Only shallow reef crests are more susceptible to sea level fluctuations with a habitat depth of 0–6 m (Montaggioni 2006).

Submersible observations carried out on Johnston atoll by Keating (1987) observed abrupt changes in slope angles with near-vertical walls at approximately 122 m. Wave cut notches were not observed, but a rock recovered from this depth has been reported with an age date of 11,630 (± 280) years comprising coralline algae interpreted as representing reef growth at depths of less than 10 m. Similarly, Anderson (1998) noted the presence of major cliffs encircling Maldivian atolls from single-beam transect profiles, with cliff bases at a modal depth 130 m below sea level, and heights of at least 30 m. Webster et al. (2006) sampled *in situ* growth of coralline and algal origin on a well-developed submerged terrace off the coast of Lanai, Hawaii, at depths of 120–160 m. The data showed that growth occurred between 30 to 14 thousand years (ka), during a time when sea levels were between 120 to 80 m lower than today. However, this represents only a thin (<5 m) veneer of re-occupying growth formed over a pre-existing or antecedent terrace foundation being at least >250 ka (Webster et al. 2006).

The observed terraces and seaward scarps at –100 m are therefore not believed to be the result of slope failures, as there are no downslope erosional mass movement features associated with them (with the exception of Funafuti). As discussed above, we also need to consider that the morphology of the atoll edifice presents an interplay of depositional and erosional processes in a time frame of several glacial/interglacial periods (McLean and Woodroffe 1994), in multiples of 100,000 years (100 ka) (Masselink and Hughes 2003), while considering the estimated subsidence rate for Funafuti of 3 m/100 ka (Ohde et al. 2002). Modern reef systems have benefited from a stable sea level for the last 6000 years, and have prograded seaward by 250 to 1000 m, as well as formed extensive reef flats through backward transport of detritus (Montaggioni 2006). Similarly, during the last glacial maximum (19–30 ka), when the global sea level was approximately 120 m lower than today, the terrace and break in slope found at 100 m water depth would have been part of an actively accreting hermatypic reef system (Figure 17). There were five glacial periods during the last half million years, and the shallow terraces and slopes are therefore interpreted to be drowned growth features that formed when sea level was at a lower level. Rather than being purely erosional features, they are believed to be equilibrium growth features that have been stable through several sea level stillstands.

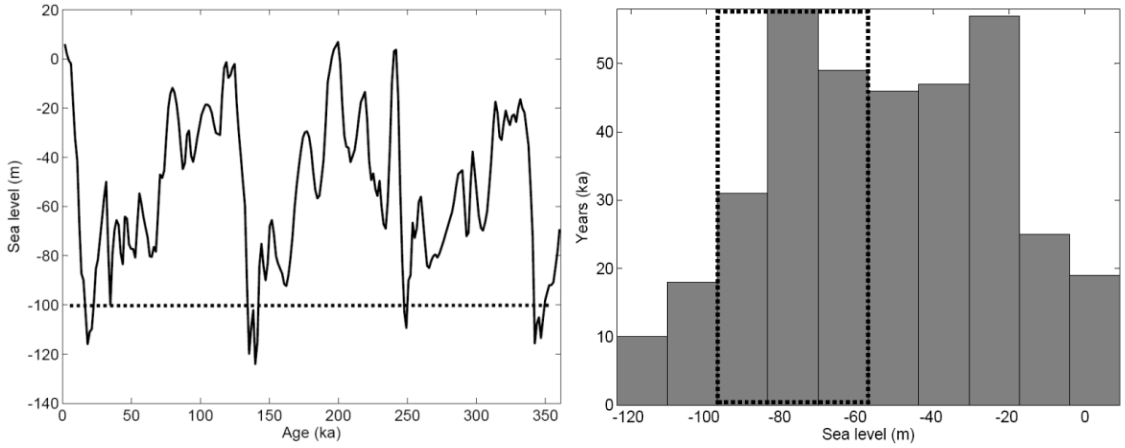

Figure 17. *Left: Sea level curve (360 ka to present, after Lea et al. 2002) and approximate position of the –100 m shallow terrace feature shown as the horizontal dashed line. Right: Histogram of the same sea level data. Assuming that light is the only growth-limiting factor, and considering that coral accretion occurs to water depths of 35 m in an open-sea, mid-Pacific atoll (Montaggioni 2006), the sea level data show that the –100 m terrace was in a growth position for 138 ka, or approximately 40% of the time over the last 360 ka (range of depths and cumulative period contained in dashed box).*

This interpretation is in agreement with the antecedent basement theory (Montaggioni 2006; Grigg et. al. 2002; Harris et al. 2008; Webster et al. 2006), whereby the formation of postglacial submerged reefs at the margins of shelves may have been aided by the existence of favourable topographic features formed by erosional or depositional terraces of earlier stillstands (Beaman et al. 2008). These submerged terraces often provide a rich habitat for modern communities. In the Western Australian Ningaloo Marine Park, prominent ridge systems have been identified on the outer shelf areas at depths of 75–125 m. The exposed limestone substrates were found to be colonised with a high cover of exotic sponges and gorgonian fans, some of which are likely to be new species (www.wamsi.org.au, accessed July 2008). Smith et al. (1990) reported a 2 m tall specimen of black coral at 60 m water depth on a vertical reef slope at Nukufetau, with locals reporting additional large specimens at greater depth. This supports the idea that previous glacial substrate such as paleo escarpments and terraces, presumed to be composed of fossilised limestone, are important marine habitats, as coralgal and sponge communities take advantage of these available substrates.

3.2 Deep (–600 m) Scarps and Submarine Landslides

The occurrence of –600 m escarpments on the flanks of Tuvalu's islands is recognised by high-gradient (>60°) slopes and walls, often associated with mass movement features such as downslope erosional canyons. While the scarps and mass failures are clearly exhibited on the high-resolution depth data, other features that are usually associated with submarine landslides such as landslide deposit near the base of the scar are not identifiable. It is likely that debris mounds were not mapped as the mid-ocean MBES system used in this survey had a depth limit of approximately –2000 m, and was thus unable to detect these deeper features. In other words, the runout distance of failures exceeded the multibeam coverage.

Due to the lack of additional ground-truthing information, we assume a simplified model of edifice and atoll formation based on that for Mururoa atoll (Guille et al. 1996), and outlined in the schematic shown in Figure 18. The Tuvalu volcanic islands probably either developed as part of a hot spot chain, or are the result of an abandoned ridge crest (cited in Locke 1991). Patterns of seamounts that build up above hotspots are typically controlled by major structural discontinuities in the oceanic crust that govern the emission of lavas (Guille et al. 1996), similar to rift-venting. This is best shown by the structural highs associated with the

southwest and southeast corners of Nukufetau and Nanumanga, which are believed to be volcanic ridges that radiate out from the present-day atoll. Therefore, the incipient submarine volcano was formed when magma broke through the fractures in the Cretaceous crust (Winterer 1976) and accumulated on the ocean floor. As the edifice grew, the volcanic lava changed in character from a deep submarine flow to shallower sub-aerial deposits and eventually to aerial explosions of volcanic ash and lava flows over the emerged island (Guille et al. 1996). Volcanic activity ceased after several million years as the crustal plate moved away from the hot spot. Sediments derived from erosional processes may be an important source of material during this post-volcanic period. As the volcanic seamount cooled, it subsided and a fringing coral reef formed. With further subsidence, erosion and sea-level changes over the following millions of years, several hundred metres of carbonates accumulated above the volcanic seamount (Brown 1998). No volcanic basement was reached during the drilling campaign in Funafuti in the late 19th century (Ohde et al. 2002), and the boundary depth was estimated at approximately 1000 m from data provided by seismic experiments (Gaskell and Swallow 1953).

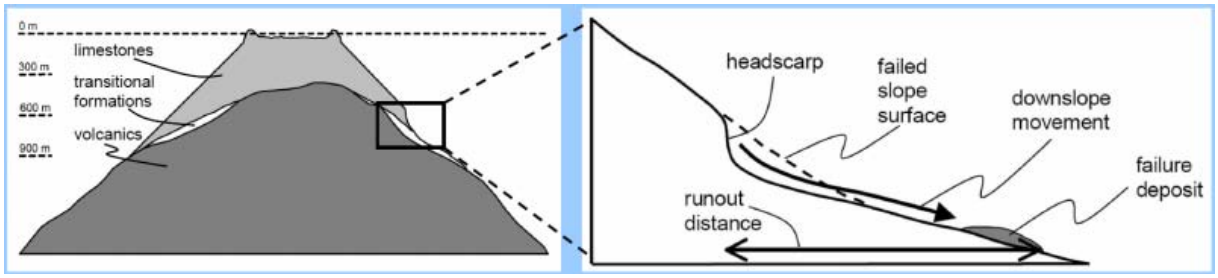

Figure 18. *Schematic atoll geology (left panel), and simplified submarine landslide morphology (right panel).*

While the geometry and size of the mapped mass failures vary, the commonality occurs in that the submarine landslides are often associated with a distinct headscarp (>60º slope angle) situated at an average depth of 600 m. The focus of our simplified model is to draw a relationship between the location of the mapped headscarps and the boundary between the sub-aerial volcanics and carbonate formation, which is presumed to be a structural weakness comprising a layer of aerial volcanic breccias and sediments. Following the model in Figure 18, the majority of the –600 m headscarps occur in a region of structural discontinuity on the edifices. The often large lateral collapses are therefore believed to be associated with areas where the toe of the limestone overlies weak transitional formations.

The processes responsible for triggering failures on the atoll and island flanks of Tuvalu are likely to be those that dominate after volcanic activity has ceased. These are termed exogenic, or extra-edifice processes, which include endo-upwelling, Karst megaporosity, fractures, oversteepening, overloading, sea level change, marine erosion, weathering by cyclones, uplift and subsidence, and earthquakes (Keating and McGuire 2000; Clouard and Bonneville 2003). Brown (1998) describes slope failures on the steep carbonate flanks of Mururoa atoll as a direct result of nuclear testing. These failures reportedly generated a tsunami, submerging the atoll rim to a maximum depth of 2 m for several minutes. Similarly, our model assumes that the observed –600 m lateral scarps in the Tuvalu group are confined to the carbonate and transitional facies, involving the overloading, strain, and subsequent tsunamigenic failure of several hundred metres of carbonates.

Only few atolls have the classic circular shape of an annular ring reef. Most atolls in the group display u-shaped notches which are convex seaward, suggesting the subaerial expression of landslide scars. This exemplifies that the carbonate formations can often fail spectacularly, probably aided by widespread megaporosity. For example, Keating (1987) found cathedral-sized caves at a depth of 400 m below sea level on the flanks of the Johnson atoll, evidence of subaerial karstic dissolution during periods of emergence during the Pleistocene. Particularly on Funafuti it was found that convex seaward notches on the

annular ring reef appear to be subaerial expressions of submarine landslide scars. Figure 19 shows that islets are pinned by terminal points between successive headscarps. Reef passes on Funafuti's southeast coastline therefore occur near the apex of the seaward convex headscarps (also refer to Figure 15).

The above discussion suggests that submarine landslides play an important role in shaping atolls and, in the case of Funafuti, clearly exert control on the position and size of modern channels and islets. By gaining an understanding of how submarine landslides look and where they occur, we can begin to infer what triggered these failures and when, and assess their importance in the construction of the island's present morphology

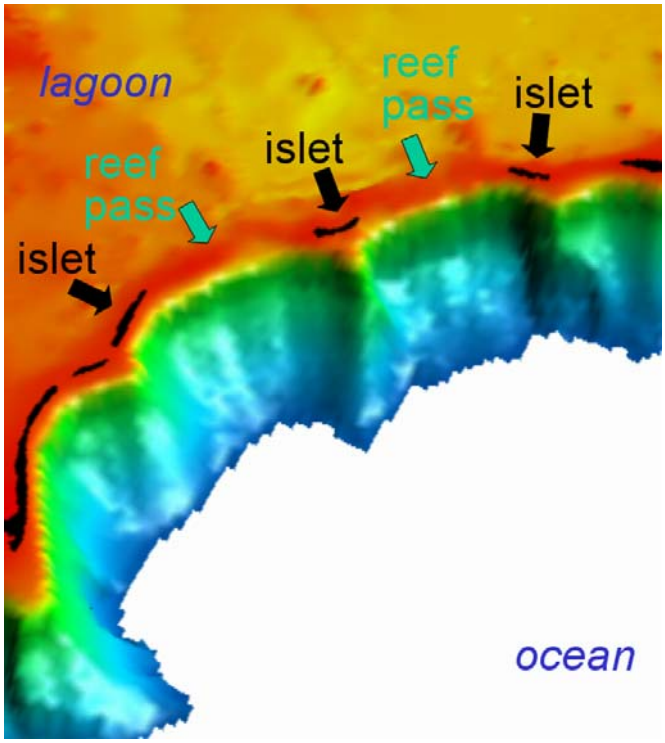

Figure 19. *Three-dimensional perspective view of Funafuti's southeast atoll rim, looking northwest. Colours red to blue indicate shallow to deep, with islets shown as black. The three islets marked by arrows are (left to right) Mateiko, Falefatu, and Funamanu. In this area, the upslope areas of the submarine slope failures correlate with the atoll rim at the surface, and reef passes occur near the apex of the seaward convex headscarps.*

3.3 Conclusion

The preliminary interpretation presented above shows that the island flanks are terraces and steep slopes (~60°) generally occur in two distinct settings. First, in the nearshore region in water depths of approximately 100 m, and 300–700 m seaward from the present day shoreline. In this setting the escarpements are often continuous and encircle the island with a headscarp height of 100 m. Second, further offshore, scarps are discontinuous and sub-parallel and occur in water depths ranging from 400 to 1000 m. Here, headscarps are often arcuate with heights of several hundred metres and have erosional mass movement features associated with them.

The terraces and steep slopes (~60°) near the 100 m isobath that surround the islands are not generally erosional features, but interpreted to mark the low stand of sea level during the last glacial maximums, which have occurred five times in the last 500 000 years (ky). These glacial maximums are associated with a glacio-eustatic drawdown in global sea level by approximately 120 m, which would have exposed the present-day islands of Tuvalu as limestone plateaus with steep cliffs. They may provide rich habitats for modern fisheries and black coral, but this can only be verified by ground truthing. It is recommended that these seabed features are investigated by remote sampling and underwater video.

The mapped slopes that occur in deeper waters are believed to be erosional headscarps associated with submarine landslides. The processes responsible for triggering these failures generally include karst megaporosity, fractures, oversteepening, overloading, and earthquakes. The majority of the headscarps where mapped at –600m, which is believed to

represents a region of structural discontinuity on the edifices. The often large lateral collapses may be associated with areas where the toe of the limestone overlies weak transitional formations, such as sedimentary rocks, deposited after volcanic activity had ceased (Figure 18). Particularly on Funafuti it was found that convex seaward notches on the annular ring reef appear to be subaerial expressions of submarine landslide scars. By gaining an understanding of how submarine landslides look and where they occur, we can begin to infer what triggered these failures and when and how they control the present-day geomorphology of atolls.

4. DATA ACQUISITION AND PROCESSING

4.1 Fieldwork Summary

Survey Particulars	
Survey vessel	MV *Turagalevu*
Fieldwork dates	08 September to 24 October 2004

All dates and times in this report are given in the local Tuvalu time zone (12:00h GMT = 24:00h local). Fieldwork dates and information on the equipment used during the different phases of the survey are listed in the table below.

Location	Survey Dates	Equipment Used
Vaitupu	20-21/09/2004	8160 MBES
Nukufetau	26-29/09/2004, 16/10/2004	8160 MBES
Nukulaelae	01-02/10/2004	8160 MBES
Nanumea	07-09/10/2004	8160 MBES
Nanumanga	10-12/10/2004	8160 MBES
Nuitao	13/10/2004	8160 MBES
Nui	14-15/10/2004	8160 MBES
Nuilakita	19-20/10/2004	8160 MBES
Funafuti	20/09/2004, 22-24/09/2007, 03-04/10/2004, 06/10/2004, 17/010/2004, 21-24/10/2004	8160 MBES, ADP

4.2 Field Personnel

SOPAC	
Jens Krüger	Physical Oceanographer
Quan Chung	Project Technician
Simon Young	Electronics Engineer

Vessel	
Steven Hay	Master
Tomasi Mara	Master / Officer
Joni Tikoikadavu	Engineer
Jobe Hargrove	Crew

Observer	
Savaliga	Lands Department
Manuela	Lands Department

4.3 Geodetic Reference System

The survey results were mapped in terms of the following geodetic reference system:

Geodetic datum	WGS84	
Ellipsoid	WGS84	
	Semi-major axis (a)	6378137.000
	Semi-major axis (b)	6356752.314
	Inverse flattening (1/f)	298.257223563
	Eccentricity sq. (e2)	0.0066943800
Projection	UTM Zone 60S	
	Projection type	Transverse Mercator
	Origin latitude	00° 00' 00.000" North
	Origin longitude	177° 00' 00.000" East
	Origin false easting	500 000.000
	Origin false northing	10 000 000.000
	Scale factor	0.9996000000
	Grid unit	Metres
Geodetic transformation	from WGS84 (GPS satellite datum) to UTM 60S	
	Source coordinate system	WGS84
	Target coordinate system	UTM 60S
	Transformation parameters	
	dX	0.00
	dY	0.00
	dZ	0.00
	rX	0.00000
	rY	0.00000
	rZ	0.00000
	Scale	0.00000

4.4 Vessel Description and Static Offsets

Sensor		X (m)	Y (m)	Z (m)
Reference point at water level		0.00	0.00	0.00
Motion Reference Unit (MRU)		0.00	0.00	–0.28
Positioning Antenna (GPS)		1.55	–3.31	5.52
Multibeam Echo Sounder (MBES)		–3.00	–4.22	–0.36
Tow point		N/A		
Winch				
Vessel				
Name	*Turagalevu*			
Length overall	18 m			
Breadth (mid)	6 m			
Draft (mid)	1.5 m			
Displacement	26 t			
Port of registry	Suva			
Official No.	041			
Radio Sign	3DN6531			
Classification	Westcoaster, Freemantle, Australia			

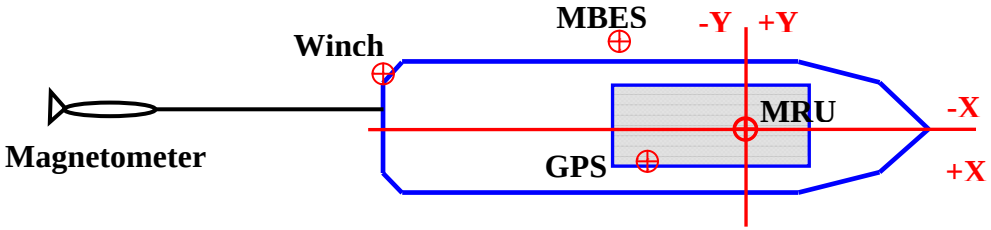

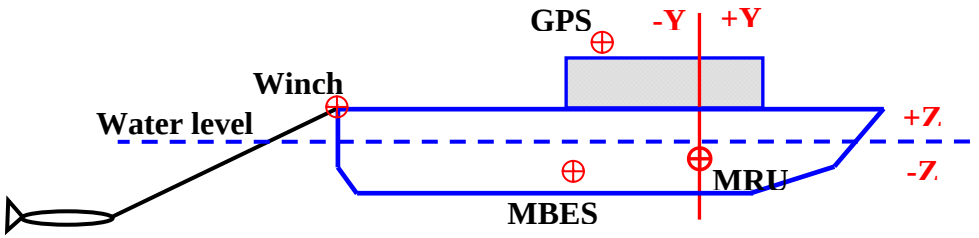

Figure 20. *Photo showing the survey vessel* Turagalevu*. The mounting pole for the 8160 Multibeam echosounder transducer can be seen over the port side.*

4.5 Positioning Control

The vessel's reference point (X=0, Y=0, Z=0) was the motion reference unit (MRU) position at the waterline. Positioning was by stand-alone GPS, using an Ashtech Aquarius receiver. A good constellation status was observed throughout the survey. The patch test was conducted in Fiji using DGPS.

4.6 Survey Computer

The survey computer was a Windows 2000 PC running Hypack 4.3. This computer was used for continuous on-line data logging and computation of positioning and digital bathymetry. The package also provided a line control display for the helm. The on-line operator continuously monitored a range of quality control parameters.

An off-line Hypack 4.3A package was used in the office for replaying and post-processing of track data and bathymetry. An A0 plotter was available for the production of charts.

4.7 Multibeam Echosounder

A Reson SeaBat 8160 multibeam echosounder (MBES) was temporarily installed on MV Turagalevu, and used to provide swathe bathymetry data. A MBES provides high resolution information about the depth of water from the surface to the seafloor in a water body. The main instrumental and operating parameters are listed below.

Instrumentation	
Multibeam echosounder	Reson SeaBat 8160
Transducer mount	Port side pole mounted
Motion reference unit	TSS DMS 2-05 Dynamic Motion Sensor
Gyro	SG Brown Meridian Surveyor Gyro Compass
Sound velocity probe at transducer	N/A. Set to 1545m/s

Operating Parameters	
Transducer frequency	50 kHz
General water depth	10–2500 m
Average ship's speed	6 knots (3 m/s) / 7.5 knots (4 m/s) in lagoon
Transmit power	Variable 1–16
Pulse length	Variable 0.5–8.0 ms
Horizontal coverage	Approx. 0.8–2.0 × water depth
No of beams / beam spacing	126 / 1.5 °
Ping rate	Variable, maximum of 4 Hz

Calibration	08/09/2004	01/11/2004
Roll correction	0.4	–1.2
Pitch correction	–2.0	–4.0
Yaw correction	2.0	–2.0
GPS latency correction	–0.2	–0.6
Gyro correction	Not determined	–1.8 °

The pre-survey patch test on 08 September 2004 was conducted in marginal weather conditions. The patch test was therefore repeated after conclusion of the survey on 01 November 2004. The post-survey patch test results were considered more reliable, and therefore applied during the data post-processing procedure.

The Tuvalu survey was conducted with a Gyro compass latitude setting of 18 °S. To account for the median latitude of 8.5 °S for Tuvalu, a magnetic deviation of –1.8 ° was applied to the survey data in post-processing.

4.8 Multibeam Echosounder Data Processing

On return to the SOPAC office in Suva, Hypack 4.3A software was used for the post-processing of the MBES survey data. Post-processing is a form of data reduction, which involves checking, calibration, cleaning and preparation necessary to convert raw measurements into a form suitable for analysis, application and presentation. The product of post-processing is in the form of ASCII listings of gridded easting, northing, and depth (XYZ) points. Gridded XYZ points from Hypack were used in Surfer 8.03 to produce final charts and figures. The processing and chart production sequences are listed below.

Post-processing Sequence	
Phase 1	Correct for heading, heave, roll, pitch, navigation errors. Apply tidal and sound velocity corrections.
Phase 2	Filter to remove poor-quality beams and spikes. Manual editing to remove outliers from individual survey lines.
Phase 3	Apply 4th standard deviation filter to remove outliers from median depth from overlapping coverage. Final manual editing to remove outliers.

Post-processing Sequence	
output	ASCII XYZ files (easting, northing, depth) are in the project coordinate system. The final output typically consist of a file that includes all post-processed sounding points, as well as files of reduced points at grid dimensions of 20, 50, and 100 m.

Chart Production Sequence	
XYZ to grid	XYZ data are reduced and gridded to 1 mm (0.1%) at the charting scale (e.g. 50 m grid size for a chart scale of 1 : 50 000).
Digital terrain model (DTM)	A surface model is created from the grid. A search radius of up to three times the grid spacing is used to fill data gaps.
Chart output	Various levels of smoothing are applied to the DTM and contours, which was felt to give a realistic impression of the seabed, without removing any real features from the data set.

4.9 Tidal Information

Observed soundings for Funafuti were reduced to chart datum (CD), using measured tidal elevations from the Fongafale tide gauge. CD was defined as 0.7859 m below LAT, 1.985 m below mean sea level (MSL 1993-1994), and 4.0123 m below the fixed height of Benchmark 22 (Figure 21).

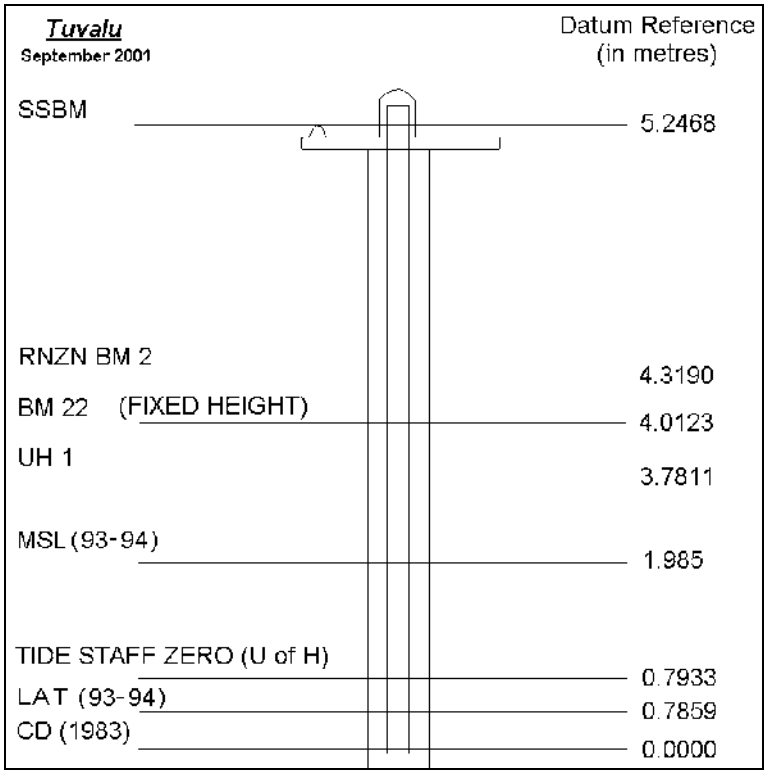

Figure 21. *SEAFRAME tide gauge datum definition and other geodetic levels at Funafuti (from NTFA 2002).*

Observed soundings for all other locations were reduced to CD using predicted tides from the tidal prediction program TideTrak 1.0 in the following relationship:

Tidal elevations = TideTrak predictions + 1.985 m

Locations for which tides were extract from TideTrak are listed in the table below.

Location	Latitude	Longitude
Vaitupu	–7.47	178.76
Nukufatau	–8.07	178.36
Nukulaelae	–9.45	179.85
Nanumea	–5.67	176.15
Nanumanga	–6.33	176.30
Nuitao	–6.12	177.31
Nui	–7.19	177.10
Nukufatau	–8.13	178.39
Nuilakita	–10.78	179.45

4.10 Sound Velocity Profiling

The accuracy of the depth soundings depends in part on the variation of the speed of sound with water depth. This is because the path of a ping of sound energy emitted from the echosounder into the water is usually not straight. Speed of sound profiles are required to correct for the refraction path travel times to find the correct depth and location of soundings. The speed of sound in seawater varies with temperature, salinity and depth, and was determined by measuring the conductivity, temperature and depth (CTD) through the water column. The main instrumental, operational, processing parameters are listed below.

CTD Instrumentation	
Make	SeaBird Electronics
Model	SeaCat 19+ (self-powered, self-contained)
Serial number	2795
Depth rating	600 m

Operating Parameters	
Sample rate	1 scan every 0.5 s
Maximum depth	Limited to 400 m due to wire rope length
Data recorded	Profiles of conductivity, temperature, and pressure

Data Processing	
Positioning	The profile position was taken at the GPS antenna near the start of the downcast. No allowance was made for instrument or vessel drift over the duration of the profile, which may be significant (>500 m).
Data conversion	Convert raw data (.hex) to a .cnv file. The following values are output from the recorded data: Pressure, dbar Depth, m (derived using salt water at local latitude) Temperature, deg C (ITS-90) Salinity, psu (derived) Density, kg m^{-3} (derived) Sound velocity, m/s (derived using Chen and Millero 1977)
Bin average	Average data into 1 m depth bins. No filtering was applied.
Output	Processed data is saved in ASCII text format with the file name date_location_bin.cnv.

CTD profiles are listed below.

Profile location	Date	Time	Easting	Northing	Depth (m)
Vaitupu	21/09/2004	13:01	693918	9174056	282
Funafuti	24/09/2004	09:00	725600	9063213	257
Nukufatau	27/09/2004	10:10	649938	9107649	220
Nukulaelae	02/10/2004	16:48	812537	8954321	270
Funafuti Lagoon	04/10/2004	13:02	735869	9063468	
Nanumea	09/10/2004	14:09	405431	9372950	328
Nanumanga	11/10/2004	17:10	423019	9300751	380
Nuitao	13/10/2004	12:55	534714	9323148	384
Nui	15/10/2004	13:58	511358	9205036	396
Nukufatau	16/10/2004	08:28	653326	9101612	392
Nuilakita	20/10/2004	15:46	768464	8807661	377
Funafuti	21/10/2004	14:04	405808	9372942	390
Funafuti Lagoon	22/10/2004	09:07	733911	9052722	27
Funafuti Lagoon	24/10/2004	09:32	735716	9057846	42

Figure 22 and Figure 23 show the locations of the open-water and lagoon CTD profiles, respectively. Summaries of the CTD profile data in graphical form are shown in Appendix 3.

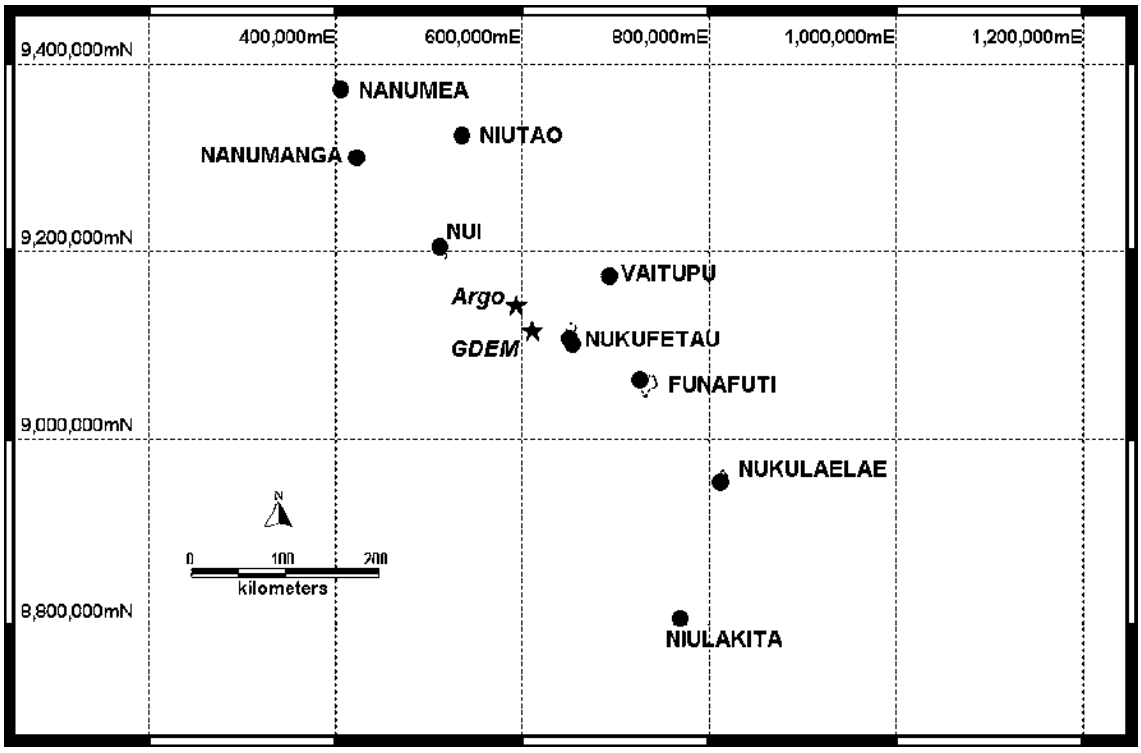

Figure 22. *Map showing the location of CTD casts (dots), and Argo and GDEM locations (stars).*

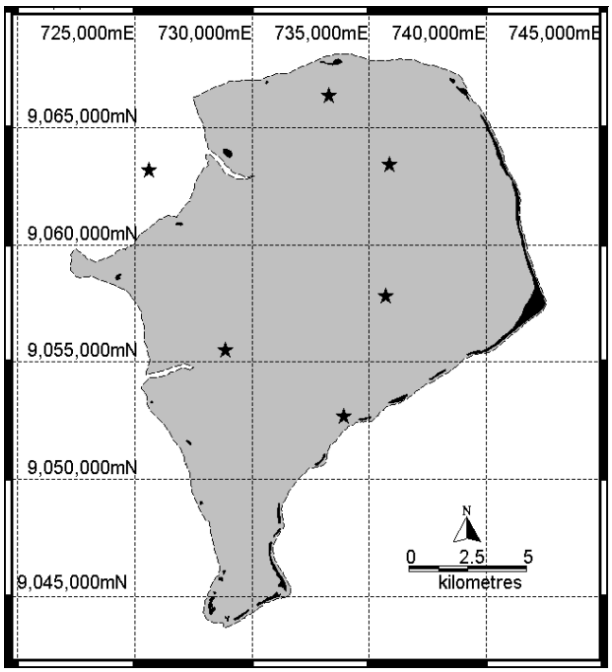

Figure 23. *Map showing the location of CTD profiles (stars) in the vicinity of Funafuti lagoon.*

The on-board CTD probe could only be operated to a maximum depth of 400 m, due to restrictions on the wire rope length. This provided data on the upper water column where the vertical temperature gradient is largest, generally consisting of a top mixed layer with warm temperatures separated from the colder waters of the deep oceans by the thermocline (Figure 24C).

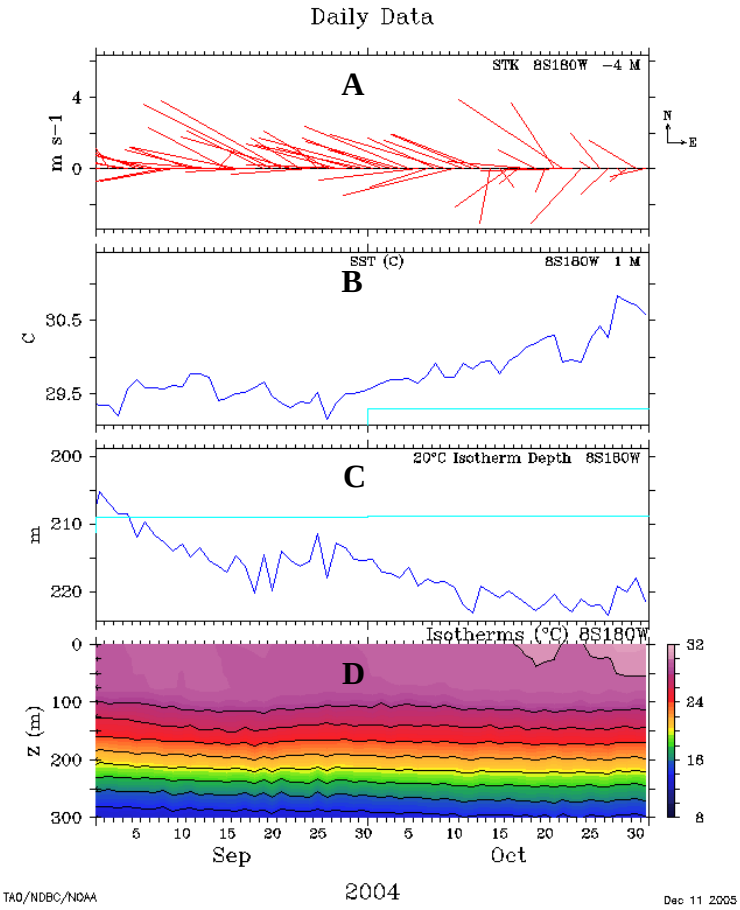

Figure 24. *Time series plot of daily averages from the TAO/TRITON buoy located at 8°S, 180°W (approximately 110 km northeast of Funafuti) for the months of September and October 2004.*
(A) Shows vectors of the direction the wind is blowing towards: the length of the vector indicates the wind speed.
(B) Shows sea surface temperatures.
(C) Shows the depth to the 20°C isotherm, used as a proxy for the depth to the thermocline.
(D) Shows constant temperature isotherms on a time-depth plot.

In order to ensure corrections to a maximum operating depth of 3000 m, the ship-based profile data were complemented with data from an ARGO float and the GDEM model. Figure 22 shows the locations of these external sources, and parameters are given below.

Argo float	
Profile ID	R5900083_118
Date	13.10.2004
Latitude	7.755 ºS
Longitude	177.84 º0E
Easting	592625 E
Northing	9142696 N
Available data	Pressure, salinity, temperature
Bin size	From 6 to 60 m, increasing with depth
Maximum Depth	1092 m

Generalised Digital Environmental Model Data (GDEM)	
Data file version	2.6, URL accessed on 3/11/2004
Date	Monthly average for October
Latitude	8.0 ºS
Longitude	178.0 ºE
Easting	610205 E
Northing	9115568 N
Available data	Depth, temperature, salinity, sound velocity
Bin size	From 10 to 100 m, increasing with depth
Maximum Depth	4968 m

The Argo temperature-salinity profiles were used to calculate the speed of sound utilising the Chen-Millero equation. This is the same method used by the SeaBird CTD software. The Argo data were collected and made freely available by the International Argo Project and the national programmes that contribute to it (www.argo.ucsd.edu, argo.jcommops.org). Argo is a pilot programme of the Pacific Islands Global Ocean Observing System (PI-GOOS). The GDEM model provided a monthly mean of sound velocity based on a 2.5 º grid.

The final sound velocity profiles used to correct MBES data were therefore a construction from three sources according to depth, as shown in the table below, and illustrated in Figure 25.

Sound Velocity Data Source	Water Depth
CTD casts	1 m to a maximum of 396 m
Argo floats	400 to 1092 m
GDEM model	1100 to 30000 m

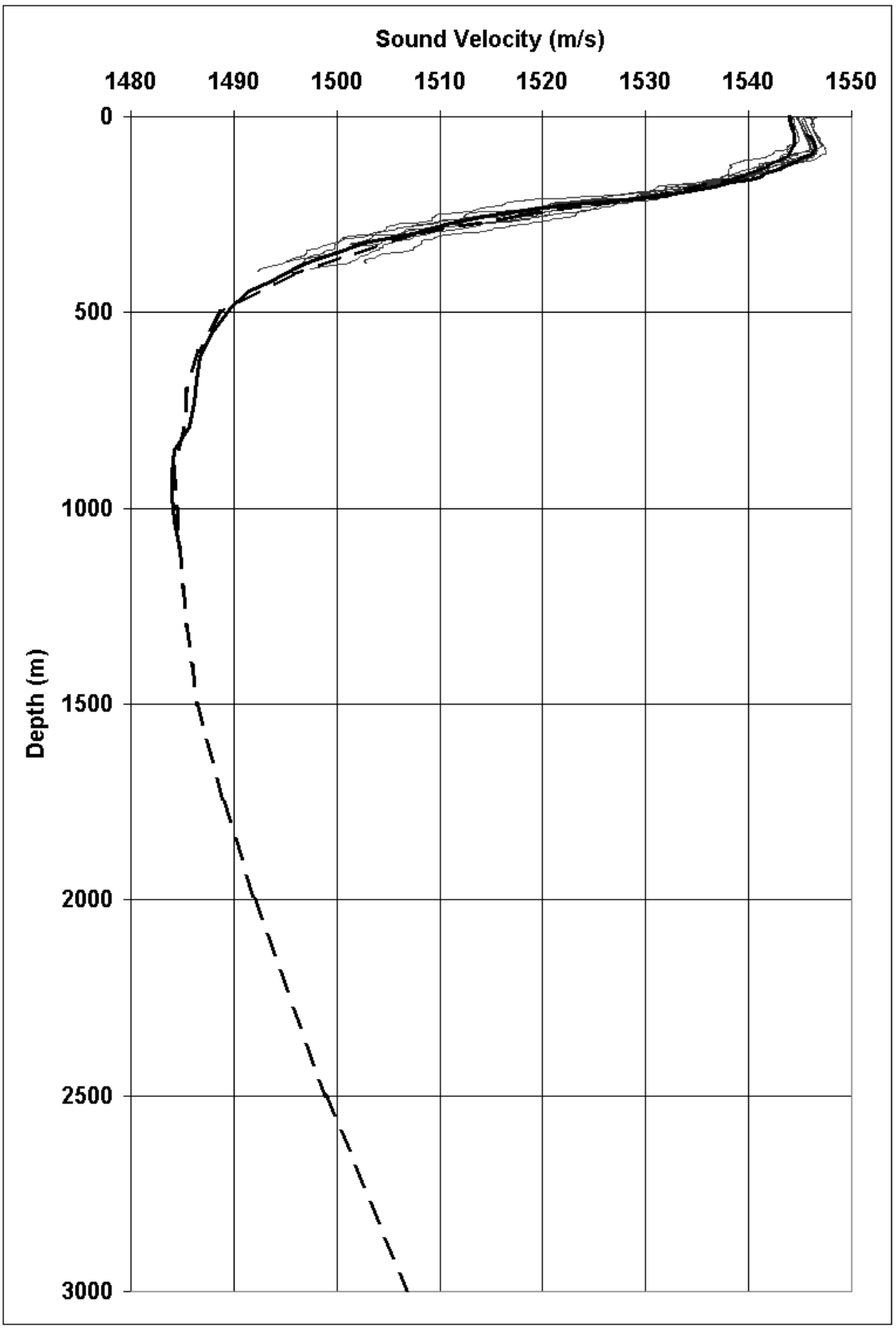

Figure 25. *Plot showing the sound velocity profiles used for MBES data correction (see Figure 22 for location). The fine lines in the upper water column are the data derived from the CTD casts. The solid black line extending to 1092 m is derived Argo data, and the dashed black line to a depth of 3000 m is the GDEM data.*

4.11 Seabed Interpretation

Bathymetric data provide information on the morphology and depth of the seafloor as well as the shape and size of submarine features. No additional information such as backscatter, seismic profiles, or ground-truth data (e.g. near-bottom visual observations or direct sampling) was available. However, three bathymetry derivatives, namely, slope angle maps, shaded relief maps, and three-dimensional rendered surfaces, were used in addition to the high-resolution bathymetry in the interpretation of the seabed morphology. These maps are included as small-scale insets on the bathymetric charts (Appendix 1 and 4).

Bathymetric Derivatives	
Slope angle	Slope is a measure of steepness between locations on the seabed, and are reported in degrees from zero (horizontal). Slope values are computed as a mean value for one grid cell from the slope gradient between it and the eight neighbouring grid cells.
Shaded relief	Shaded relief maps use shades of grey to indicate the local orientation of the seafloor relative to a user-defined light source direction. The light source can be thought of as the sun shining on a topographic surface, much like artificial hillshading that illuminates bathymetric roughness. Portions of the surface that face away from the light source reflects less light toward the viewer, and thus appear darker.
Three-dimensional surface	For three-dimensional surfaces the height of the surface corresponds to the depth of the seafloor.

All slope angles exceeding 60° (degrees from horizontal) were interpreted as scarps. Any inclined area of the seafloor that was laterally confined by distinctive slopes, with or without a distinctive upslope headscarp, was interpreted as a channel. Bathymetric highs that may have been failure deposits were not mapped in the absence of information on the seabed texture (backscatter data) as discussed above. Therefore, no attempt was made to determine whether a mass movement process originated from a slump, slide, debris flow, etc. The interpretation of the seafloor in this report is thus based on the acquired bathymetric data, and is limited to mesoscale (km scale) erosive features such as scarps and channels.

The broad terminology used to describe submarine landslides is summarised in the table below, and illustrated in Figure 26 and Figure 27. The interpretations presented in this report may be refined as additional data become available in the future.

Seabed Morphology	
Landslide, or slope failure	Landslides are common on inclined areas of the seafloor, and refer to an area of disturbed seafloor caused by the downslope movement of a failed mass
Headscarp	Distinctive break in slope, steep upslope regions usually associated with submarine landslides
Channel	Low-relief gully with sidewalls perpendicular to slope. Channels transport sediment into deeper waters.

Seabed Morphology	
Runout	Runout distance is the limit of the disturbed seafloor downslope of the failure's scarp. In cohesive failures this corresponds to the distance of the furthest piece of blocky debris from the upslope scarp. This cannot be easily determined with disintegrative failures
Deposit	The deposit of the failed seabed mass, transported downslope from the scarp source area by the runout distance

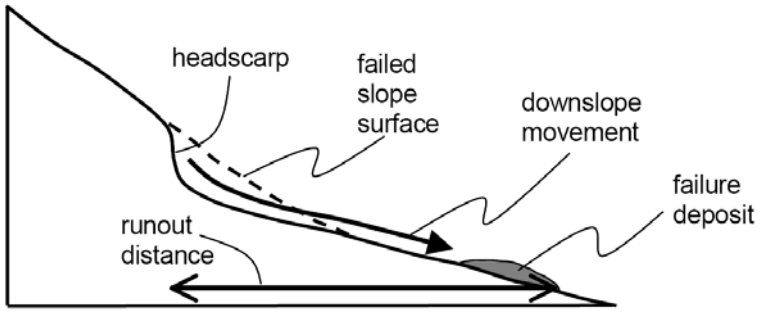

Figure 26. *Illustration of the submarine scarp geometry. The headscarp resulting from the submarine landslide is steeper than the slope on which the failure occurred.*

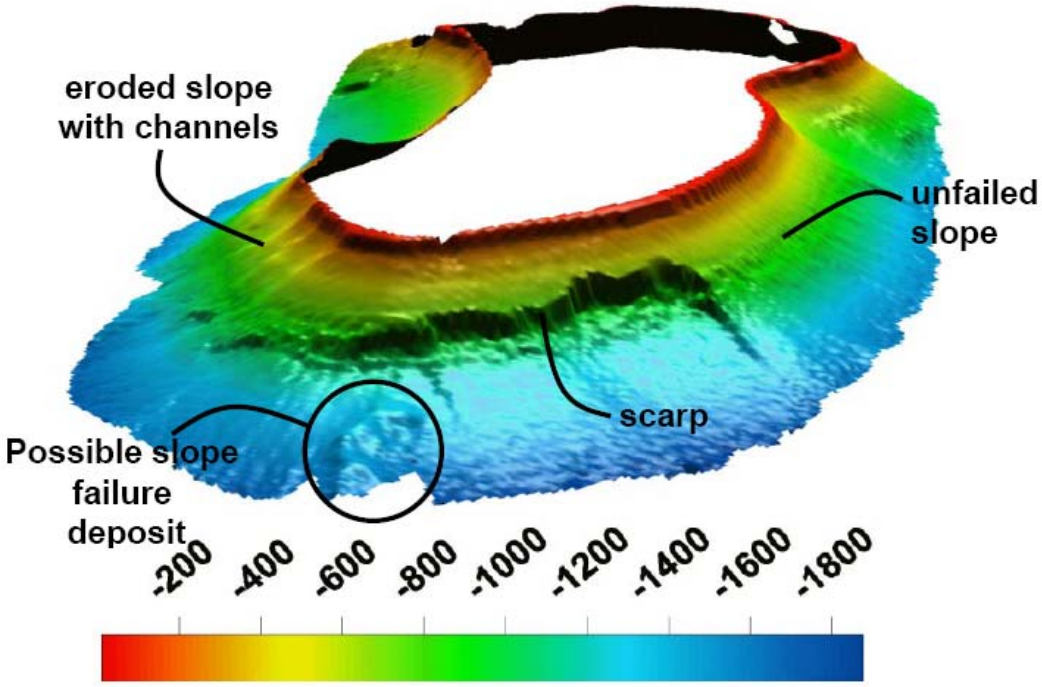

Figure 27. *Three-dimensional perspective image of the Nukulaelae edifice. View is looking northwest with no vertical exaggeration. Scale varies with distance in the perspective. The dominant feature of the headscarp extends over a distance of approximately 5 km, with a maximum scarp height of 420 m. A possible failure deposit is evident as a mound near the base of the scarp. However, there is a general lack of bathymetric evidence of failed material within the survey area, indicating that runout distances are large, and are presumed to fall outside of the coverage area. The area interpreted as an eroded slope with channels, refers to a region where material has presumably been transported downslope, resulting in gullies with low relief sidewalls.*

5. REFERENCES

Anderson, R.C. 1998. Submarine topography of Maldivian atolls suggests a sea level of 130 metres below present at the last glacial maximum. *Coral Reefs 17:* 339–341.

ARGO: Array for real-time geostrophic oceanography. http://www.argo.ucsd.edu/

Augustin, J.M., Le Suave, R., Lurton, X., Voisset, M., Dugelay, V. and Satra, C. 1996. Contribution of the multibeam acoustic imagery to the exploration of the sea-bottom. *Marine Geophysical Researches 18*: 459–486.

Beaman, R.J., Webster, J.M. and Wust, R.A.J. 2008. New evidence for drowned shelf edge reefs in the Great Barrier Reef, Australia. *Marine Geology 247*: 17–34.

Brown, E.T. 1998. The consequences of underground nuclear testing in French Polynesia. *ATSE Focus – Supplement No 104*. http://www.atse.org.au.

Chen, C.T. and Millero, F.J. 1977. Speed of sound in seawater at high pressure. *Journal of the Acoustic Society of America 32(10)*: 1357 p.

Church, J.A., White, N. and Hunter, J.R. 2006. Sea-level rise at tropical Pacific and Indian Ocean islands. *Global and Planetary Change 53*: 155–168.

Clouard, V. and Bonneville, A. 2003. Submarine landslides in Society and Austral Islands, French Polynesia: evolution with the age of edifices. In: Locat, J. and Mienert, J. (eds): Submarine Mass Movements and their Consequences, pp. 335–341, Kluwer Academic Publishers, 2003.

Collen, J.D and Garton, D.W. 2004. Larger foraminifera and sedimentation around Fongafale Island, Funafuti Atoll, Tuvalu. *Coral Reefs 23*: 445–454.

Connell, J. 2003. Losing ground? Tuvalu, the greenhouse effect and the garbage can. *Asia Pacific Viewpoint 44(2)*: 89–107.

Creak, E.W. 1904. Report on the results of the magnetic survey of Funafuti Atoll by officers of HMS Penguin, 1896. In: Bonney (ed.), The atoll of Funafuti. Borings into a coral reef and the results, Report, Coral Reef Boring Committee, Royal Society of London. Harrison and Sons, Section III, pp. 33–39.

Cronan, D.S. and Hodkinson, R.A 1990. Manganese nodules and cobalt-rich crusts in the EEZ's of the Cook Islands, Tuvalu and Kiribati. Part IV: Nodules and crusts in the Ellice Islands region, Tuvalu. *SOPAC Technical Report 102*, 59 p.

Dahl, A.L. 1980. Regional ecosystems survey of the South pacific Areas. *SPC/IUCN Technical Paper 179*. South Pacific Commission, Noumea, New Caledonia.

Darwin, C. 1842. *The structure and distribution of coral reefs.* London, Elder and Co.

David, T.W.E. and Sweet, G. 1904. The geology of Funafuti. In: Bonney (ed) The atoll of Funafuti. Borings into a coral reef and the results, Report, Coral Reef Boring Committee, Royal Society of London. Harrison and Sons, Section V, pp. 61–124.

Dickinson, W.R. 1999. Holocene sea-level record on Funafuti and potential impact of global warming on central Pacific atolls. *Quaternary Research 51* 124–132.

Dickinson, W.R. 2004. Impacts of eustasy and hydro-isostasy on the evolution and landforms of Pacific atolls. *Palaeogeography, Palaeoclimatology, Palaeoecology, 213*: 251–269.

Duncan, R.A., 1985. Radiometric ages from volcanic rocks along the New Hebrides–Samoa lineament. In: Brocher, T.M. (ed.), Investigations of the northern Melanesian borderland: *Circum-Pacific Council for Energy and Mineral Resources Earth Science Series 3*: 67–76.

Gaskell, T.F. and Swallow, M.A. 1953. Seismic experiments on two Pacific atolls. *Occasional papers of the Challenger Society No.3*, 14p.

GIBB 1985. Tuvalu lagoon bed resource survey. Australian Development Assistance Survey by GIBB Australia, Consulting Engineers. Volume 2 of 2.

Global Topography. GTOPO. http://topex.ucsd.edu/marine_topo/mar_topo.html. Global topography data is available from: http://topex.ucsd.edu/cgi-bin/get_data.cgi.

https://128.160.23.42/gdemv/gdemv.html

Grigg, R.W., Grossmann, E.F., Earle, S.A., Gittings, S.R., Lott, D. and McDonough, J. 2002. Drowned reefs and antecent karst topography, Au'au Channel, S.E. Hawaiian islands. *Coral Reefs 21*: 73– 82.

Guille, G., Goutiere, G., Sornein, J.F., Buigues, D., Gachon, A.M. and Guy, C. 1996. The atolls of Mururoa and Fangataufa, I., Geology – Petrology – Hydrogeology. Musée océanographique, Monaco, 175 p.

Harris, P.T., Heap, A.D., Marshall, J.F., McCulloch, M. 2008. A new coral reef province in the Gulf of Carpentaria, Australia: Colonisation, growth and submergence during the early Holocene. *Marine Geology 251*: 85–97.

IFREMER 1994. SOPACMAPS Project. Final Report – South Tuvalu Banks Area. *SOPAC Technical Report 199*.

Kaly, U.L. and Jones, G.P. 1994. Long-term effects of blasted boat passages on intertidal organisms in Tuvalu: a mesoscale human disturbance. *Bulletin of Marine Science, 54*: 164–179.

Kaly, U.L. and Jones, G.P. 1994. Pilot dredging project Funafuti, Tuvalu: Assessment of ecological impacts on lagoon communities: Final report. Commissioned by SPREP, Western Samoa, 200 p.

Keating, B.H. 1987. Structural failure and drowning of Johnston atoll, central Pacific basin. In: Keating, B.H., Fryer, P., Batiza, R., Boehlert, G.W. (eds.), Seamounts, Islands and Atolls. *Geophysical Monograph 43*, American Geophysical Union, pp.49–59.

Keating, B.H. and McGuire, W. 2000. Island edifice collapse and associated tsunami hazards. *Pure and Applied Geophysics 157*: 899–956.

Kroenke, L.W. 1995. A morphotectonic interpretation of SOPACMAPS 1 : 500 000 charts, central Solomon Islands – southern Tuvalu. *SOPAC Technical Report 220*.

Lea, D.W., Martin, P.A., Pak, D.K. and Spero, H.J. 2002. Reconstructing a 350 ky history of sea level using planktonic Mg/Ca and oxygen isotope records from a Cocos Ridge core. *Quaternary Science Review 21*: 283–293.

Lewis, J. 1989. Sea level rise: some implications for Tuvalu. *The Environmentalist 9(4)*: 269–275.

Locke, C.A. 1991. Geophysical constraints on the structure of Funafuti. *The South Pacific journal of natural science 11:* 129–140.

Masselink, G. and Hughes, M.G. 2003. Introduction to coastal processes and geomorphology. Arnold, London, 354 p.

McLean, R.F. and Hoskins, P.L. 1991. Geomorphology of reef islands and atoll Motu in Tuvalu. *The South Pacific Journal of Natural Science, (11)*: 167–189.

McLean, R.F., Hoskins, P.L. 1992. Tuvalu Land Resources Survey: Funafuti, Tuvalu Land Resources Survey Island Report No7, Food and Agriculture Organisation, Rome.

McLean, R.F. and Woodroffe, C.D. 1994. Coral atolls. In: Carver, R.W.G., Woodroffe, C.D. (Eds.), Coastal Evolution: Late Quaternary Shoreline Morphodynamics. Cambridge University Press, Cambridge, pp. 267–302.Montaggioni, L.F. 2006. History of Indo-Pacific coral reef systems since the last glaciations: development patterns and controlling factors. *Earth-Science Reviews 71*: 1–75.

NTFA 2002. Pacific Country Report, Sea Level & Climate: Their Present State, Tuvalu. 22 p. National Tidal Facility Australia.

Ohde S., Greaves M., Masuzawa T., Buckley H.A., Van Woesik, R., Wilson P.A., Pirazzoli, P., and Elderfield, H. 2002. The chronology of Funafuti Atoll: revisiting an old friend. *Proceedings of the Royal Society of London 458*: 2289–2306.

Patel, S.S. 2006. A sinking feeling. *Nature 440:* 734–736.

Paulay, G.P., McEdwards, L.R. 1990. A simulation model of island reef morphology: the effects of sea level fluctuations, growth, subsidence and erosion. *Coral Reefs 9:* 51–62.

Pearce, H. 2008. Inventory of geospatial data and options for tsunami inundation and risk modelling: Tuvalu. SOPAC/GA tsunami hazard and risk assessment project report 06. SOPAC MR 656. p. 58.

Pelletier, B., and Auzende, J.M. 1996. Geometry and structure of the Vitiaz Trench Lineament (SW Pacific). *Marine Geophysical Researches 18*: 305–335.

Radke, B.M. 1986. Bathymetric and seismic features of Nukufetau lagoon, Tuvalu: an appraisal of submarine phosphate potential. *SOPAC Technical Report 57:* 29 p.

Ramsay, D.L., Kaly, U.K. 2004. Tuvalu reef channel review. New Zealand Agency for International Development, National Institute of Water & Atmospheric Research, NIWA, project TUV04201. HAM2003-137, 207 p.

Reson, 2002. SeaBat 8160 Multibeam Echo Sounder System operator's manual, v3.00.

Rogers, K.A. 1992. Occurrence of phosphate rock and associated soils in Tuvalu, Central Pacific. *Atoll Research Bulletin 360*: 1–31.

Scott, G.A.J. and Rotondo, G.M. 1983. A model for the development of types of atolls and volcanic islands on the Pacific lithospheric plate. *Atoll Research Bulletin 260*: 33 p.

Sheppard, C.R.C. 1982. Coral populations on reef slopes and their major controls. *Marine Ecology Progress Series 7*: 83–115.

Smith, R. 1992a. Bathymetric map of Tuvalu – Nukulaelae lagoon. 1 : 12500. *SOPAC Bathymetric Series Map 3*.

Smith, R. 1992b. Bathymetric map of Tuvalu – Nukufetau lagoon. 1 : 25000. *SOPAC Bathymetric Series Map 4*.

Smith, R. 1995. Bathymetric and physical monitoring of the pilot project dredging site in Funafuti Atoll, Tuvalu. *SOPAC Technical Report 216*, 24 p.

Smith, R. and Woodward, P. 1992. Bathymetric map of Tuvalu – Funafuti lagoon. 1 : 40000. *SOPAC Bathymetric Series Map 2*.

Smith, R.B., Rearic, D.M., Saphore, E. and Seneka, F. 1990. Survey of Nukulaelae and Nukufetau lagoons, Tuvalu. *SOPAC Technical Report 105*, 59 p.

Smith, R.B., Saphore, E. and Seneka, F. 1991. Geophysical survey of lagoon sediments, Funafuti Atoll, Tuvalu. SOPAC Preliminary Report 33, 15 p.

Smith, W.H.F. and Sandwell, D.T. 1997. Global seafloor topography from satellite altimetry and ship depth soundings, *Science 277*: 1957–1962.

SOPAC 2000. Tuvalu. *SOPAC Country Profile 13*, 13 p.

TAO Tropical Atmosphere Ocean Array. http://tao.noaa.gov/

Webb, A. 2005, Coastal change analysis using multi-temporal image comparisons – Funafuti atoll, Tuvalu. *EU-SOPAC Project Report 54*, 19 p.

Webster, J.M., Clague, D. A., Braga, J.C., Spalding, H., Renema, W., Kelley, C., Applegate, B., Smith, J.R., Paull, C.K., Moore, J.G. and Potts, J.G. 2006. Drowned coralline algal dominated deposits off Lanai, Hawaii; carbonate accretion and vertical tectonics over the last 30 ka. *Marine Geology 225*: 223–246.

Winterer, E.L. 1976. Bathymetry and regional tectonic setting of the Line Islands chain. In Schlanger, S.O., Jackson, E.D., et al., Initial Reports., DSDP, 33: Washington (U.S. Govt. Printing Office), pp. 731–748.

Xue, C. 1996a, Coastal Geology of Tuvalu – Southwest Nukufetau. 1 : 50000 *SOPAC Coastal Series Map 8*.

Xue, C. 1996b. Coastal Geology of Tuvalu – Vaitupu. 1 : 10000 *SOPAC Coastal Series Map 9*.

Xue, C. 1996c. Coastal erosion and management of Amatuku island, Funafuti atoll, Tuvalu. *SOPAC Technical Report 234*, 33 p.

Xue, C. and Malologa, F. 1995. Coastal sedimentation and costal management of Fongafale, Funafuti atoll, Tuvalu. *SOPAC Technical Report 221*, 53 p.

Yamano, H., Kayanne, H., Yamaguchi, T., Kuwahara, Y., Yokoki, H., Shimazaki, H. and Chikamori, M. 2007. Atoll island vulnerability to flooding and inundation revealed by historical reconstruction: Fongafale Islet, Funafuti Atoll, Tuvalu. *Global and Planetary Change 57*: 407–416.

APPENDICES

Appendix 1 – Multibeam Echosounder Coverage

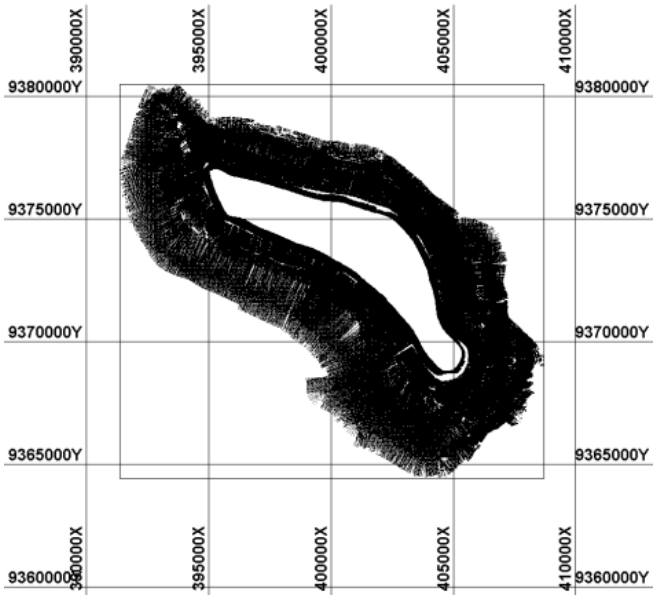

Nanumea

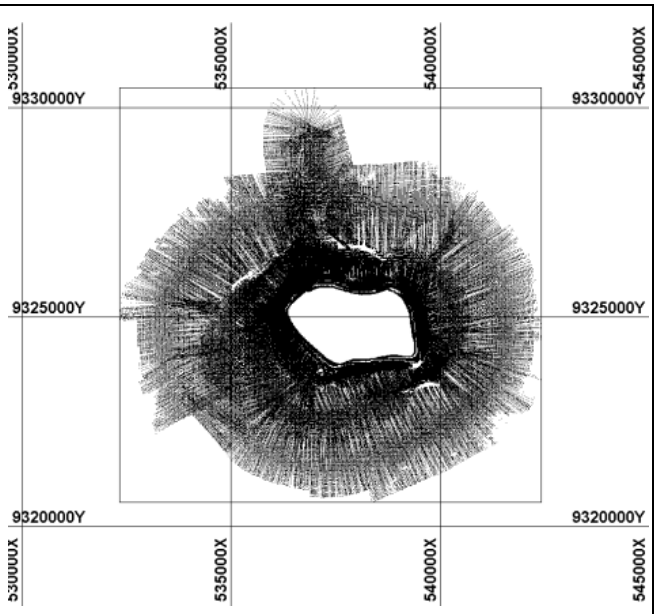

Niutao

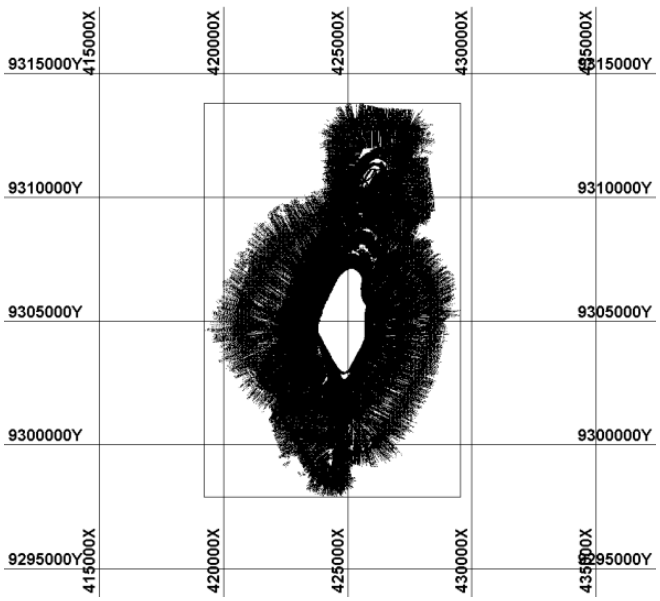

Nanumanga

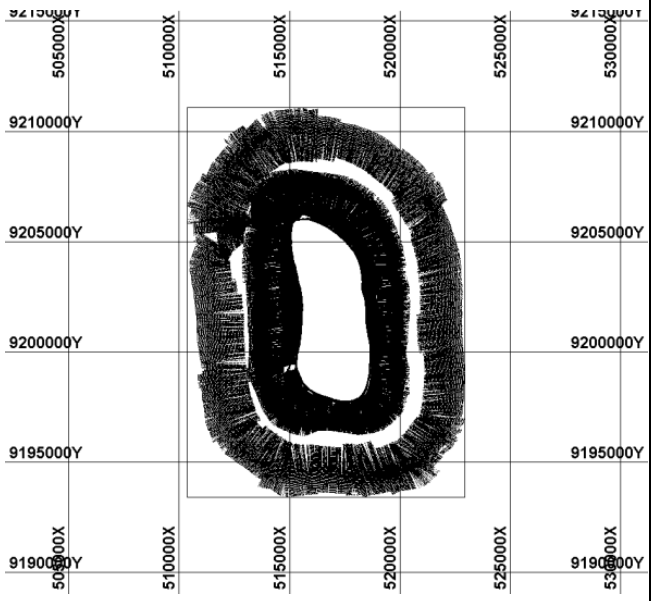

Nui

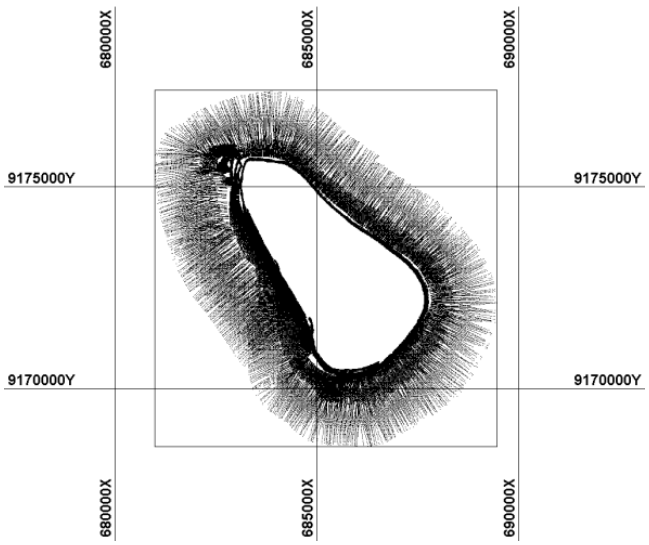

Vaitupu

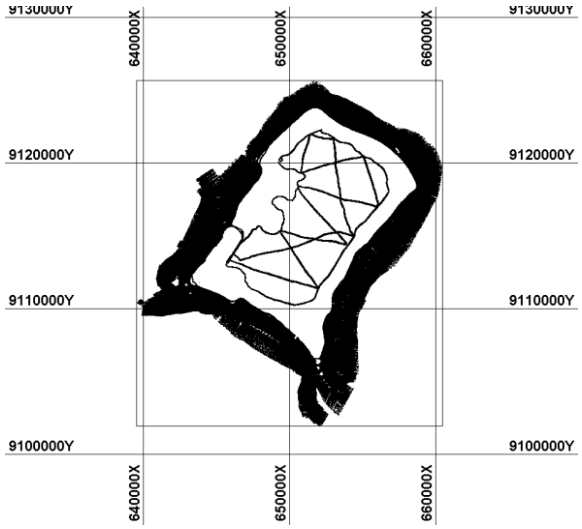

Nukufetau

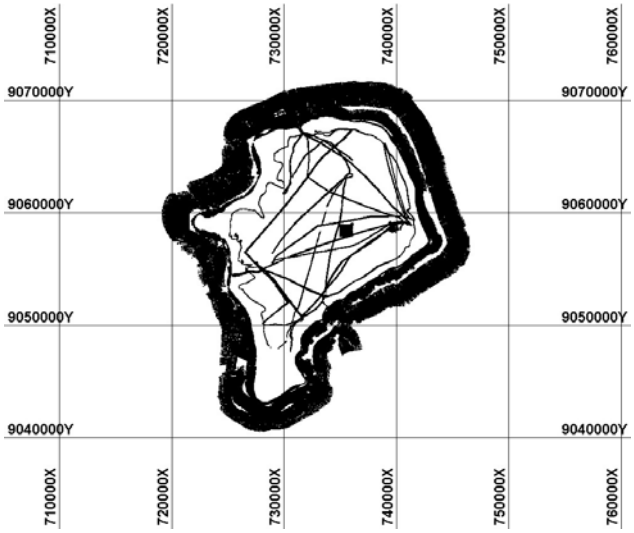

Funafuti

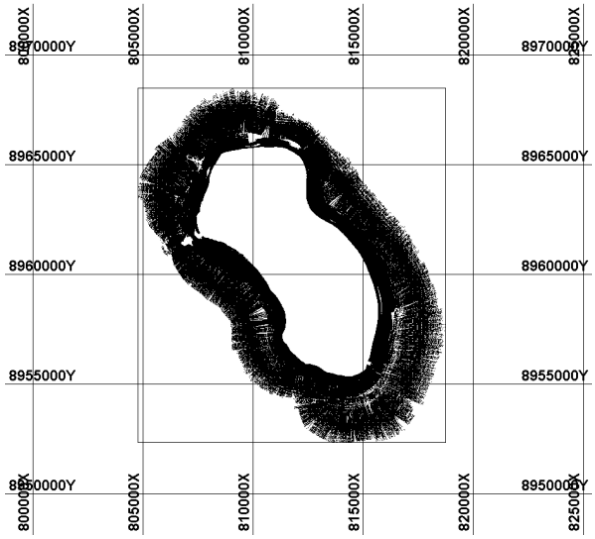

Nukulaelae

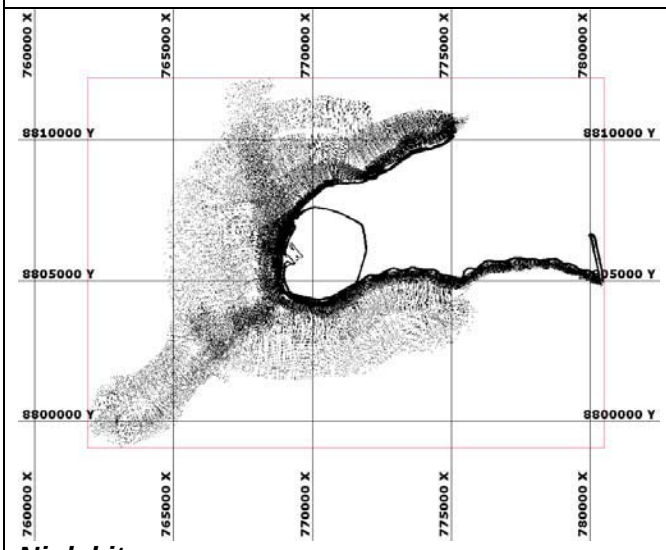

Niulakita

Appendix 2 – Equipment Performance and Statement of Uncertainty

Bathymetric maps are topographic maps of the seafloor. The bathymetric map serves the basic tool for performing scientific, engineering, marine geophysical and environmental studies. The information presented in this report and enclosed charts are intended to assist persons and authorities engaged in recreation, tourism, marine resource related industries, hydrographic mapping, coastal development, trade and commerce, sovereignty and security, and environmental management. It is therefore important that users be informed of the uncertainties associated with the data and with products constructed from it. The following is an outline of the survey equipment used and the operating principles, including limitations and estimates regarding the data accuracy.

A2.1 Horizontal positioning

The methods used to acquire survey data will affect the final product accuracy. The global positioning system, GPS, uses radio signals from satellites that orbit the earth to calculate the position of the GPS receiver. Stand-alone GPS has an estimated accuracy as good as approximately 10 m, depending on satellite configuration and atmospheric conditions. In addition to this, equipment and measurements errors also need to be considered.

A general rule of thumb is that surveys should be conducted with a positioning accuracy of 1 mm at the scale of the chart. Therefore, at a scale of 1 : 10 000, the survey would be required to be accurate to 10 m.

The present S-44 4th Edition Standard of the International Hydrographic Office (IHO) includes a depth-dependent factor that takes into account the added uncertainty of the positions of soundings from multibeam echosounder systems as depth increases. The relevant survey orders are listed n Table A2.1, with multibeam surveys conducted by SOPAC generally falling into orders 2 and 3.

Table A2.1. *Recommended accuracy of survey orders*

Survey order	Application	Recommended Accuracy
Order 1	Harbours and navigation channels	5 m + 5% of depth
Order 2	Depths < 200 m	20 m + 5% of depth
Order 3	Depths > 200 m	150 m + 5% of depth

For the purpose of this survey, it was assumed that the use of GPS provided adequate precision in terms of horizontal position. Therefore, it is not recommended to interpret nearshore data at scales larger than 1 : 10 000, or a grid size smaller than 10 m. For areas with water depths greater than 200m, a charting scale of least 1 : 50 000 is recommended.

A2.2 Depth measurements

Bathymetric maps provide information about the depth of water from the water surface to the seabed. Through the use of detailed depth contours and full use of bathymetric data, the size, shape and distribution of underwater features are clearly revealed. The depth is measured using a ship-mounted multibeam echosounder (MBES). The MBES transducer produces an acoustic pulse designed as a fan that is wide in the across-track and narrow in the along-track direction (Figure A2.1). The seabed covered by this beam typically returns good data over a swath that is two to three times the water depth. The pulse of sound emitted from the MBES travels through the water column and is reflected back as an echo and received as numerous narrow beams by the receiving elements of the MBES. The measurements are time-based, and by using the speed of sound in seawater each time is converted first to a range and then, knowing the beam angle, to a depth. The distance to the seabed is then combined with the movement of the vessel to stabilise it into a real-world framework. The framework is then positioned to provide XYZ soundings for each beam's interaction with the seabed. A series of these swaths are then combined to produce a three-dimensional representation of the seafloor topography.

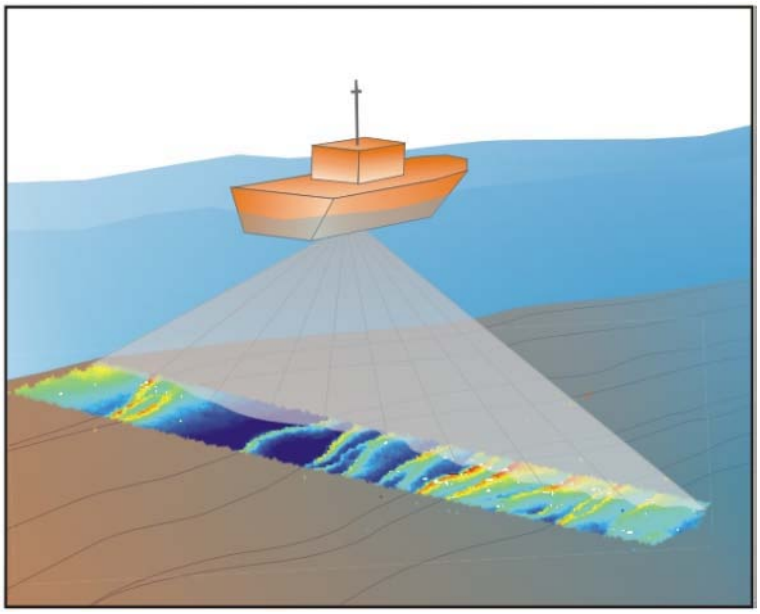

Figure A2.1. *Conceptual illustration of bathymetric data acquisition with a Multibeam echosounder, MBES (source: http://www.rcom.marum.de, accessed 10/01/2007).*

The accuracy of the MBES system is critically dependent on the corrections applied for vessel motion (heave, pitch, roll, yaw, and heading). However, the absolute accuracy of single-beam and multibeam bathymetry depends on several factors that are not easy to determine. For single beam data, probably the principal errors that may be introduced are due to topographic features falling between survey lines. Multibeam systems give far better coverage.

The S-44 4th Edition Standard of the IHO lists values “a” and “b”(Table A2.2) that should be introduced into the following equation to calculate the error limits for depth accuracy:

$\pm\sqrt{a^2+(b\times d)^2}$, where d = depth.

Table A2.2. *Values for calculating error limits for depth accuracy*

Survey order	Application	Constants
Order 1	Harbours and navigation channels	a = 0.5 m, b = 0.013
Order 2	Depths < 200 m	a = 1.0 m, b = 0.023
Order 3	Depths > 200 m	a = 1.0 m, b = 0.023

For example, the IHO recommends that a nearshore coastal survey (Order 2) in water depths of 20 m should have a maximum error of ±1.1 m.

A MBES has, as any other measuring instrument, an inherent limit in its achievable accuracy. The total measurement accuracy, i.e. the uncertainty in the depth and location of the soundings, also depends upon the errors of the auxiliary instruments such as the motion reference unit, the gyro compass, and the measurements of the speed of sound through the water column. The sea state at the time of the survey also contributes significantly to the quality of the data. The possible accuracy of the measured depths may be estimated by considering the following main error sources.

A2.3 Error budget analysis for depths

Measurement

The nadir-beam bottom detection range resolution of the multibeam system has a maximum limit of 0.1 m (Reson 2002). However, multibeam systems are particularly susceptible to errors in the far range (outer beams), and detection is estimated at ±0.3 m plus 0.5% of the depth. Errors also include the detection of the sea floor due to local variations of depth within the beam

footprint, especially in the outer beams, and a varying density of the bottom material. This may be significant if a relatively low-frequency transducer is used on soft marine muds in shallow water.

Transducer draft — The transducer depth may be accurate to ± 0.1 m. However, the draft of the vessel due to the variability in vessel loading, e.g. fuel and fresh water storage, was not determined. It is estimated that this introduced a water depth-independent error of up to ± 0.2 m. Dynamic draft errors, e.g. vessel squat, may also be significant.

Sound velocity — The sound velocity profiles measured by the conductivity-temperature-depth sensor (CTD) probe did not reach full survey depths in waters exceeding 400 m water depths. An inaccurate sound path from the transducer to the bottom and back will affect not only the observed depth of water, but also the apparent position of the observed sounding. This error is presumed to exceed 0.5% of the water depth beyond the direct CTD measurements. In order to minimise this error, ARGO and GDEM data may be used to supplement the CTD data.

Heave — This error is directly dependent on the sea state and the sensitivity of the motion sensor and installation parameters. The MRU installation did not account for the offset distance between MRU, the centre of gravity, and the MBES transducer mount. However, the software was able to perform lever arm calculations and heave compensation during post-processing, and the vertical error is assumed to be significant only in heavy seas.

Tide/water level — Uncertainties due to tides may be significant, especially where predicted tides some distance from the survey area are used. Perhaps ± 0.3 m for uncertainty in tidal datum need to be considered.

From the listing above, it is estimated that the measured depths in 20 m have an uncertainty of ± 1.5 m. However, the complete bathymetric model, or digital terrain model (DTM), is based on some form of interpolation between the sampled depths from several survey lines. Consequently, the total uncertainty associated with a bathymetric model will include uncertainties due to horizontal positioning, and uncertainties introduced by the interpolation process, and will therefore be larger than the depth sounding uncertainty.

A2.4 Multibeam echosounder data density

The density of data used to construct a bathymetric grid is an important factor in its resolution – the denser the data, the higher the resolution that can be achieved. Sounding density is critical in terms of seabed feature detection and delineation. The two main factors that control the potential bathymetric target resolution capability of a multibeam echosounder are the distance between individual soundings (both in the cross-track and along-track dimensions), and the footprint size. The footprint is the area on the bottom covered by the sound pulse. Footprint size is a function of range, beam angle, and receiver and transmitter beam widths. A high sounding density and small footprint will result in higher resolution data. Conversely, the target detection capability is going to decay as a result of a growing projected beam footprint and decreasing data density.

The along-track spacing is controlled by the ping rate, which in turn is limited by the two-way travel time from the source to the furthermost point imaged. The maximum across-track spacing depends again primarily on the range, but also on the equiangular beam spacing. The size of the beams received by the MBES system is between one and one-and-a-half degrees. This means that a system mounted on a ship will have a larger projected footprint as the water depth increases. The footprint will also be larger at the outer beams than at the centre of the swath, as the range and incident angles increase with distance from the nadir beam. It is possible to have local variations of depth within the beam footprint, causing vertical error and affecting amplitude detection.

Table A2.3 shows a summary of the projected beam footprint size under varying water depths for

the two MBES systems currently in use by SOPAC. It should be noted that the higher-frequency system (SeaBat 8101) is not appropriate for applications in waters deeper than 200 m. Due to the constant beam width, the sounded area varies according to the depth and slope, which results in a variable data density in the survey area.

Table A2.3. *Projected footprint size under varying water depths*

Water depth	SeaBat 8160 (deep water) 50 kHz, 126 beams at 1.5 °		SeaBat 8101 (shallow water) 240 kHz, 101 beams at 1.5 °	
(m)	Inner footprint, nadir (m)	Outer footprint (m)	Inner footprint, nadir (m)	Outer footprint (m)
20	0.4	5.8	0.5	3.5
50	1.0	14.4	1.3	17.6
100	2.1	28.8	2.6	35.3
200	4.2	57.6	5.2	70.6
500	10.5	143.9	N/A	N/A
1000	20.9	287.9	N/A	N/A
1500	31.4	431.8	N/A	N/A

Table A2.3 assumes a horizontal seabed, and shows the variation in across-track footprint size with water depth and beam angle. The sounding density and swath width will also vary when surveying steep slopes, or highly incised margins, as the footprint size varies strongly with topography. Therefore, deeper sections have larger projected footprints and fewer data point. This has the effect that a bathymetric feature, whose lateral dimensions are less than the beam footprint size, will not be resolved.

It should also be noted that the along-track resolution usually exceeds the across-track resolution due to ping rates, especially in deep water. Since ping rates are limited by the two-way travel time, rates for water depths of 20 m and 1500 m are 12.9 and 0.2 pings per second, respectively. Using maximum ping rates, or when surveying in deep water, the same area may be measured with the outer beams for several pings, which may give inconsistent sounding data due to the poor repeatability on uneven seabed.

In order to take into account depth-dependent point density, it is generally accepted to grid bathymetric data at a resolution that is on the order of the average beam footprint size, typically 10% of the water depth.

Appendix 3 – CTD profiles

Salinity is determined from measurements of conductivity, temperature and pressure.

Downcast and upcast unfiltered data

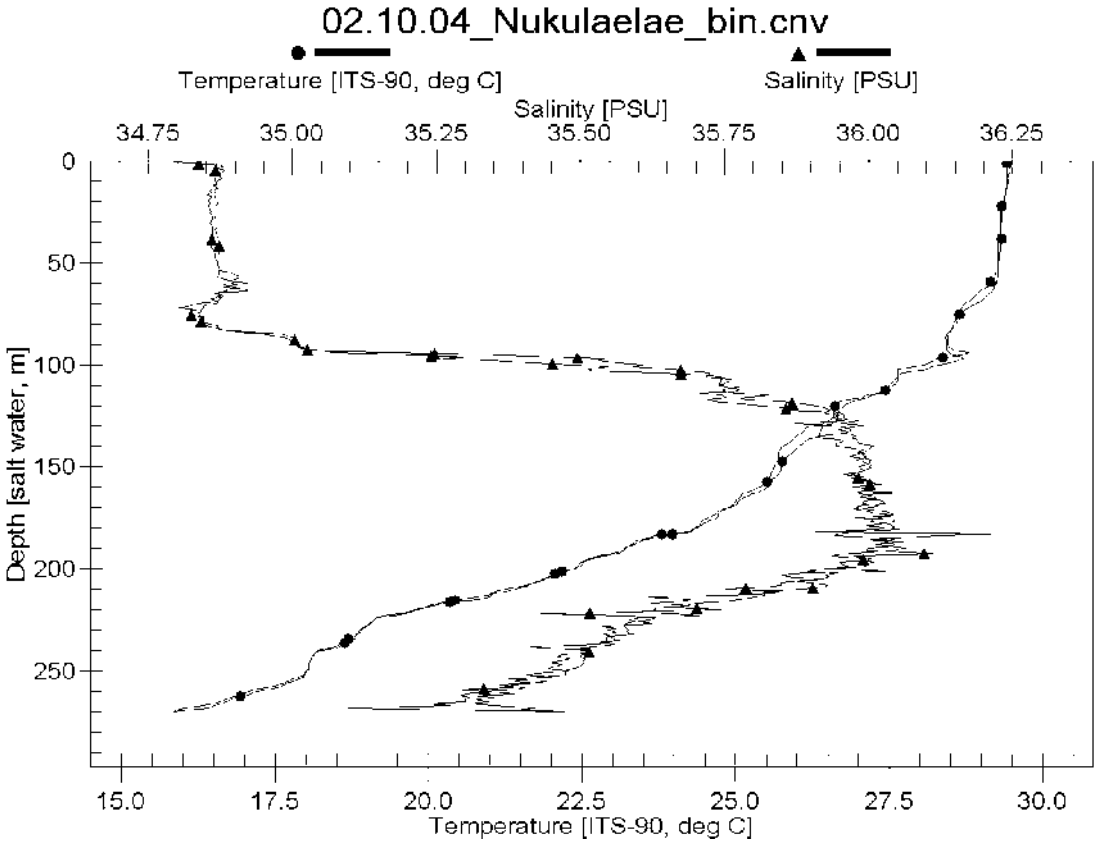

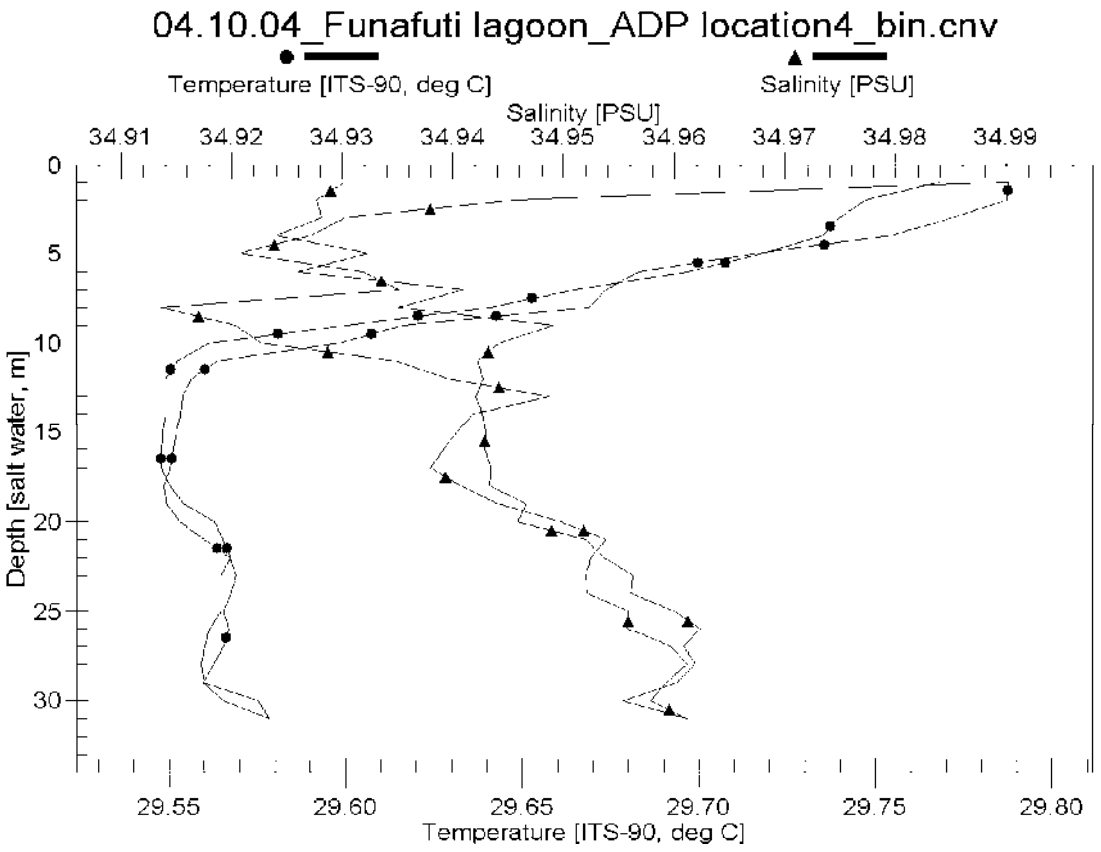

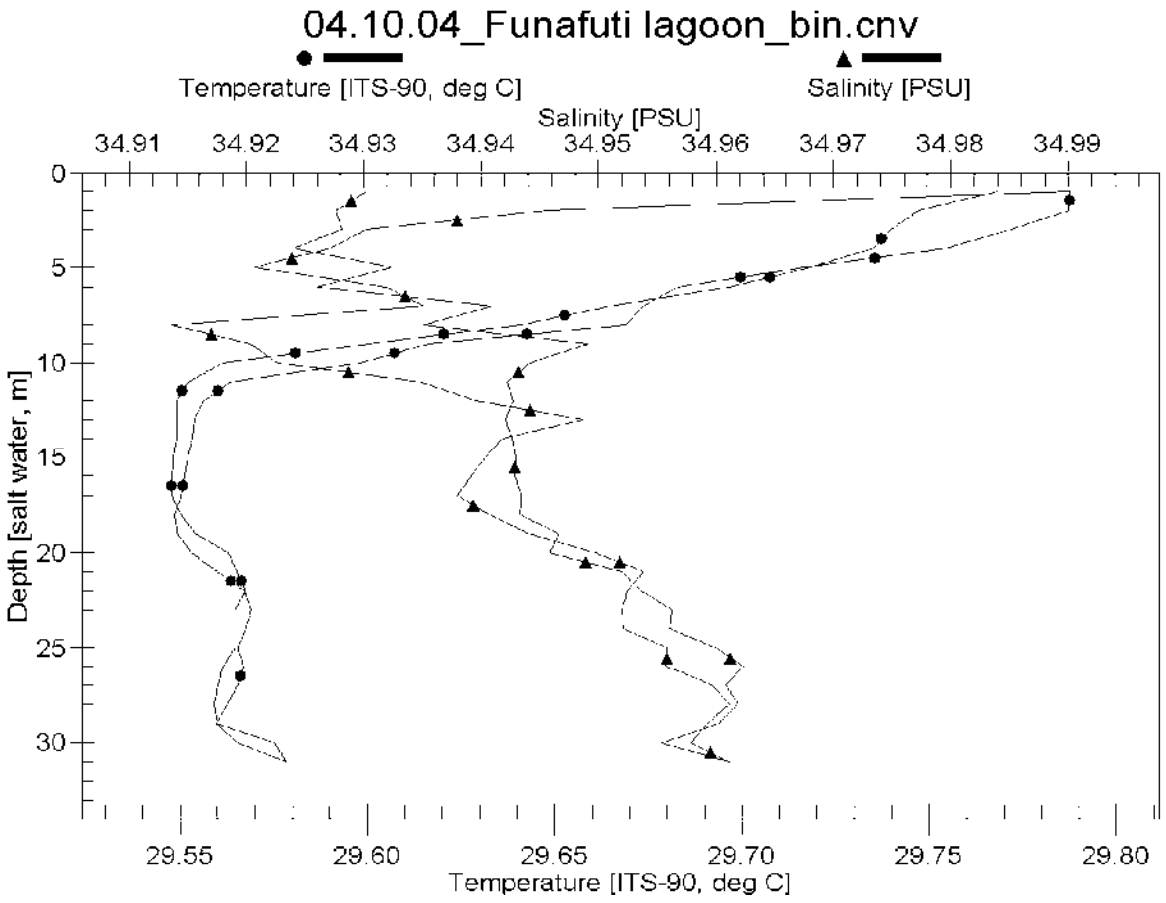
04.10.04_Funafuti lagoon_bin.cnv
Temperature [ITS-90, deg C]
Salinity [PSU]
Salinity [PSU]
34.91 34.92 34.93 34.94 34.95 34.96 34.97 34.98 34.99
Depth [salt water, m]
0 5 10 15 20 25 30
29.55 29.60 29.65 29.70 29.75 29.80
Temperature [ITS-90, deg C]

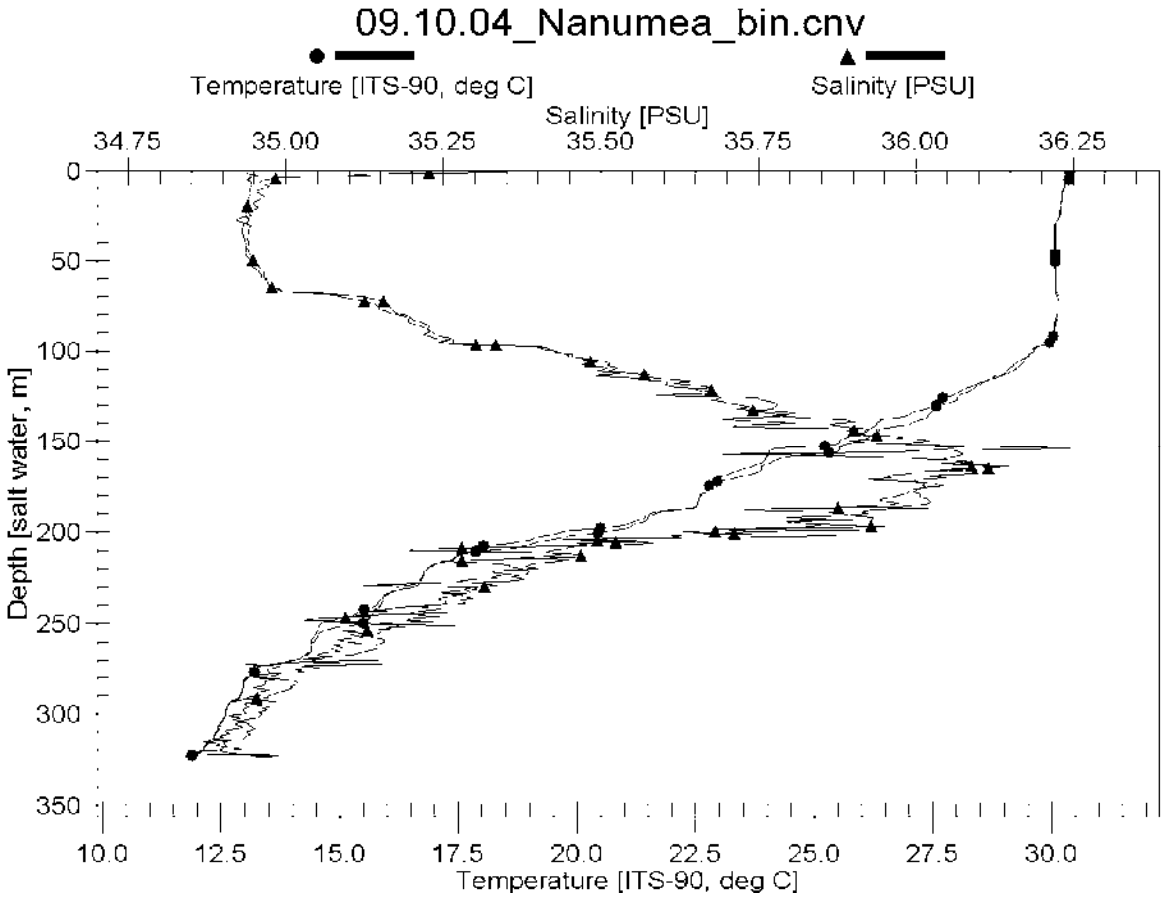
09.10.04_Nanumea_bin.cnv
Temperature [ITS-90, deg C]
Salinity [PSU]
Salinity [PSU]
34.75 35.00 35.25 35.50 35.75 36.00 36.25
Depth [salt water, m]
0 50 100 150 200 250 300 350
10.0 12.5 15.0 17.5 20.0 22.5 25.0 27.5 30.0
Temperature [ITS-90, deg C]

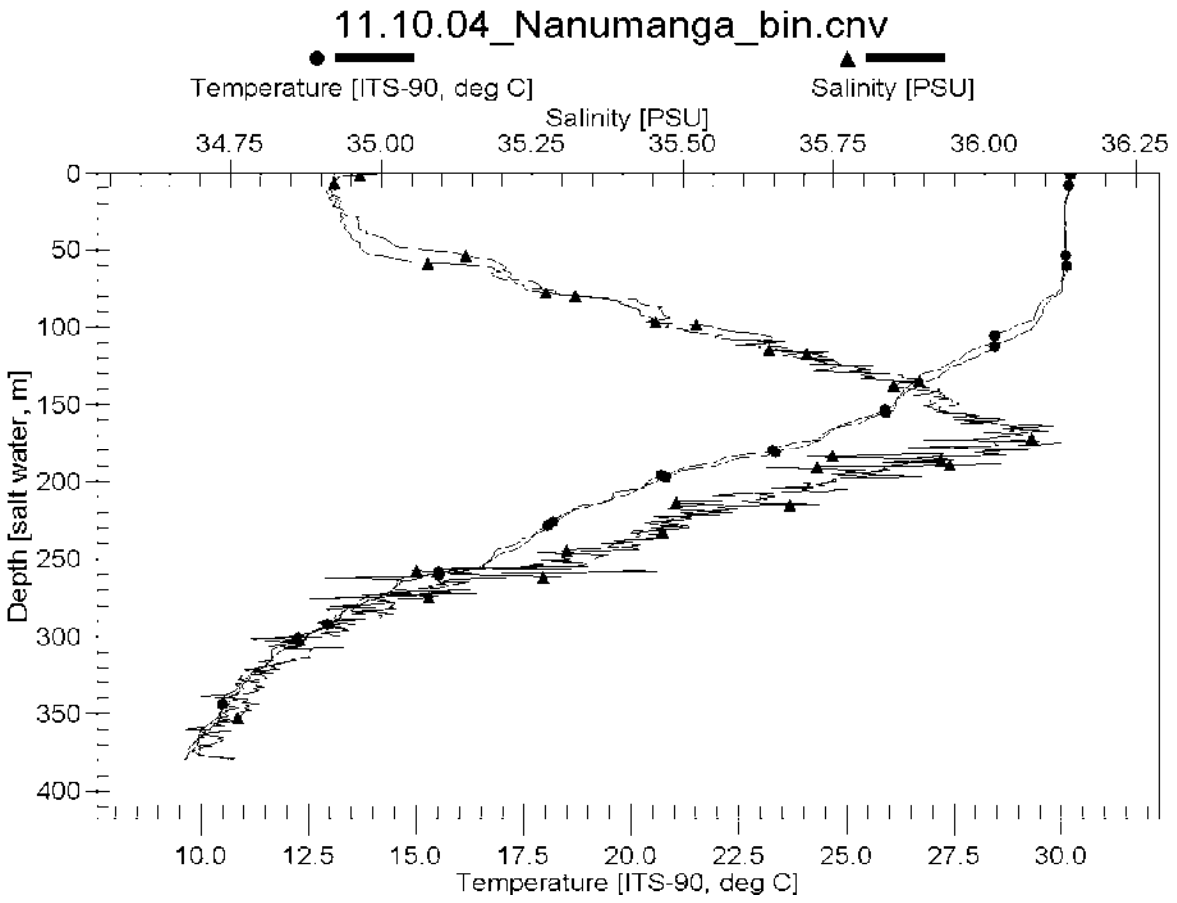
11.10.04_Nanumanga_bin.cnv
Temperature [ITS-90, deg C]
Salinity [PSU]
Salinity [PSU]
34.75
35.00
35.25
35.50
35.75
36.00
36.25
0
50
100
150
200
250
300
350
400
Depth [salt water, m]
10.0
12.5
15.0
17.5
20.0
22.5
25.0
27.5
30.0
Temperature [ITS-90, deg C]

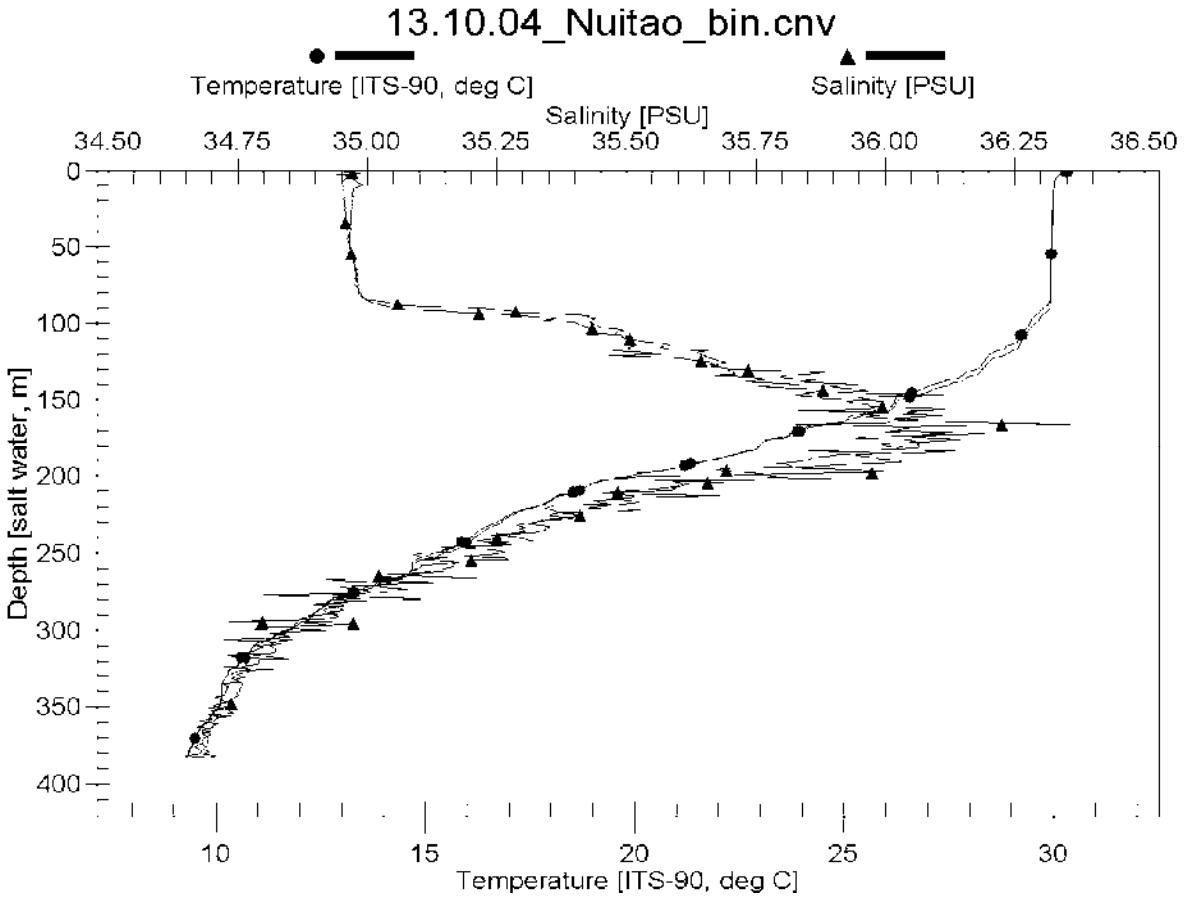
13.10.04_Nuitao_bin.cnv
Temperature [ITS-90, deg C]
Salinity [PSU]
Salinity [PSU]
34.50
34.75
35.00
35.25
35.50
35.75
36.00
36.25
36.50
0
50
100
150
200
250
300
350
400
Depth [salt water, m]
10
15
20
25
30
Temperature [ITS-90, deg C]

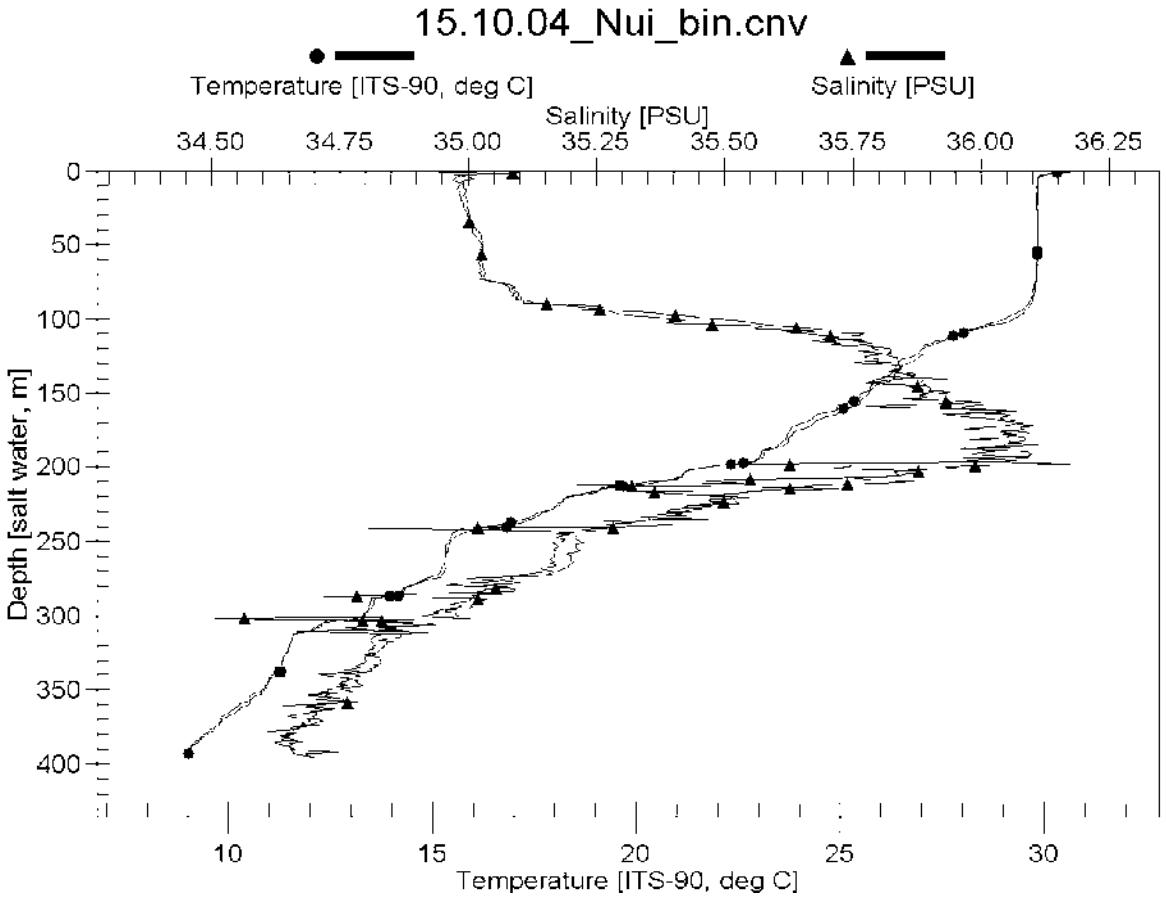
15.10.04_Nui_bin.cnv
Temperature [ITS-90, deg C]
Salinity [PSU]
Salinity [PSU]
34.50 34.75 35.00 35.25 35.50 35.75 36.00 36.25
Depth [salt water, m]
0 50 100 150 200 250 300 350 400
10 15 20 25 30
Temperature [ITS-90, deg C]

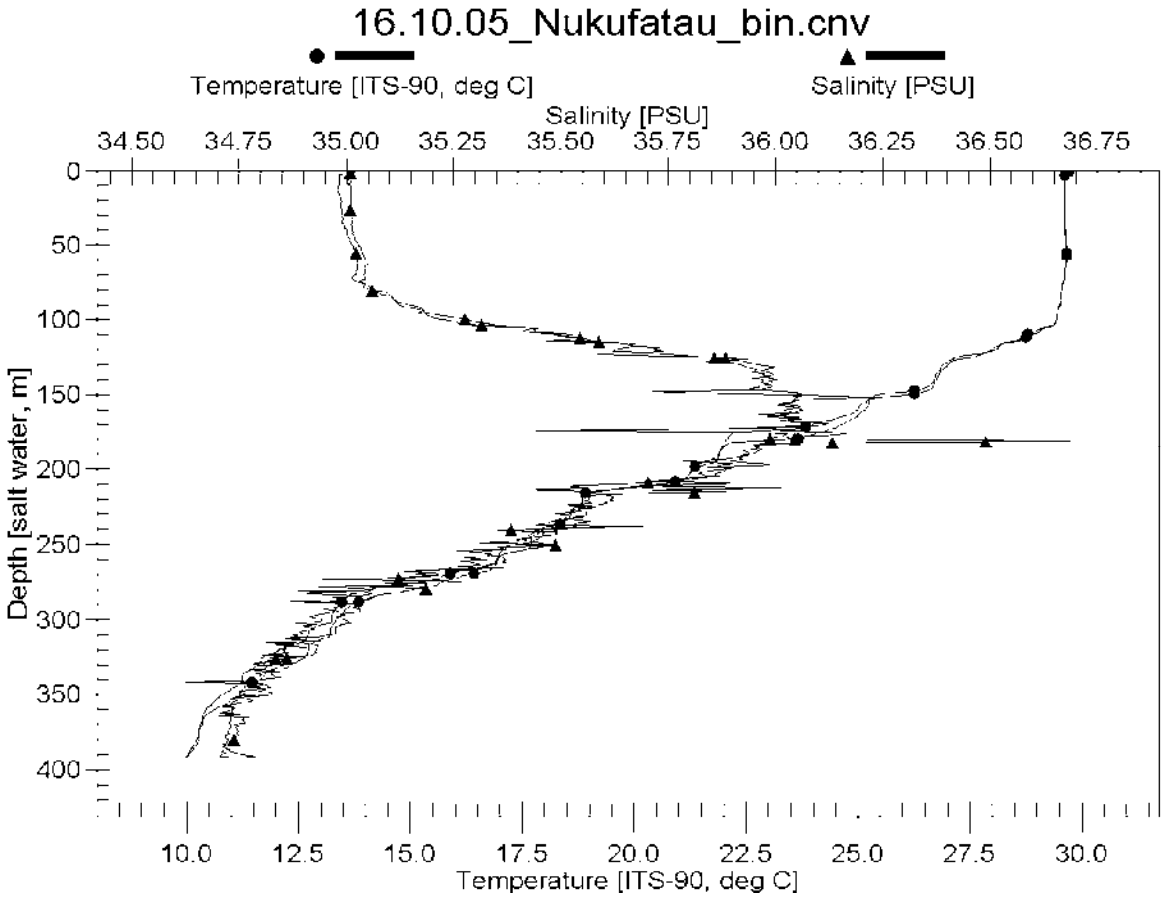
16.10.05_Nukufatau_bin.cnv
Temperature [ITS-90, deg C]
Salinity [PSU]
Salinity [PSU]
34.50 34.75 35.00 35.25 35.50 35.75 36.00 36.25 36.50 36.75
Depth [salt water, m]
0 50 100 150 200 250 300 350 400
10.0 12.5 15.0 17.5 20.0 22.5 25.0 27.5 30.0
Temperature [ITS-90, deg C]

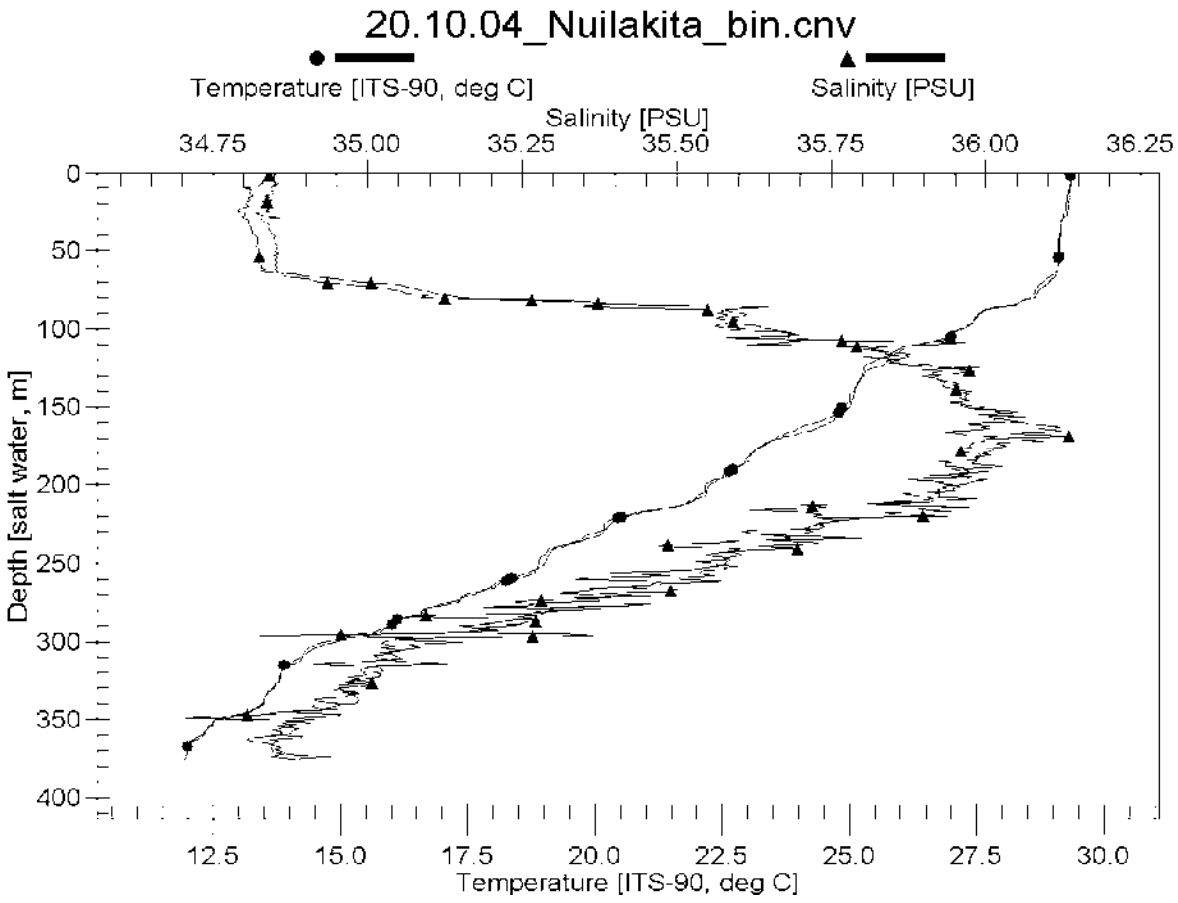
20.10.04_Nuilakita_bin.cnv
Temperature [ITS-90, deg C]
Salinity [PSU]
Salinity [PSU]
34.75 35.00 35.25 35.50 35.75 36.00 36.25
Depth [salt water, m]
0 50 100 150 200 250 300 350 400
12.5 15.0 17.5 20.0 22.5 25.0 27.5 30.0
Temperature [ITS-90, deg C]

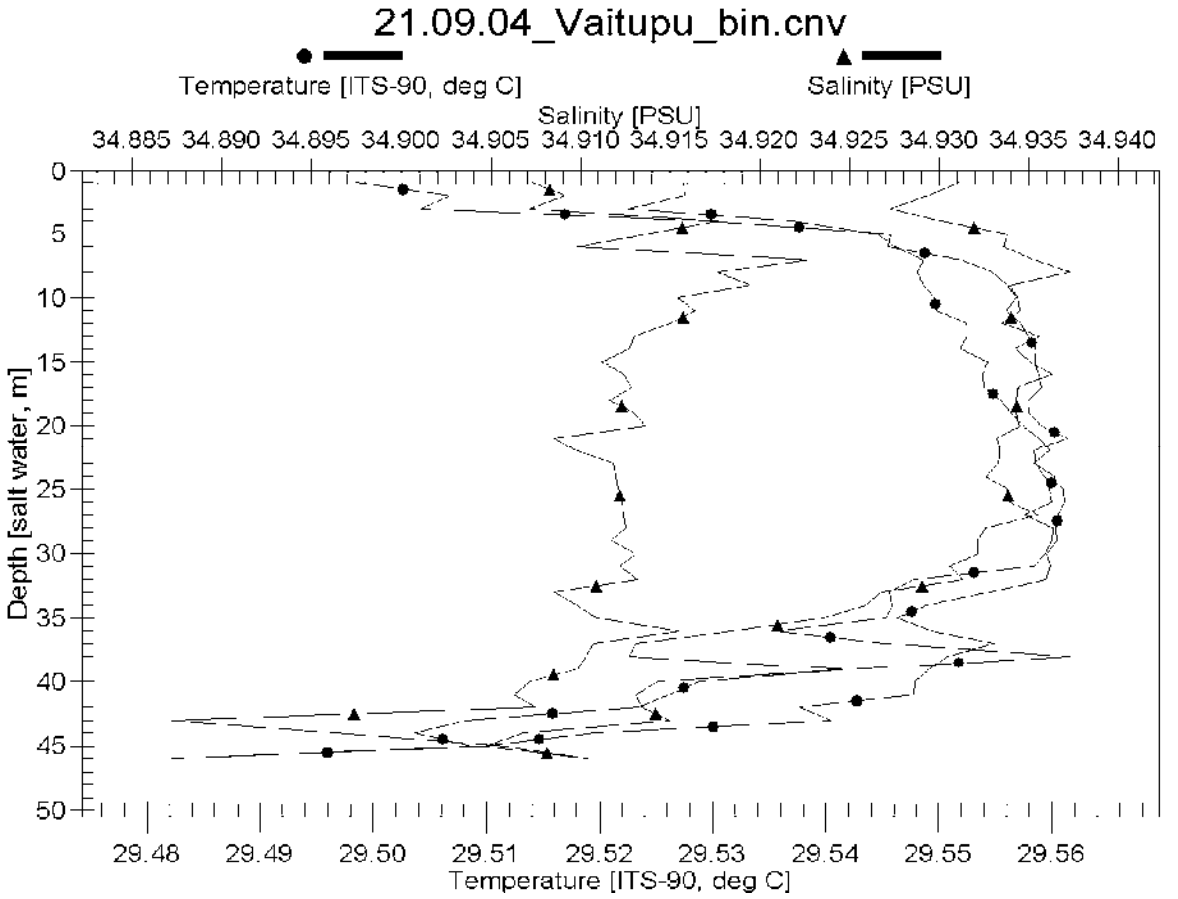
21.09.04_Vaitupu_bin.cnv
Temperature [ITS-90, deg C]
Salinity [PSU]
Salinity [PSU]
34.885 34.890 34.895 34.900 34.905 34.910 34.915 34.920 34.925 34.930 34.935 34.940
Depth [salt water, m]
0 5 10 15 20 25 30 35 40 45 50
29.48 29.49 29.50 29.51 29.52 29.53 29.54 29.55 29.56
Temperature [ITS-90, deg C]

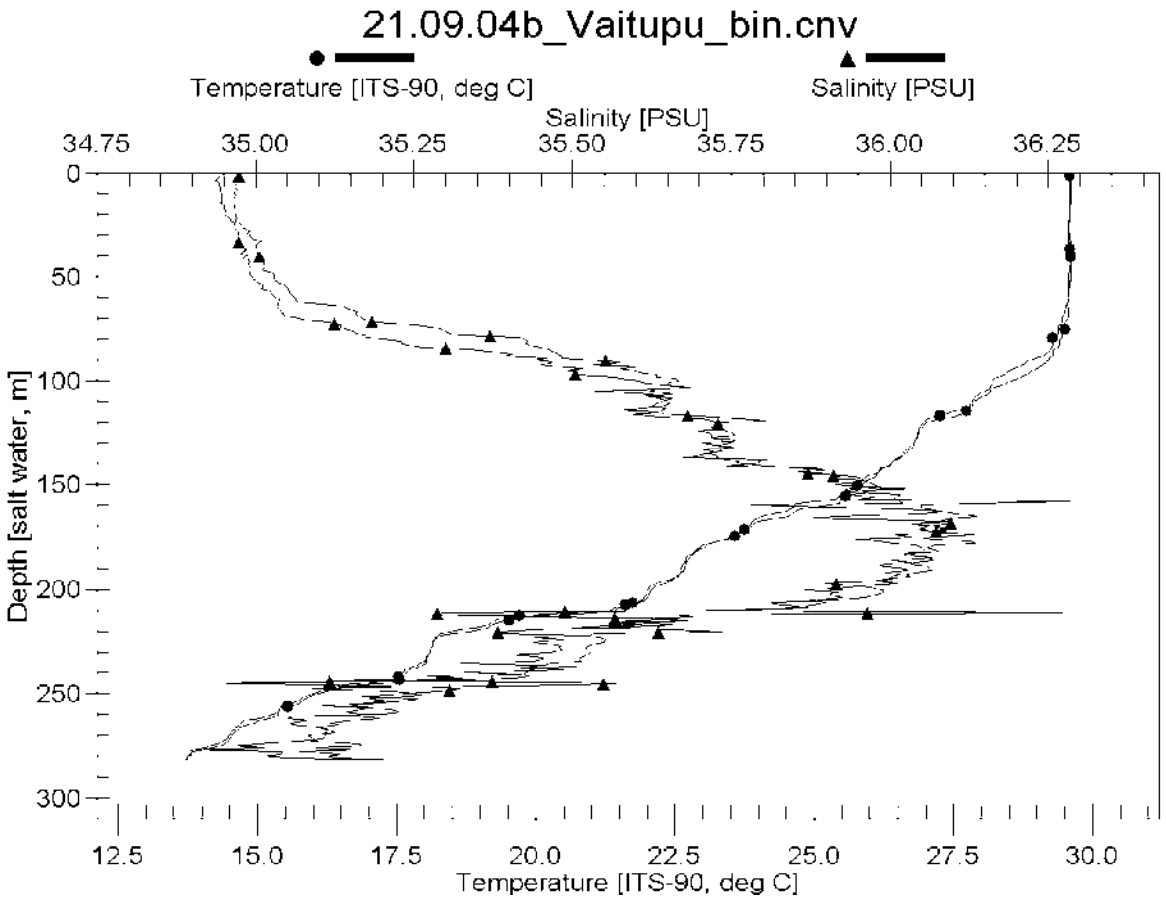
21.09.04b_Vaitupu_bin.cnv
Temperature [ITS-90, deg C]
Salinity [PSU]
Salinity [PSU]
34.75
35.00
35.25
35.50
35.75
36.00
36.25
0
50
100
150
200
250
300
Depth [salt water, m]
12.5
15.0
17.5
20.0
22.5
25.0
27.5
30.0
Temperature [ITS-90, deg C]

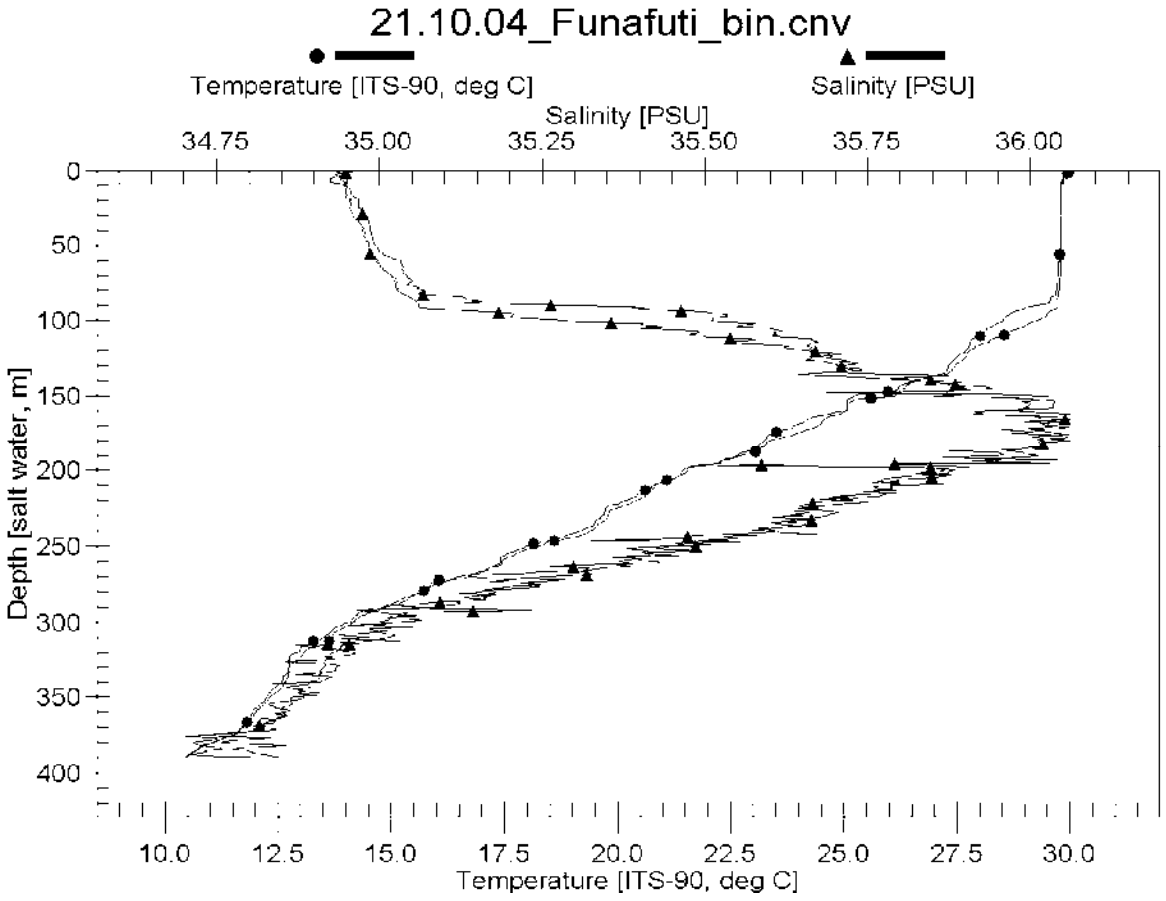
21.10.04_Funafuti_bin.cnv
Temperature [ITS-90, deg C]
Salinity [PSU]
Salinity [PSU]
34.75
35.00
35.25
35.50
35.75
36.00
0
50
100
150
200
250
300
350
400
Depth [salt water, m]
10.0
12.5
15.0
17.5
20.0
22.5
25.0
27.5
30.0
Temperature [ITS-90, deg C]

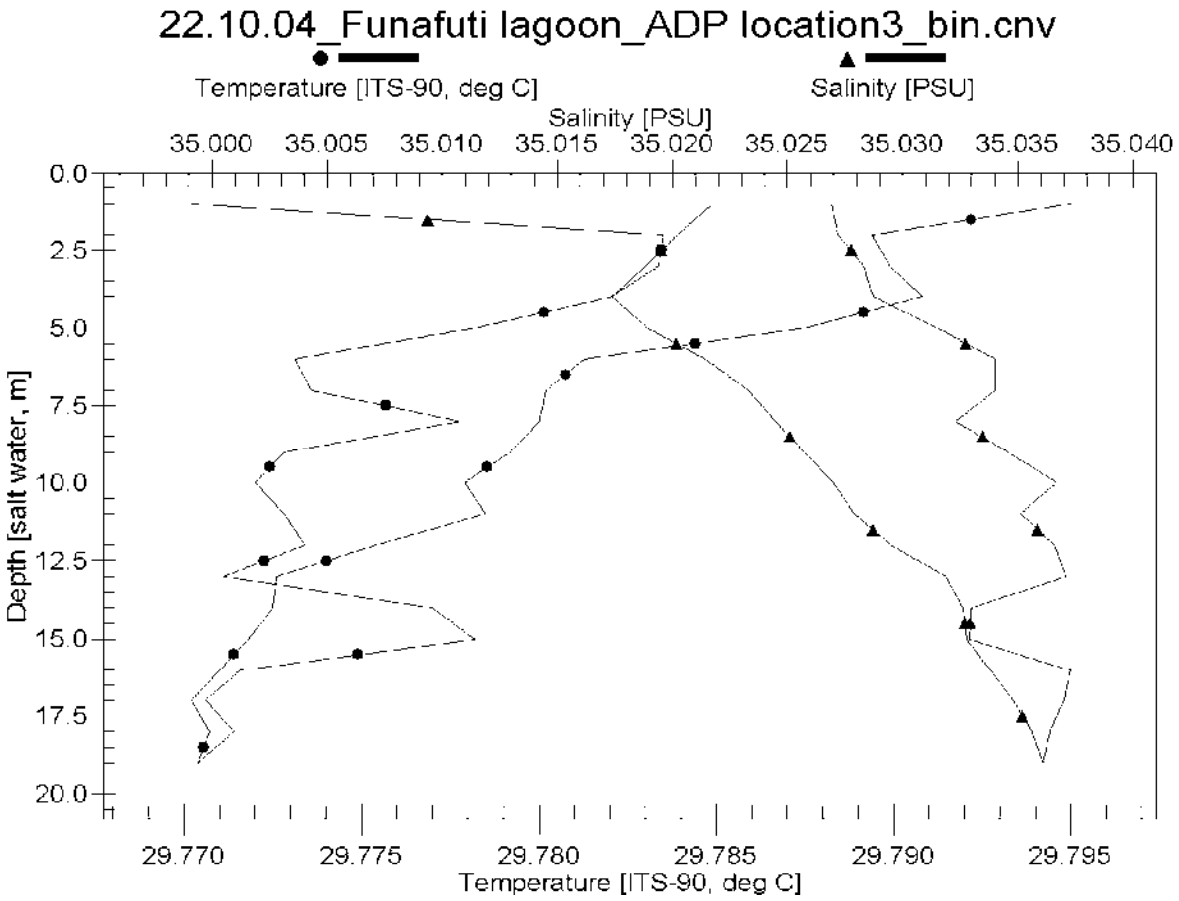
22.10.04_Funafuti lagoon_ADP location3_bin.cnv
Temperature [ITS-90, deg C]
Salinity [PSU]
Salinity [PSU]
35.000 35.005 35.010 35.015 35.020 35.025 35.030 35.035 35.040
0.0 2.5 5.0 7.5 10.0 12.5 15.0 17.5 20.0
Depth [salt water, m]
29.770 29.775 29.780 29.785 29.790 29.795
Temperature [ITS-90, deg C]

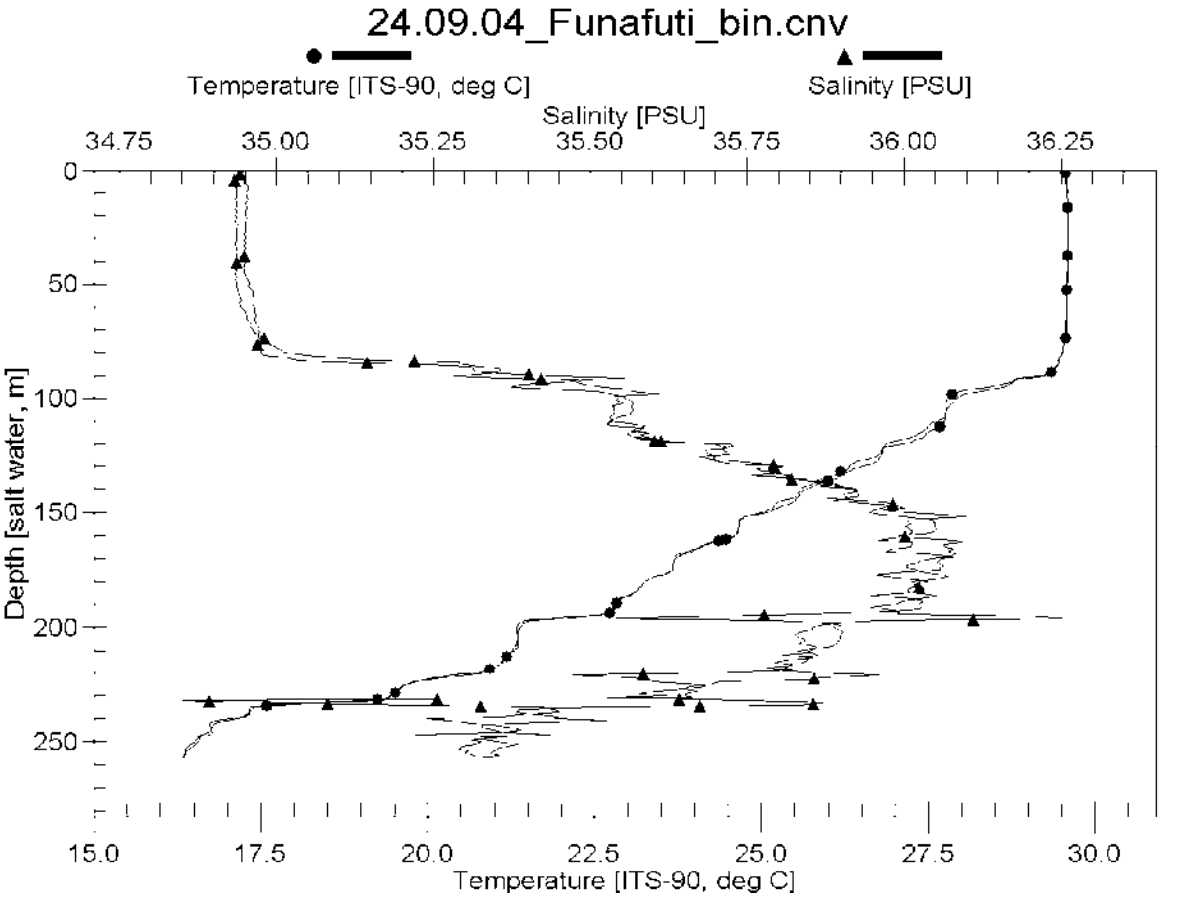
24.09.04_Funafuti_bin.cnv
Temperature [ITS-90, deg C]
Salinity [PSU]
Salinity [PSU]
34.75 35.00 35.25 35.50 35.75 36.00 36.25
0 50 100 150 200 250
Depth [salt water, m]
15.0 17.5 20.0 22.5 25.0 27.5 30.0
Temperature [ITS-90, deg C]

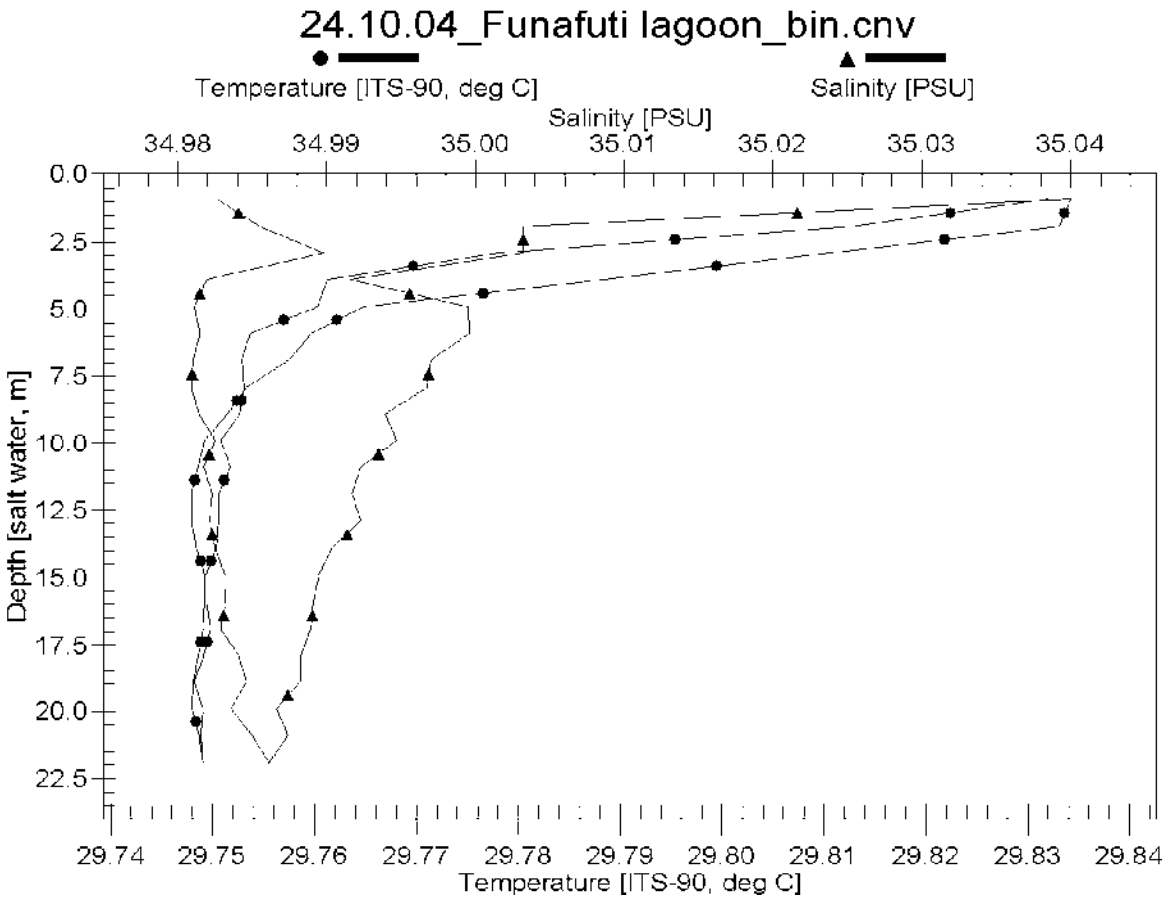
24.10.04_Funafuti lagoon_bin.cnv
Temperature [ITS-90, deg C]
Salinity [PSU]
Salinity [PSU]
34.98
34.99
35.00
35.01
35.02
35.03
35.04
Depth [salt water, m]
0.0
2.5
5.0
7.5
10.0
12.5
15.0
17.5
20.0
22.5
29.74
29.75
29.76
29.77
29.78
29.79
29.80
29.81
29.82
29.83
29.84
Temperature [ITS-90, deg C]

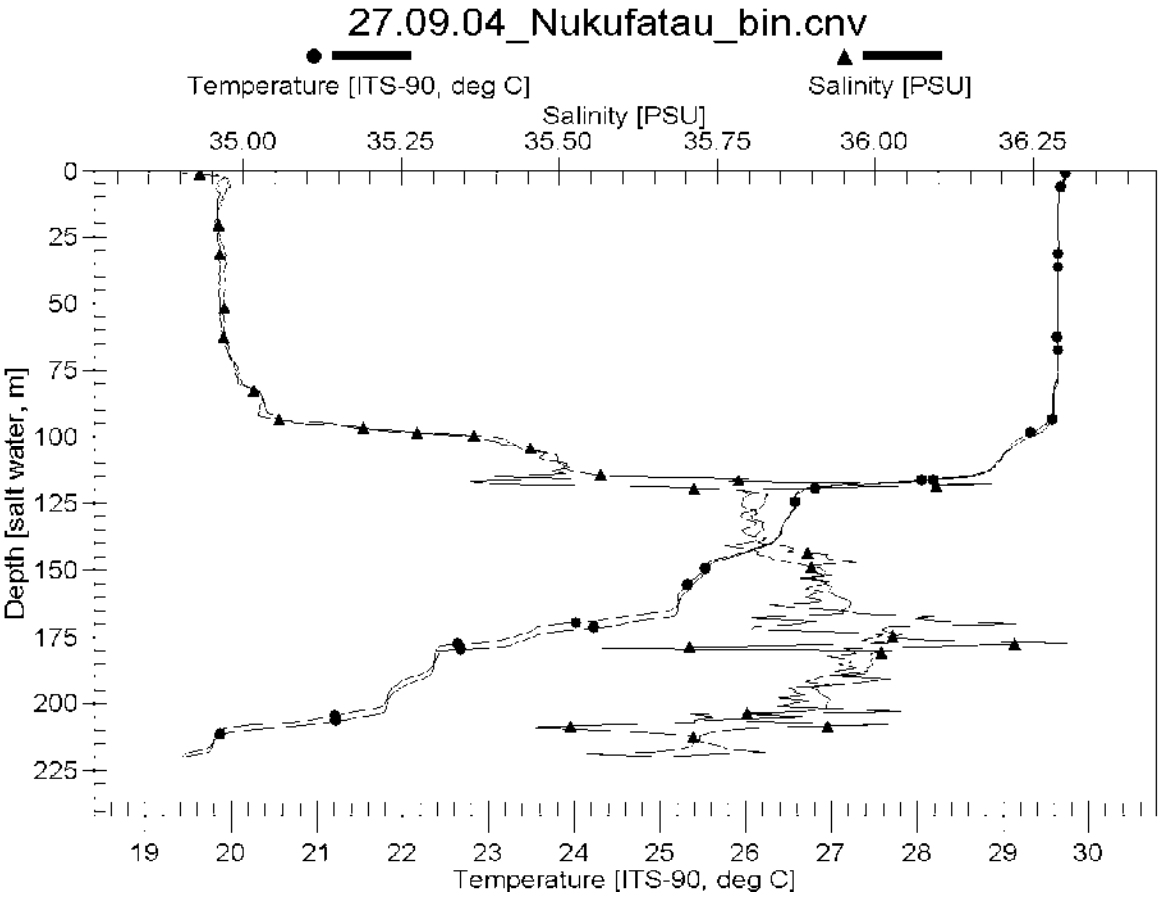
27.09.04_Nukufatau_bin.cnv
Temperature [ITS-90, deg C]
Salinity [PSU]
Salinity [PSU]
35.00
35.25
35.50
35.75
36.00
36.25
Depth [salt water, m]
0
25
50
75
100
125
150
175
200
225
19
20
21
22
23
24
25
26
27
28
29
30
Temperature [ITS-90, deg C]

Appendix 4 – High-resolution A0 Charts, Tuvalu Bathymetry

Charts are available from SOPAC, and can be downloaded from its virtual library.

(Low-resolution A4 representations follow, 9 pages)

List of drawings			
Chart No	Title	Scale	Drawing No.
1	Nanumea, Tuvalu, Bathymetry	1 : 25 000	ER050.1
2	Niutao, Tuvalu, Bathymetry	1 : 20 000	ER050.2
3	Nanumanga, Tuvalu, Bathymetry	1 : 25 000	ER050.3
4	Nui, Tuvalu, Bathymetry	1 : 25 000	ER050.4
5	Vaitupu, Tuvalu, Bathymetry	1 : 20 000	ER050.5
6	Nukufetau, Tuvalu, Bathymetry	1 : 50 000	ER050.6
7	Funafuti, Tuvalu, Bathymetry	1 : 50 000	ER050.7
8	Nukulaelae, Tuvalu, Bathymetry	1 : 25 000	ER050.8
9	Niulakita, Tuvalu, Bathymetry	1 : 25 000	ER050.9

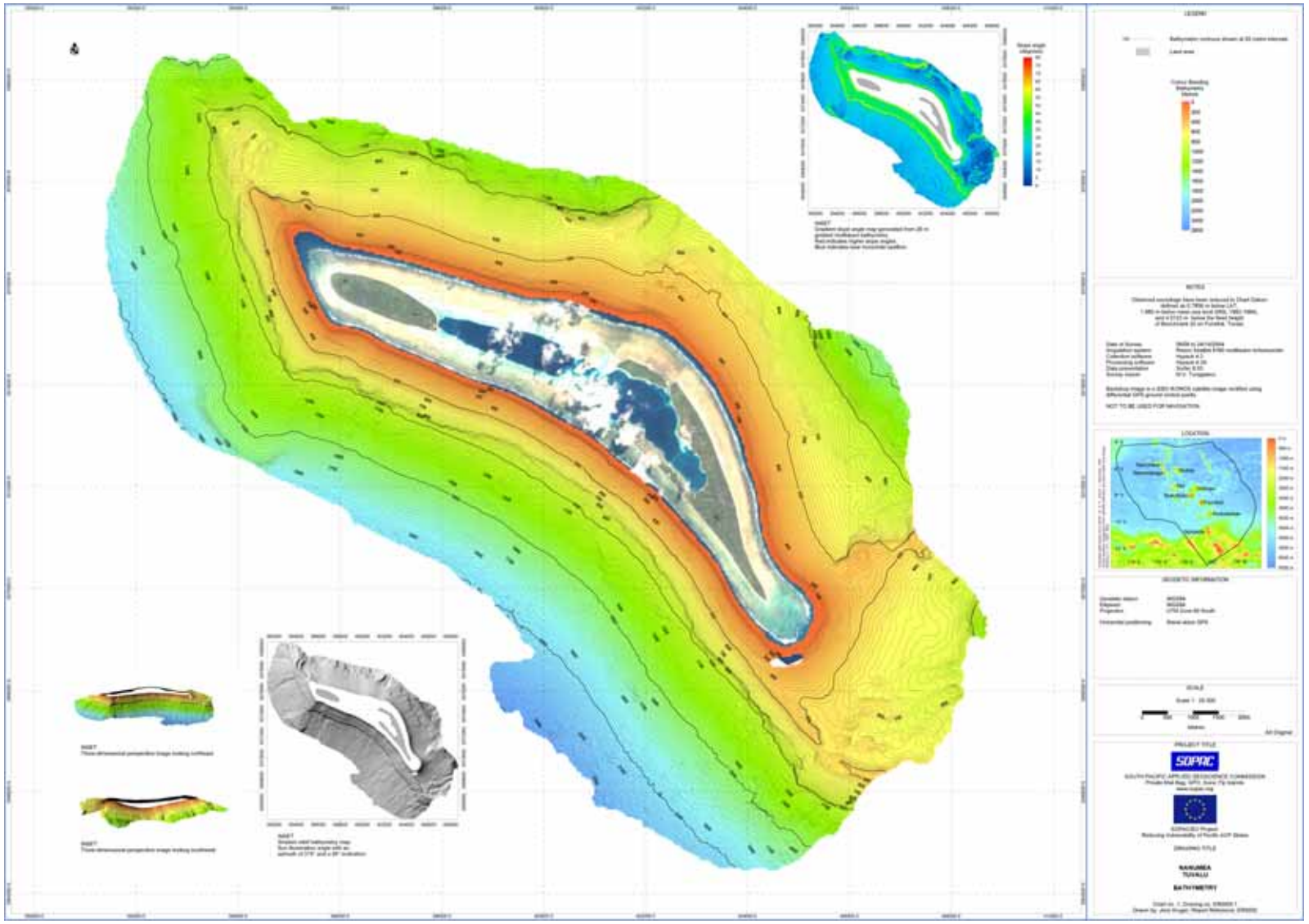
LEGEND
NOTES
LOCATION
GEODETIC INFORMATION
SCALE
PROJECT TITLE
SOPAC
NANUMEA
TUVALU
BATHYMETRY

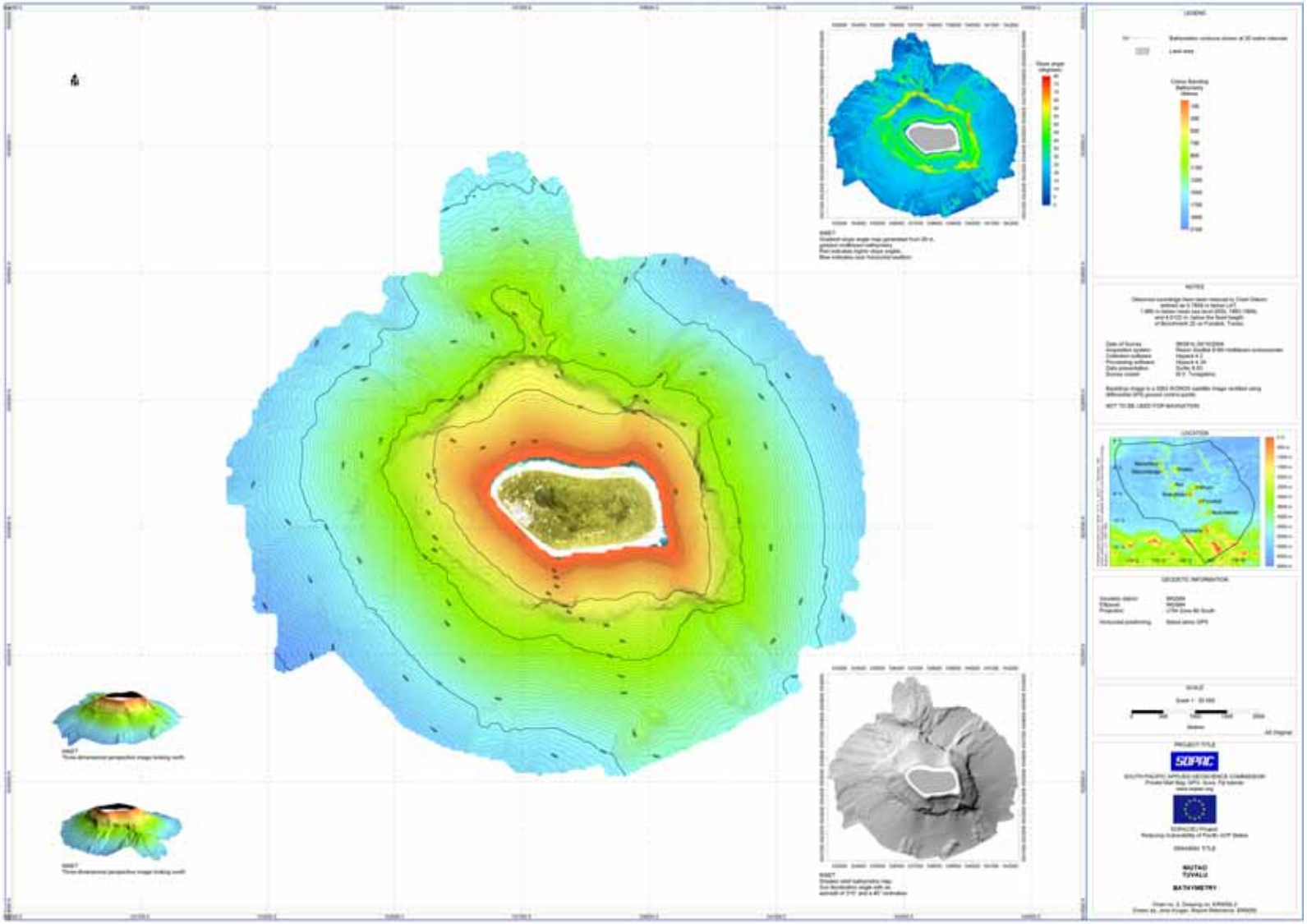

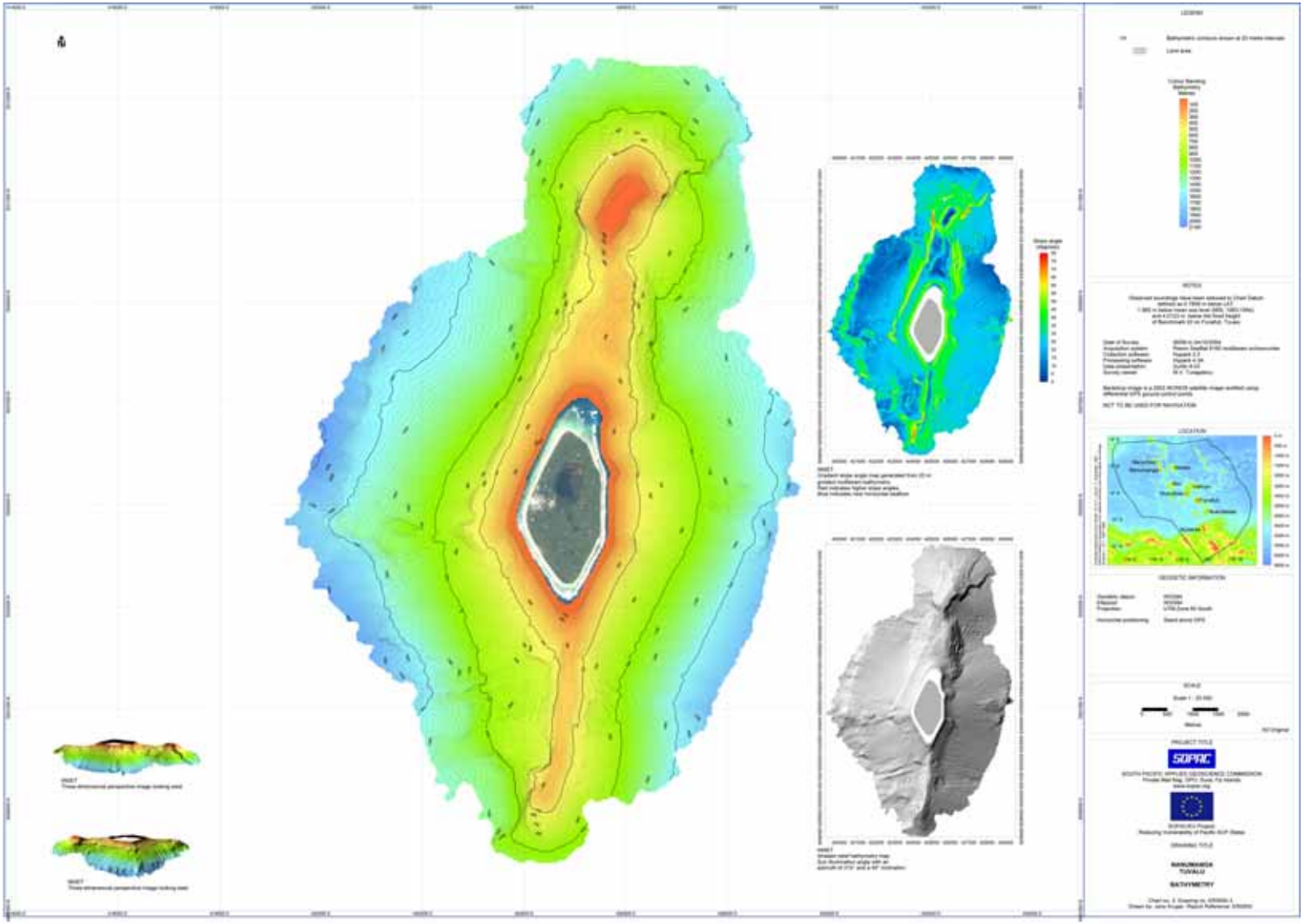
LEGEND
Bathymetric contours shown at 25 metre intervals
Land area
Colour Banding
Bathymetry
Metres
NOTES
Observed soundings have been reduced to Chart Datum
(MSL) which is 1.885 m below LAT.
1.885 m below mean sea level (MSL, 1983-1994)
and 4.27233 m below Mid Road Height
of Benchmark 01 on Funafuti, Tuvalu
Date of Survey
Acquisition system
Collection software
Processing software
Data presentation
Survey vessel
LOCATION
GEODETIC INFORMATION
Geodetic datum
Projection
Horizontal positioning
SCALE
Scale 1 : 25 000
Metres
PROJECT TITLE
SOPAC
SOUTH PACIFIC APPLIED GEOSCIENCE COMMISSION
Private Mail Bag, GPO, Suva, Fiji Islands
www.sopac.org
SOPAC/EU Project
Reducing Vulnerability of Pacific ACP States
Grandiez TITLE
NANUMANGA
TUVALU
BATHYMETRY
Chart no. 2, Drawing no. 0050002-2
Drawn by: Jaime Kruger Report Reference: 0050002

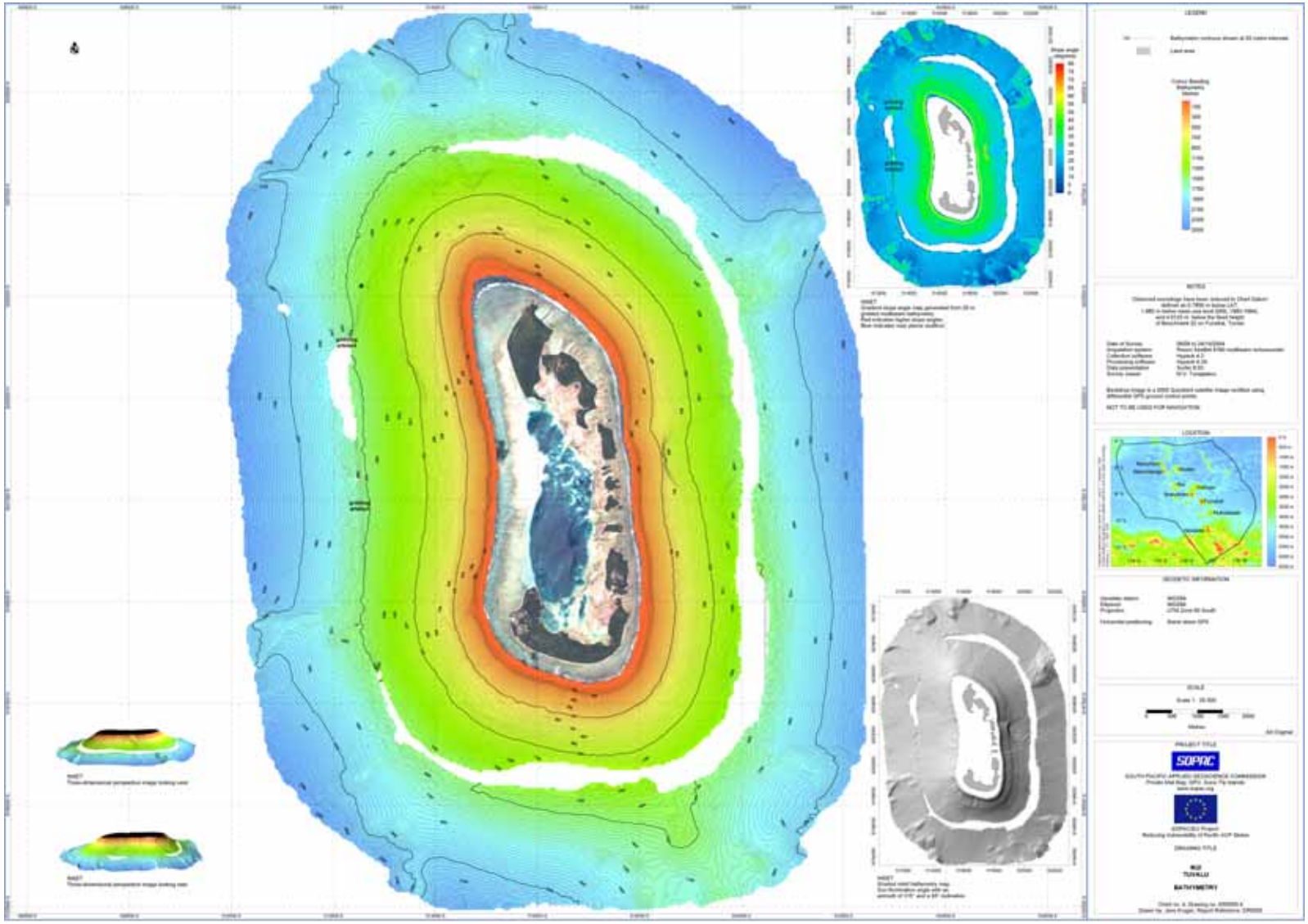

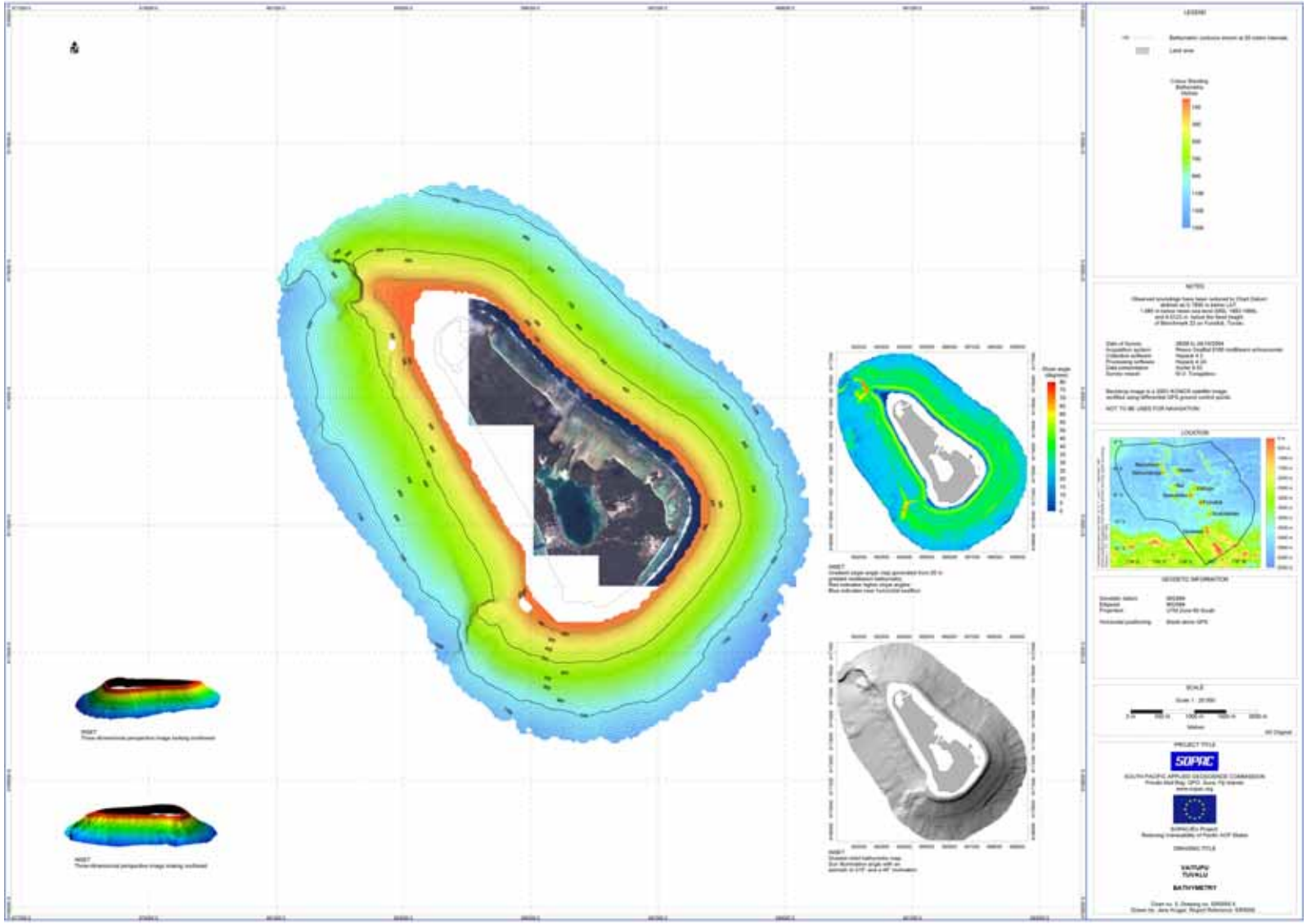
LEGEND
NOTES
LOCATION
GEODETIC INFORMATION
SCALE
PROJECT TITLE
SOPAC
SAMOA Project
VAITUPU
TUVALU
BATHYMETRY

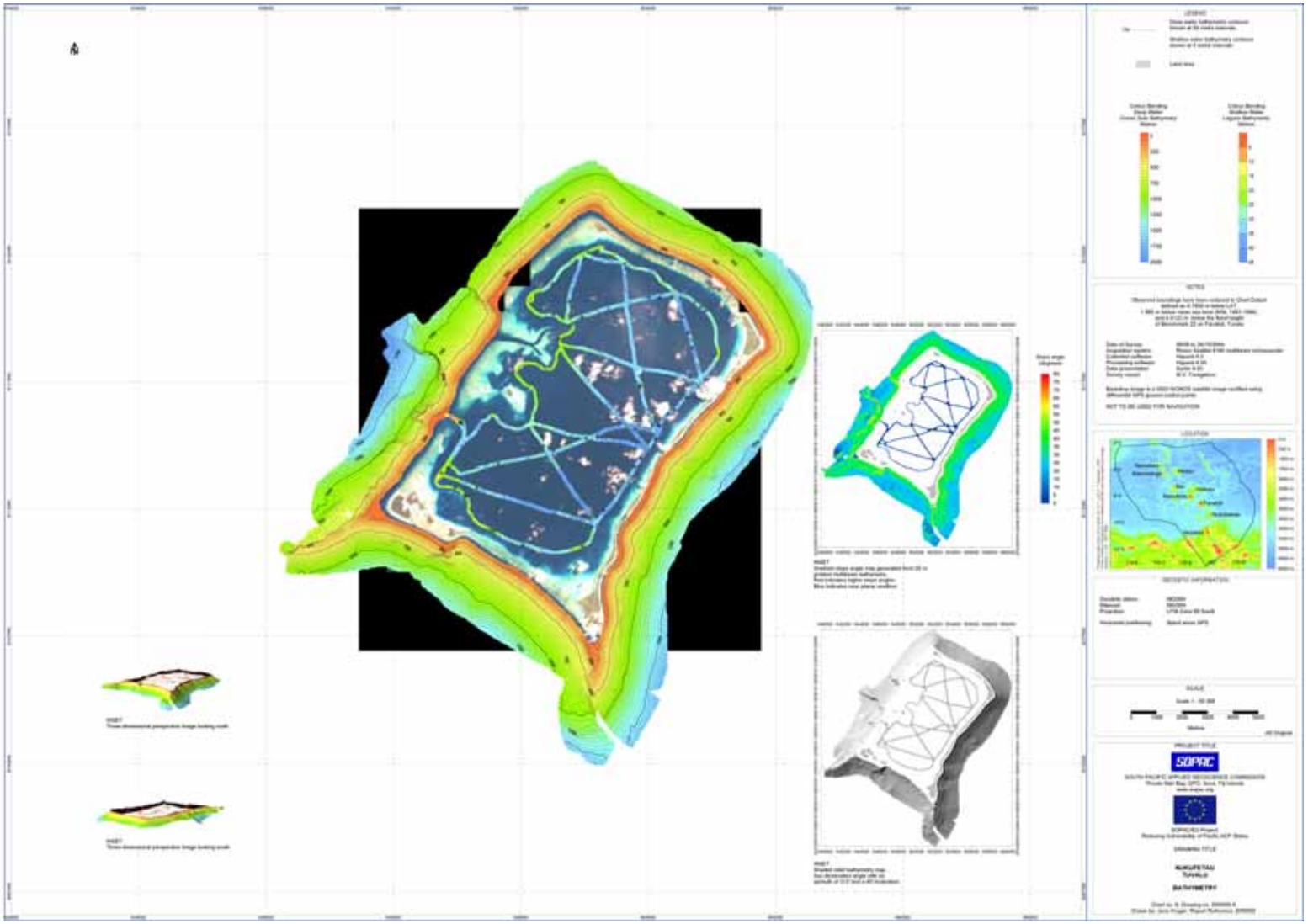

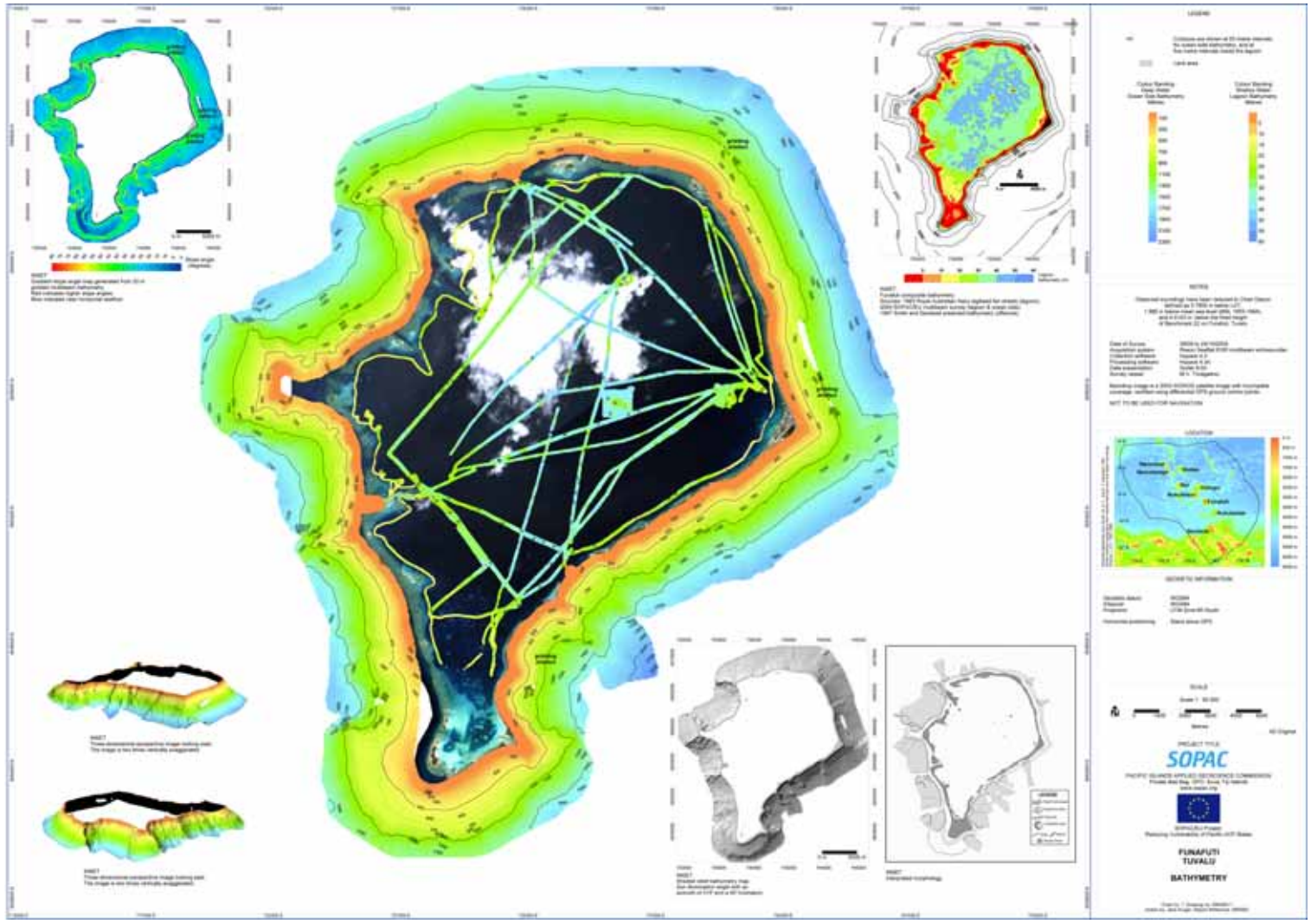
LEGEND
NOTES
LOCATION
SOURCE OF INFORMATION
SCALE
PROJECT TITLE
SOPAC
FUNAFUTI
TUVALU
BATHYMETRY

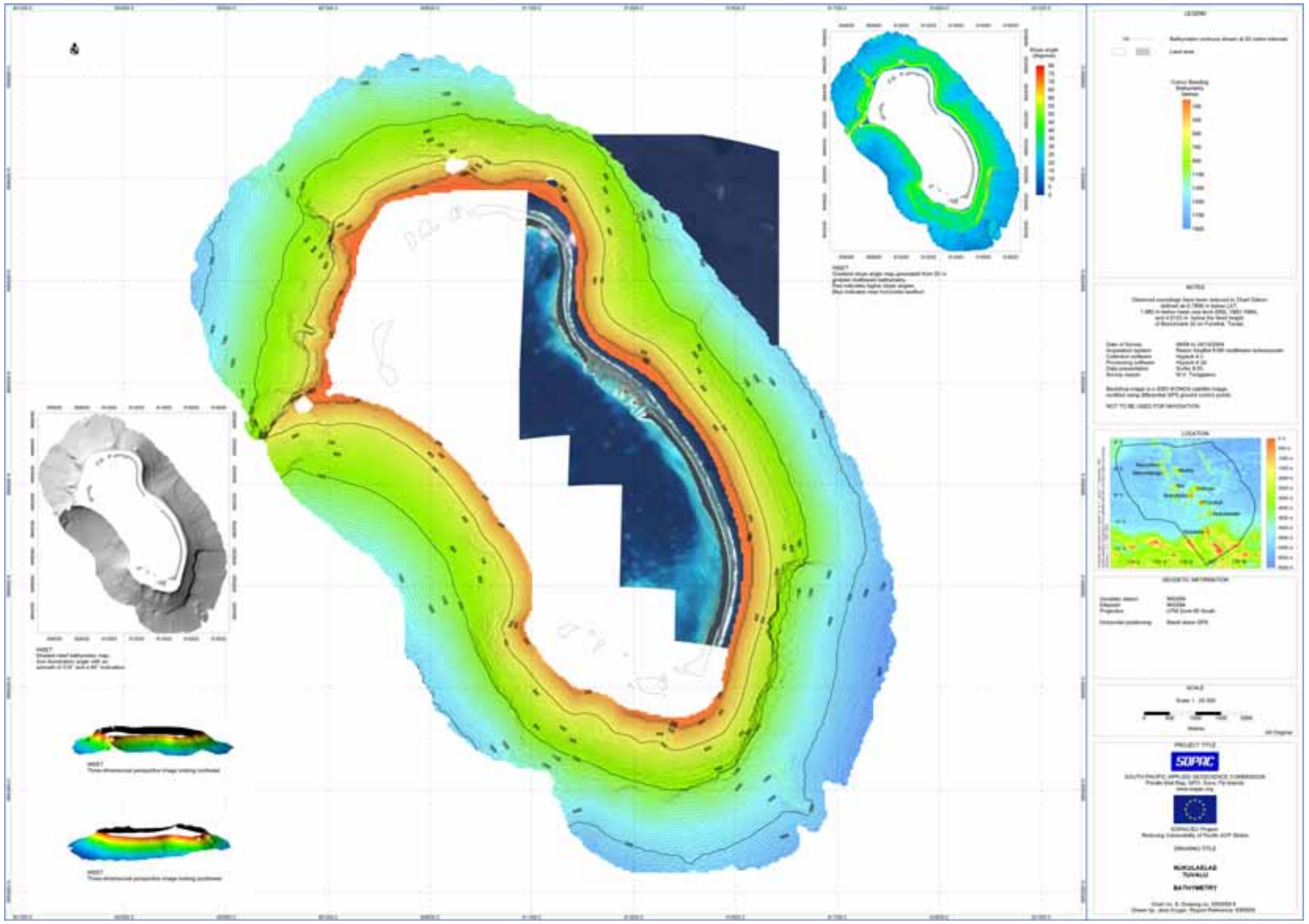
LEGEND
NOTES
LOCATION
GEODETIC INFORMATION
SCALE
PROJECT TITLE
SOPAC
NUKULAELAE
TUVALU
BATHYMETRY

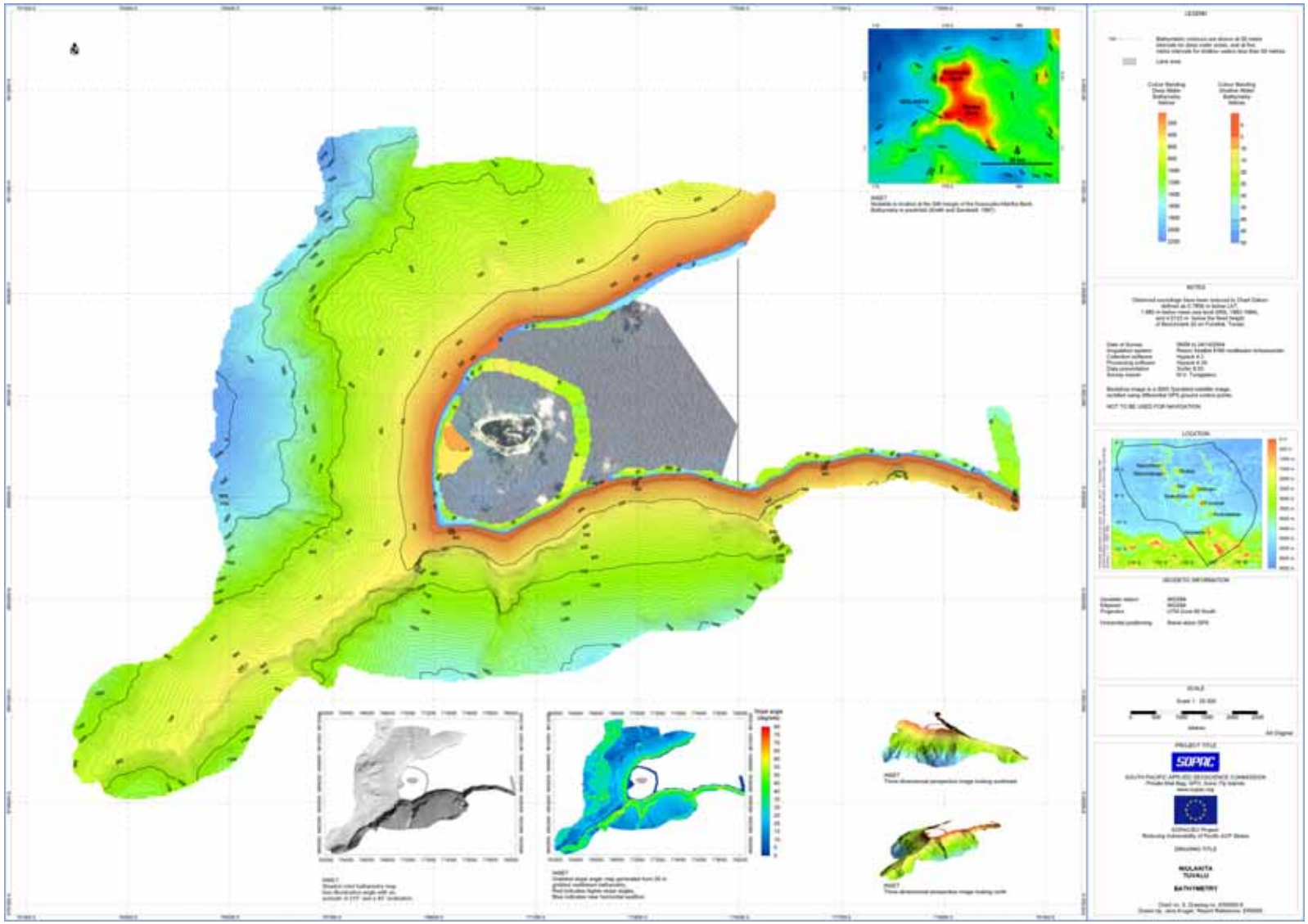
LEGEND
NOTES
LOCATION
GEODETIC INFORMATION
SCALE
PROJECT TITLE
SOPAC
SOPAC/EU Project
Reducing Vulnerability of Pacific ACP States
DRAWING TITLE
NUI,AVITA
TUVALU
BATHYMETRY